

Bulletin of The Geological Society of America

VOLUME 63

November 1952

NUMBER 11

CONTENTS

	Pages
Gravity and magnetic investigation of the structure of the Cortlandt Complex, New York. By Nelson C. Steenland and George P. Woollard.....	1075-1104
Continental shelf sediments of southern California. By K. O. Emery.....	1105-1108
Glaciation and drainage changes in the Fish Lake Plateau, Utah. By Clyde T. Hardy and Siegfried Muessig.....	1109-1116
Hypsometric (area-altitude) analysis of erosional topography. By Arthur N. Strahler..	1117-1142
Probable Illinoian age of part of the Missouri River, South Dakota. By Charles R. Warren.....	1143-1156

Subscription \$15.00 per year.

Publication Office: Mt. Royal & Gullford Aves., Baltimore 2, Md.

Communications for publication should be addressed to The Geological Society of America, Dr. H. R. Aldrich, Secretary, 419 West 117 Street, New York, N. Y.

NOTICE—Four weeks notice of change of address is necessary. In accordance with the rules established by the Council, claims for non-receipt of the preceding number of the Bulletin must be sent the Secretary of the Society within three months of the date of the receipt of this number in order to be filled gratis.

Entered as second-class matter at the Post-Office at Baltimore, Md.,
under the Act of Congress of July 16, 1904.

Accepted for mailing at special rate of postage provided for in Section 1103
Act of October 3, 1917, authorized on July 8, 1918.

PAPERS IN PRESS FOR FORTHCOMING ISSUES

SEDIMENTARY VOLUMES IN GULF COASTAL PLAIN OF UNITED STATES AND MEXICO

FOREWORD AND SUMMARY. By Grover E. Murtay

PART I: VOLUME OF MESOZOIC SEDIMENTS IN FLORIDA AND GEORGIA. By Paul L. Applin

PART II: VOLUME OF CENOZOIC SEDIMENTS IN FLORIDA AND GEORGIA. By Lyman D. Toulmin

PART III: VOLUME OF MESOZOIC AND CENOZOIC SEDIMENTS IN CENTRAL GULF COASTAL PLAIN OF UNITED STATES. By Grover E. Murtay

PART IV: VOLUMES OF MESOZOIC AND CENOZOIC SEDIMENTS IN WESTERN GULF COASTAL PLAIN OF UNITED STATES. By Jack Colle, W. F. Cooke, Jr., R. L. Denham, H. C. Ferguson, J. H. McGuirt, Frank Reedy, Jr., and Paul Weaver

PART V: VOLUMES OF MESOZOIC AND CENOZOIC SEDIMENTS IN MEXICAN GULF COASTAL PLAIN. By Eduardo J. Guzmán

PART VI: GEOPHYSICAL ASPECTS. By L. L. Nettleton

CARIBBEAN RESEARCH PROJECT. By H. H. Hess and J. C. Maxwell

GEOLOGY OF THE CARACAS REGION, VENEZUELA. By Gabriel Dengo

GEOLOGY OF THE LOS TEQUES-CUA REGION, VENEZUELA. By Raymond J. Smith

GEOLOGY OF THE ST. BARTHOLOMEW, ST. MARTIN, AND ANGUILLA, LESSER ANTILLES. By Robert A. Christman

GEOLOGY OF THE AGUA FRIA QUADRANGLE, BREWSTER COUNTY, TEXAS. By C. Gardley Moon

GRAVITY AND MAGNETIC INVESTIGATION OF THE STRUCTURE OF THE CORTLANDT COMPLEX, NEW YORK

BY NELSON C. STEENLAND AND GEORGE P. WOOLLARD

ABSTRACT

This report is based on 185 gravity and magnetic stations established over the Cortlandt Complex and contiguous areas. The total area of the survey is approximately 75 square miles. The Complex consists of a group of basic igneous rocks near Peekskill, New York, in a region of granitic rocks and lower Paleozoic sediments.

The gravity observations show a pronounced gravity anomaly of about 30 mgals, centered over the olivine pyroxenitic region on the east side of the Complex, and a smaller anomaly of about 15 mgals on the west side of the Complex in an area of augite norite and norite with prismatic hornblende. The larger anomaly corresponds in position to one of the foliation structures Balk mapped within the Complex. No separate anomaly occurs in the central area where a foliation structure exists with almost perfect zoning of rock types grading from norite with poikilitic hornblende to augite norite. The results of density determinations show the intrusive rocks to have an average density 0.4 gm/cc higher than the country rock. Calculations are presented to determine theoretical bodies that would satisfy the observed anomalies. The principal anomaly (30 mgals) is closely approximated by a vertical cylinder 2.4 miles in diameter and 4.7 miles thick, whereas the lesser anomaly of 15 mgals is approximated by a vertical cylinder 1.2 miles in diameter and 5.0 miles thick. These thicknesses are minimal values because infinitely long cylinders of the same cross sections have essentially the same gravity effect. The intermediate area between the cylinders is characterized by a residual gravity anomaly of 8 mgals suggesting that here the Complex is about 0.3 mile thick.

The magnetic map shows no well-defined anomaly associated with the Complex as a whole. A central anomaly of 1200 gammas, occurring in the middle of the Complex, is ascribed to the rocks beneath the Complex and affords a basis for estimating the depth to the host rock, 0.3 mile. This verifies the thickness computed from the gravity data. In addition, four local anomalies of approximately 1000 gammas are developed near the boundaries of the Complex. Three of these are associated with known magnetite-bearing emery deposits.

CONTENTS

TEXT		Page	
Introduction	1076	Recapitulation of geological and geophysical results	1089
General description	1076	Conclusions	1090
Geological investigations	1076	References cited	1091
Present investigation	1076	Appendix	1094
Purpose of geophysical investigations	1076		
Description of geophysical work	1076		
Gravity survey	1079		
Instruments used	1079		
Method of reduction	1079		
Bouguer anomalies	1079		
Density of rocks in Cortlandt Complex	1081		
Interpretation of gravity anomalies	1081		
Magnetic survey	1085		
Instruments used	1085		
Reductions of observations	1085		
Magnetic anomalies	1085		
Magnetic susceptibility of rocks of Complex	1086		
Interpretation of magnetic anomalies	1086		

ILLUSTRATIONS		Page	
Figure			
1. Location and geologic setting of Cortlandt Complex	1077		
2. Foliation structure within the Cortlandt Complex	1077		
3. Geologic map of the Cortlandt Complex	1078		
4. Network of gravity and magnetic stations in and around the Cortlandt Complex	1078		
5. Topography of the area in and adjacent to the Cortlandt Complex	1079		
6. Bouguer gravity anomaly map of Cortlandt Complex	1080		

Figure	Page	Figure	Page
7. Residual gravity map of Cortlandt Complex.....	1081	12. Magnetic susceptibility of rocks in the Cortlandt Complex.....	1088
8. Rock-density distribution in the Cortlandt Complex.....	1083	13. Comparative geologic and geophysical profiles.....	1090
9. Comparison of observed and theoretical gravity profiles.....	1084	14. Contour map of dip of structural lineaments within Cortlandt Complex.....	1092
10. Second residual gravity map of Cortlandt Complex.....	1084	15. Block diagram showing proposed subsurface structure of Cortlandt Complex... ..	1092
11. Vertical component magnetic anomaly map of Cortlandt Complex.....	1086		

INTRODUCTION

General Description

The Cortlandt Complex is an unusual body of igneous rocks, composed of norite, diorite, and pyroxenite. The Complex outcrops in a general area of metamorphic rocks and granites along the east bank of the Hudson River, near Peekskill, New York, at Lat. 41°16' N., and Long. 73°54' W. (Fig. 1). The area embraced by the Complex is approximately 24 square miles. Outstanding features associated with the Complex are: (a) the unusual suite of basic rocks; (b) a systematic zoning of rock types; (c) a conspicuous banding in parts of the Complex (resulting from alternations of dark and light minerals); and (d) a suggested funnel shape for the Complex as a whole and a similar shape for some of its constituent parts.

Geological Investigations

J. D. Dana's report on the Cortlandt Complex (1880) classifies the series as a group of metamorphosed sediments on the basis of the notable banding. G. H. Williams (1886) recognized the rocks as igneous, and he described many of the rock types in detail. The first geologic map of the area is included in a paper by G. S. Rogers (1911). Seventeen rock types are recognized, but his distinctions are based upon an inappropriate classification and do not adequately describe the complexity of the rock types.

Robert Balk (1927) mapped the strike and dip of the planes of foliation both within the pluton and in the surrounding metamorphic rocks. His maps suggest that the entire pluton is funnel-shaped and, moreover, that two and possibly three smaller funnel-shaped bodies exist in the interior (Fig. 2).

S. J. Shand (1942) mapped important petrologic phases in the development of the Complex in order to describe the rock types. His map is used as the petrographic reference of this study (Fig. 3). Shand concludes that hornblende is the most critical mineral phase in the development of the Complex and that there is a correlation between the distribution of rock types and the structure as mapped by Balk. In particular the coincidence of Balk's central structure with the zoned area of norite containing poikilitic hornblende led Shand to postulate that this area is the source area for the whole Complex. This interpretation is at variance with Balk's original hypothesis that the internal funnels were derived from large globs of early-crystallized material suspended in rising currents of magma.

Other geologic reports on the Cortlandt Complex consist of studies of local areas within the Complex in connection with the mining of emery (*e.g.*, Butler, 1936).

PRESENT INVESTIGATION

Purpose of Geophysical Investigations

No geophysical data are included in any of the previously published reports. The authors' purpose in making a geophysical study of the Cortlandt Complex is to ascertain the feasibility of using gravity and magnetic measurements to determine (1) whether the Complex represents one or more distinct lithologic units, and (2) what their shapes are beneath the surface.

Description of Geophysical Work

The field data for this report consist of a reconnaissance survey made in June 1946 and an additional network in 1947. The final network of 185 stations covering 75 square miles is shown in Figure 4. Sixty-five of these stations

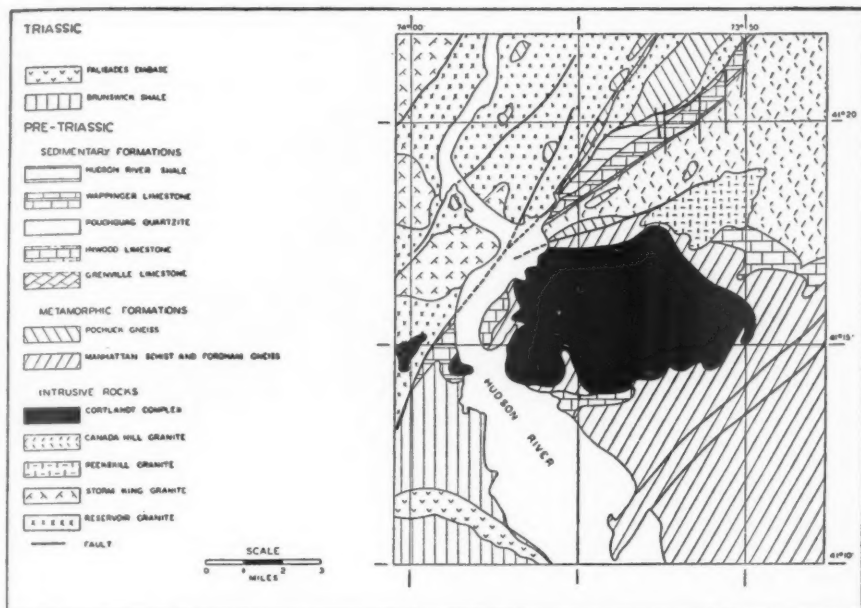


FIGURE 1.—LOCATION AND GEOLOGIC SETTING OF CORTLANDT COMPLEX



FIGURE 2.—FOLIATION STRUCTURE (after Balk) WITHIN THE CORTLANDT COMPLEX

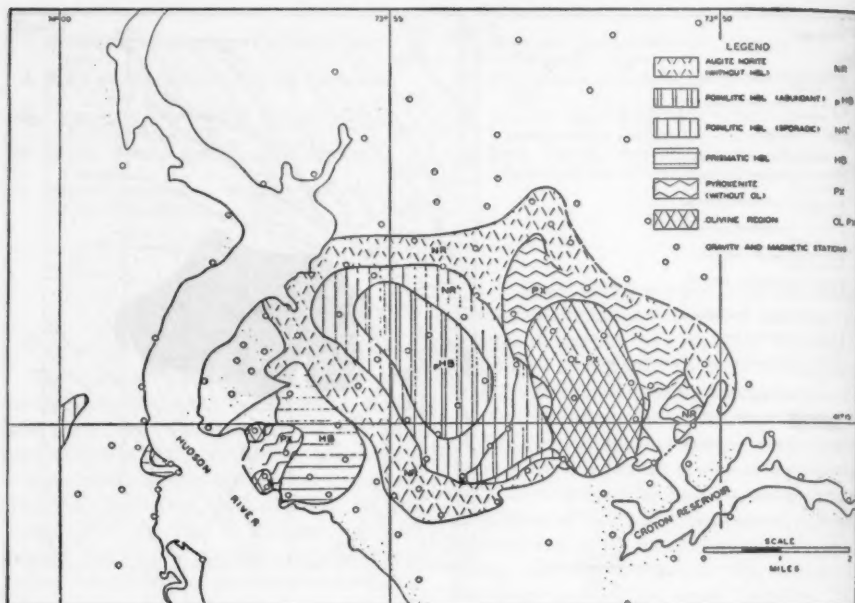


FIGURE 3.—GEOLOGIC MAP (after Shand) OF THE CORTLANDT COMPLEX

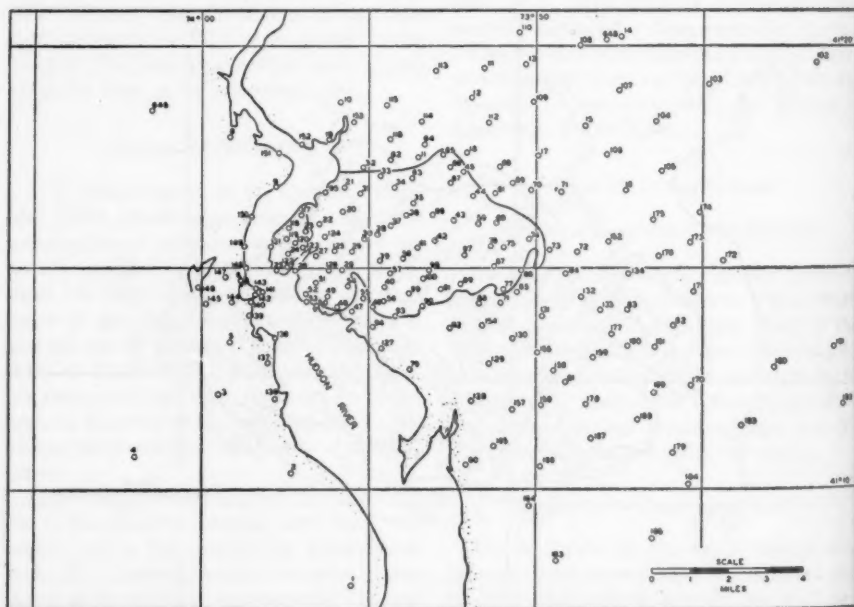


FIGURE 4.—NETWORK OF GRAVITY AND MAGNETIC STATIONS IN AND AROUND THE CORTLANDT COMPLEX

are within the outcrop of the Complex with a resulting density of observations of about three per square mile. This coverage is adequate for

above sea level, results in the Bouguer anomalies. The Bouguer corrections are computed using a density of 2.67 gm/cc for the surface rocks.

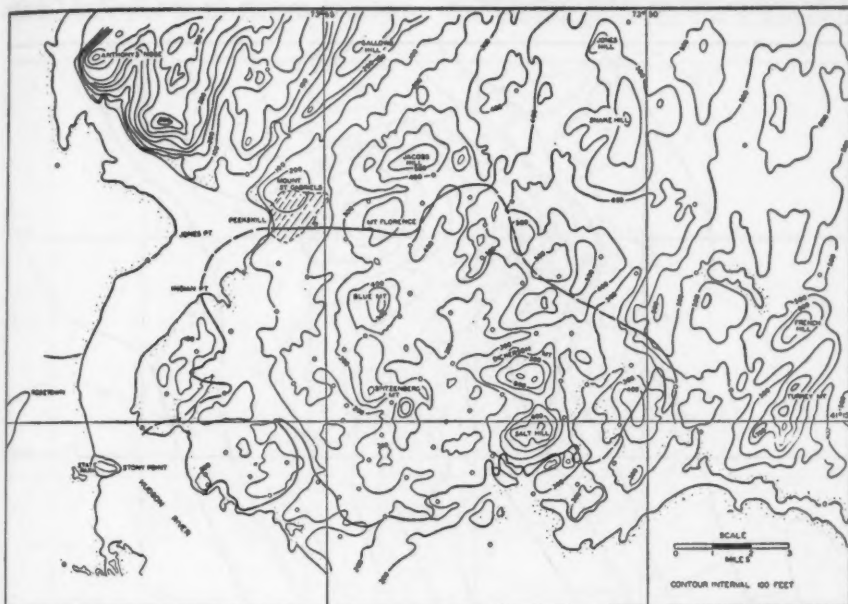


FIGURE 5.—TOPOGRAPHY OF THE AREA IN AND ADJACENT TO THE CORTLANDT COMPLEX

the gravity and magnetic anomalies except for the local magnetic anomalies over the emery deposits.

Gravity Survey

Instruments used.—The data for stations 1-100 and 135-162 are computed from observations made with a Humble Oil and Refining Company X-type gravity meter with a scale value of 0.176 mg/scale division. The data for the remaining 57 stations are computed from observations with a Frost gravity meter, scale value 2.26 mg/scale division.

Method of reduction.—Observed gravity values, after corrections for drift and closure, are put on an absolute gravity basis through tie-observations to the pendulum gravity station network of the U. S. Coast and Geodetic Survey. These observed values, corrected for variations in latitude (according to the International gravity formula), elevation, and mass

Principal facts for all stations are included in Appendix 1.

The elevations at the stations are derived from the pertinent topographic quadrangle sheets of the U. S. Geologic Survey. These sheets provide individual elevations at road intersections and other prominent land marks, in addition to the topographic contours. Only the elevations in areas of contours are substantiated by ties made with altimeters. All station elevations are considered accurate to within 2 feet.

The topography is mostly rolling and without excessive relief (Fig. 5). No corrections for terrain are included since these would not exceed 1 mgal at any station site. An inspection of the Bouguer anomaly map (Fig. 6) shows that errors of this magnitude would not significantly affect the anomalies. There is no correlation between the anomalies and topography.

Bouguer anomalies.—Figure 6 shows a regional gradient of approximately 6 mgals per

mile decreasing to the east; this is derived from Woollard's regional gravity map of eastern United States. Superimposed on this gradient is the positive anomaly of the Cortlandt Com-

gravitational effect of surface and near-surface geologic features, and these are plotted along the profile lines. These residual values, when contoured, produce the first Residual Gravity

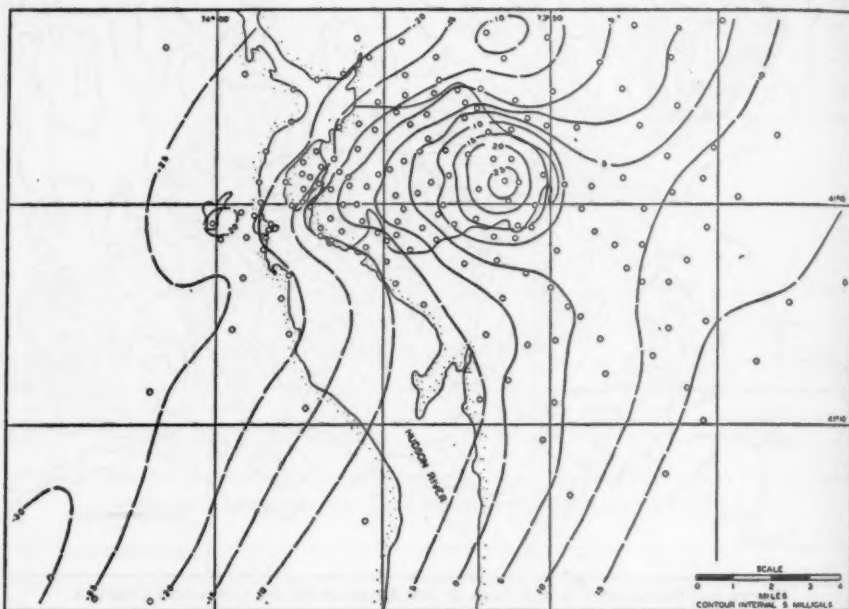


FIGURE 6.—BOUGUER GRAVITY ANOMALY MAP OF CORTLANDT COMPLEX

plex. The first step in the analysis is the removal of this gradient and the isolation of the Bouguer anomaly attributable to the intrusive.

The removal of any regional effect is essentially "the removal of the undesirable." Many techniques are available and range from complicated grid calculations of fourth derivatives to the simple method of sketching residual anomalies on an observed map. The resolution of the Cortlandt Bouguer map is not difficult. The two fundamental elements, the regional gradient and the anomaly over the intrusive, are easily and objectively resolved by the use of profiles, in this case by north-south and east-west profiles, constructed over the Bouguer anomaly map at 1-mile intervals. On these profiles smooth curves, representing the regional gradient, are drawn. The differences between the observed profiles and the smooth regional curves are the residual values representing the

Anomaly Map (Fig. 7). This map, contoured with a 5-mgal interval and superimposed on Shand's petrographic map of the Complex, shows an anomaly of more than 30 mgals reaching its maximum value over the olivine pyroxenitic area on the east side of the Complex. The zero contour is parallel to, but outside, the outcropping limits of the Complex except north of the intrusive where a small closure of 5 mgals distorts the zero contour.

In addition to the maximum of almost circular contours over the eastern pyroxenitic area, a prominent westward-plunging nose includes the pyroxenitic area along the eastern bank of the Hudson River. A local closure of 5 mgals occurs within this nose (within the 15-mgal contour) over an area of out-cropping norite with prismatic hornblende. The zero contour extends westward to include the Rosetown ex-

tension. At both Rosetown and Stony Point closed gravity maxima of 5 mgals occur.

The small local gravity maximum, on the northwestern edge of the poikilitic hornblende

comparison. Sharpe's results are from pycnometer determinations using samples the size of a kernel of corn. On the whole, the corroboration is good. Of the 32 comparisons, 24 have differences of 0.05 or less, with an average difference of 0.025. Eight have differences greater than 0.05. If these are in-

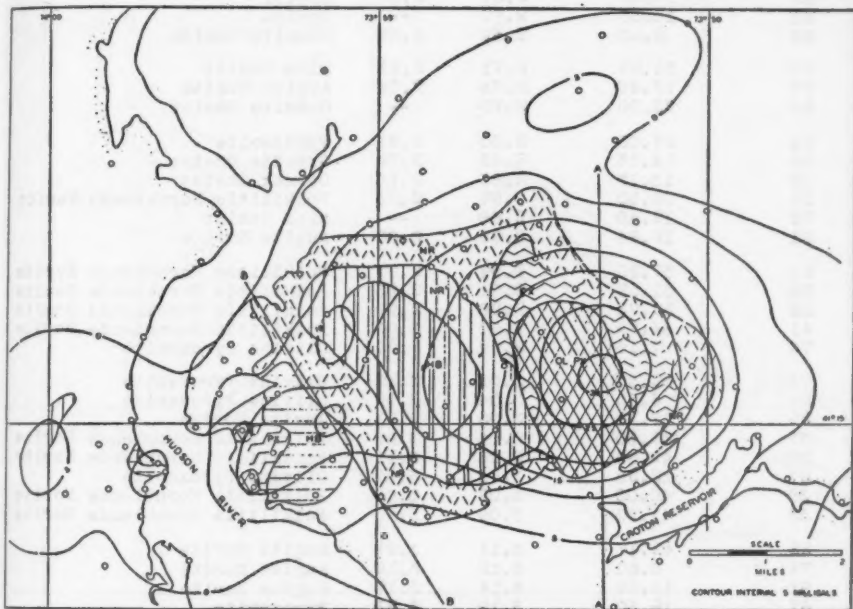


FIGURE 7.—RESIDUAL GRAVITY MAP OF CORTLANDT COMPLEX

area and within the 10-mgal contour, is not clearly identifiable with any known geologic element.

Density of rocks in Cortlandt Complex.—The relations between the anomalous areas and surface geologic features suggest that the gravity anomalies depend upon the density of the outcropping rocks. Determinations of the bulk densities of 26 samples of the Complex and 9 samples of the host rock are listed in Table 1 in order of increasing densities. The petrologic identifications of the samples are based on their location within Shand's boundaries and the megascopic examination of "hand" specimens.

Since the rocks are impervious, the buoyancy method of determining specific gravity may be used without taking special precautions against the absorption of water. In Table 1, a series of measurements made by Joseph Sharpe and J. C. Rollins (Frost Geophysical Company) are included for

cluded, the mean difference is 0.06. In view of the larger size of the original samples used in the buoyancy method, these values form the basis for the subsequent analysis of the gravity results.

In Table 2, average values for the different rock types are grouped for comparison along with the spread in density observed within each group. The mean density values of the individual intrusive types within the Complex are confined within a range of ± 0.05 gm/cc. On the other hand, the mean value of the Complex rocks as a whole (3.05) differs significantly from that of the country rock (2.74).

In Figure 8 the data of Table 1 are plotted and contoured to show the variation in density of the surface rocks. Although there are individual idiosyncrasies, the density distribution within the Complex conforms in general to the Bouguer gravity-anomaly pattern.

Interpretation of gravity anomalies.—The

TABLE 1. ROCK DENSITIES

Station	Sample Weight grams	Density (gm/cc)		Rock Description ³
		S & W ¹	Frost ²	
94	25.23	2.62	2.65	Granite
62	26.30	2.67	2.67	Gneiss
83	15.50	2.67	--	Gneiss
88	8.20	2.69	2.69	Granite Gneiss
72	33.26	2.71	2.71	Mica Schist
93	12.40	2.74	2.74	Augite Norite
84	73.90	2.78	--	Granite Gneiss
96	27.05	2.80	2.81	Pyroxenite
18	14.73	2.83	2.72	Granite Gneiss
55	13.17	2.83	3.16	Garnet Gneiss
31	32.50	2.88	2.83	Poikilitic Hornblende Norite
72	12.40	2.88	--	Mica Schist
91	12.84	2.89	2.86	Augite Norite
21	37.30	2.94	2.92	Poikilitic Hornblende Norite
58	31.51	2.94	2.93	Poikilitic Hornblende Norite
35	22.75	2.96	2.99	Poikilitic Hornblende Norite
41	64.75	2.97	3.00	Poikilitic Hornblende Norite
76	7.19	2.98	2.94	Olivine Pyroxenite
76	52.83	3.01	3.28	Olivine Pyroxenite
89	6.35	3.04	3.09	Olivine Pyroxenite
29	17.70	3.05	2.91	Augite Norite
37	31.30	3.05	3.01	Poikilitic Hornblende Norite
30	49.88	3.06	3.11	Poikilitic Hornblende Norite
87	12.25	3.06	3.07	Olivine Pyroxenite
36	40.00	3.07	3.05	Poikilitic Hornblende Norite
38	41.53	3.09	3.23	Poikilitic Hornblende Norite
22	42.17	3.11	3.27	Augite Norite
74	6.80	3.12	3.12	Augite Norite
95	16.65	3.14	3.17	Augite Norite
67	18.50	3.19	3.23	Pyroxenite
59	8.95	3.20	3.24	Olivine Pyroxenite
43	4.10	3.20	3.29	Olivine Pyroxenite
26	106.20	3.21	3.09	Olivine Pyroxenite
75	7.35	3.24	3.22	Pyroxenite
39	58.72	3.27	3.22	Poikilitic Hornblende Norite

¹ Buoyancy method.

² Pycnometer method.

³ Identification by hand specimen study and area of occurrence.

TABLE 2.—SUMMARY OF ROCK DENSITIES

Rock Description	No. of Samples	Average Density gm/cc	Range of Values gm/cc
Host Rock.....	9	2.74	0.26
Cortlandt Complex.....	26	3.05	0.53
Augite Norite.....	6	3.01	0.40
Poikilitic Hornblende Norite.....	10	3.02	0.39
Pyroxenite.....	3	3.08	0.44
Olivine Pyroxenite.....	7	3.10	0.23

large gravity anomaly over the eastern olivine pyroxenite is the primary feature of the first Residual Gravity Anomaly Map (Fig. 7). This anomaly has almost circular contours, suggesting a subsurface body of circular cross section. The density contrast between pyroxenitic rock of the anomaly area and the metamorphic host rocks is approximately 0.4 gm/cc (Table 1). The mean diameter of the pluton in the eastern anomaly area is 2.4 miles. No conical body, having a surface diameter of 2.4 miles, contains

enough mass to produce an anomaly of 31 mgals. For example, the maximum effect of a cone extending to a depth of 12 miles, with this surface dimension, is 24 mgals. A cylin-

approximated by a cylinder with a diameter of 1.2 miles extending to a depth of 5 miles (26,000 feet). Using the density contrast of 0.4 gm/cc, this depth, again mathematically equivalent to

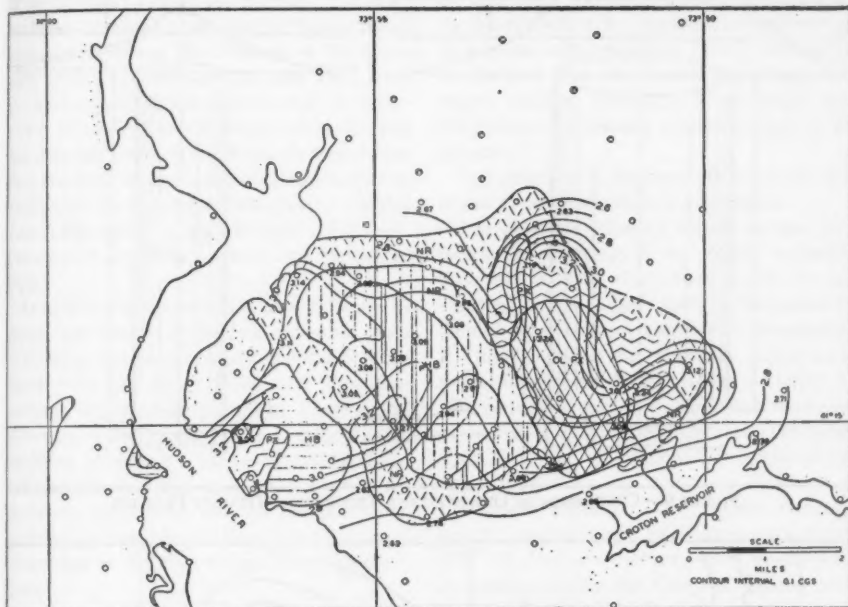


FIGURE 8.—ROCK-DENSITY DISTRIBUTION IN THE CORTLANDT COMPLEX

drical body 2.4 miles in diameter and 4.7 miles (25,000 feet) in depth, however, yields a value of the desired amplitude. This depth is a minimum value because an infinitely deep cylinder of the same radius would have an effect of only 32 mgals. A comparison between the theoretical anomaly for the above cylinder and the first residual anomaly contours along Section A-A of Figure 7 is shown in Figure 9. The theoretical curve fits the residual anomaly curve reasonably well except at the extremities where the residual curve maintains a steeper gradient. This may indicate that the actual subsurface shape is conical near the surface.

The 15-mgal anomaly in the area of prismatic hornblende adjacent to the pyroxenitic area on the Hudson River's eastern bank is similarly analyzed. The residual gravity-anomaly profile along Section B-B (Fig. 7) can be

infinity, is essentially the same as that required to produce the large eastern anomaly. Since the anomaly of 15 mgals is not centered over any of the zoned petrographic units suggestive of a magma pipe, its surface geologic counterpart is probably displaced or masked.

It is of interest to evaluate the effect of removing the gravitational field of the two cylinders. To do this, their circular contours (shown in background, Fig. 10) are subtracted from the first Residual Gravity Anomaly Map. A contoured map of these residues results in the Second Residual Gravity Anomaly Map (Fig. 10).

This second residual map contains only residues of a few milligals in the areas where anomalies of more than 30 and 15 mgals had appeared. The amplitude of these residues reflects the departure of the mass distribution

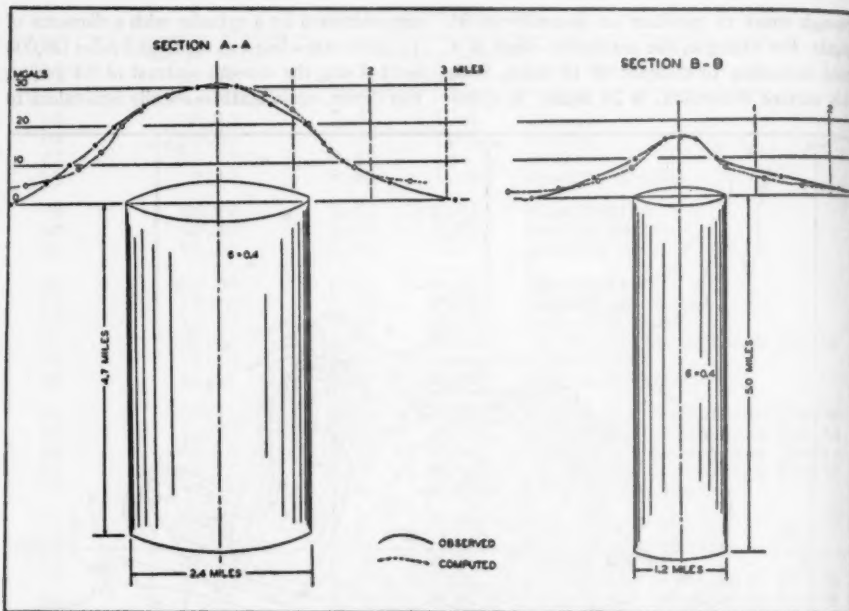


FIGURE 9.—COMPARISON OF OBSERVED AND THEORETICAL GRAVITY PROFILES

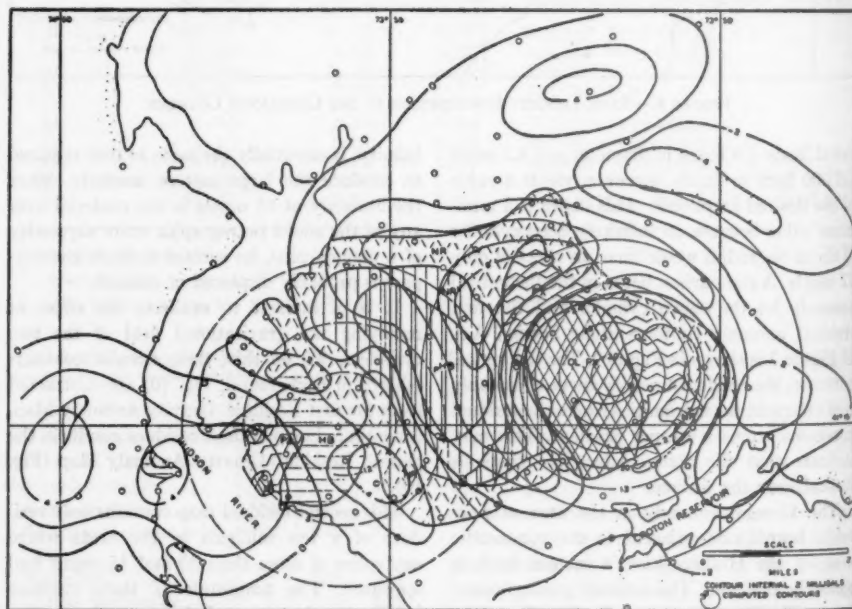


FIGURE 10.—SECOND RESIDUAL GRAVITY MAP OF CORTLANDT COMPLEX

of the actual subsurface masses from the hypothetical cylinders. From Figure 10 it is seen that the largest residue, 8 mgals, is in the area between the pyroxenitic areas (the central region of norite with poikilitic hornblende). This is an elongated anomaly broadening to the north and presumably reflects the thickness of the Complex developed in the central area away from the feeder pipes. If it is assumed that the intrusive in the central area is shaped like a slab and has a density contrast of 0.3 (on the supposition that the bulk of the intrusive is norite in this area), then the thickness of the Complex in this area is calculated to be 0.35 mile (1800 feet). (Method of calculation shown by Nettleton, 1942.)

In addition to the central anomaly, Figure 10 shows that two small residual anomalies, each of 4 mgals, occur on the west side of the Hudson River over the Stony Point and Rosetown outcrops of Cortlandt-type rocks. These anomalies suggest small feeder pipes at each of these localities. In addition, the configuration of the 2-mgal contour which crosses the river to include the pyroxenitic area on the east bank suggests the possible existence of another small feeder pipe in the river adjacent to the eastern shore.

Magnetic Survey

Instruments used.—The magnetic data are reduced from observations made with two Askania Schmidt type vertical-component magnetometers. The scale values and temperature coefficients for the magnetometers are:

Inst. No.	Year	S.V.	T.C.
1	1946	30.2 gammas/scale div.	7.6 gammas/°c
1	1947	33.5 gammas/scale div.	7.6 gammas/°c
2	1947	31.6 gammas/scale div.	7.6 gammas/°c

Reduction of observations.—Corrections for the diurnal variation in the earth's magnetic field during the period of the survey are taken

from magnetograms obtained from the U. S. Coast & Geodetic Survey's Cheltenham (Maryland) Magnetic Observatory. The correction is acceptable because the observed misclosure for each day's operations is essentially removed by this procedure. For example, a misclosure of 91 gammas obtained on 16 June is reduced to 16 gammas after the diurnal correction. The largest value of misclosure of any single day, after correcting for the diurnal change, is 38 gammas.

The accuracy of the magnetic values is estimated to be approximately 10 gammas.

The observed intensity values are also corrected for variations of the earth's magnetic field with latitude. Corrections applied to the observed values consist, then, of temperature, diurnal, base (closure) and latitude corrections. A "tare" value is also added to adjust each day's observations to the datum of station 1. The reduced values (ΔZ anomalies), plotted and contoured, are shown in Figure 11. The principal facts for all stations are included in Appendix 2.

Magnetic anomalies.—No general anomaly may be associated with the Complex as a whole (Fig. 11). The zero contour, which would have to remain outside the Complex, crosses and recrosses the Complex's boundary as it follows the four pronounced sharp anomalies developed at random along the boundary. These four anomalies may be easily removed and leave no general anomaly. Their removal does leave a broad, irregular maximum of 1200 gammas in the central area about 0.7 mile east of the center of the area of poikilitic hornblende.

The very large anomalies outside the Complex are only partially surveyed and have no known geologic counterparts. Presumably they reflect local concentrations of magnetite.

A number of rock specimens from one of these areas are amphibolitic schists. R. A. Geyer, who has done extensive work in investigating magnetic anomalies in the Carmel region just north of this area (Geyer, 1951) and who has examined the specimens, identifies them as similar to schists in the area of his investigations. These schists contain significant amounts of disseminated magnetite.

A local anomaly occurs over the Rosetown extension of the Cortlandt rocks (Fig. 11). Kemp (1888), in describing these rocks, men-

tions considerable magnetite in association with abundant hornblende. No anomaly is found over the pyroxenites on Stony Point.

The agreement between the zonal arrangement of the susceptibility values and Shand's geologic map is quite striking. Further agree-

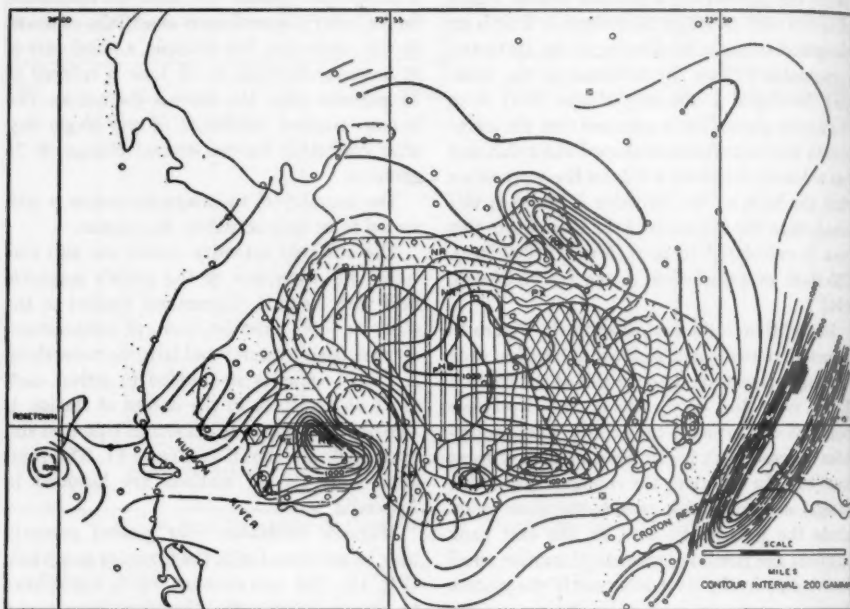


FIGURE 11.—VERTICAL COMPONENT MAGNETIC ANOMALY MAP OF CORTLANDT COMPLEX

Magnetic susceptibility of rocks of the complex.

—The magnetic susceptibilities of the suite of rocks obtained for density determinations are given in Table 3. The authors are again indebted to Frost Geophysical Company for these measurements. The susceptibility values, plotted and contoured, are shown in Figure 12. An examination of this map shows: (1) both the pyroxenitic areas and the central area of abundant poikilitic hornblende are characterized by rocks of low magnetic susceptibility; (2) an intervening area of rocks of moderate susceptibility separates these areas of low susceptibility; (3) the rocks of high susceptibility are confined to the periphery of the Complex, and (4) the adjacent host rock has low susceptibility, similar to (1). The abnormally high susceptibility value listed, $20,283 \times 10^{-6}$ cgs, is for a specimen of pyroxenite from the Emery Hill ore deposit.

ment is also supplied by Shand's thin-section studies of the rocks of the Complex which show that spinel is an accessory mineral of the rocks as well as of the ore deposits. Spinel is

"not uncommon as a minor constituent of norite and diorite throughout the Complex. . . . The sections of nonfeldspathic rocks (pyroxenite, hornblende, peridotite) did not reveal a single grain of spinel . . . the spinel is always enclosed with irregular plates as skeletons of an iron ore. . . . If this iron ore has the same composition as that in the emery deposits, it is a mixture of magnetite and ilmenite" (Shand, 1942, p. 419).

The absence of spinel from the central zoned areas of norite and pyroxenite thus explains the low susceptibility values found in these regions.

Interpretation of magnetic anomalies.—Thus the magnetic expression of the Cortlandt rocks is more complex than the gravity expression, and the two sets of data do not conform in

pattern. In particular, no distinct pattern is associated with the eastern olivinitic area where the gravity maximum occurs.

The broad anomaly of 1200 gammas, situated centrally within the Complex, should corroborate the slablike form postulated for this area

TABLE 3.—MAGNETIC SUSCEPTIBILITIES

Station Location	Description	Susceptibility Kv x 10 ⁶
88	Granite gneiss	14
62 (2)	Gneiss	18
72	Mica schist (weathered)	28
62 (1)	Gneiss	52
39	Poikilitic hornblende norite (badly weathered)	64
76 (1)	Olivine pyroxenite	82 (?)
38	Poikilitic hornblende norite (weathered)	106
59	Olivine pyroxenite	109.6
18	Granite Gneiss	125
75	Pyroxenite	190
37 (3)	Poikilitic hornblende norite) (same fragment)	313
37 (1)	Poikilitic hornblende norite)	327
94	Granite	342
26	Olivine pyroxenite	361
36	Poikilitic hornblende norite (badly weathered)	407
37 (2)	Poikilitic hornblende norite	425
43	Olivine pyroxenite	441
18	Granite gneiss	455
87	Olivine pyroxenite	762
41	Poikilitic hornblende norite (badly weathered)	812
31	Poikilitic hornblende norite (weathered)	1046
58	Poikilitic hornblende norite (weathered)	1069
74	Norite	1324
30	Poikilitic hornblende norite	1487
29	Augite norite	1703
93	Augite norite	1770
95	Augite norite	2012
96	Pyroxenite	2297
55	Garnet gneiss (weathered)	2775
35	Poikilitic hornblende norite (lightly weathered)	3060
22	Augite norite	3148
91	Augite norite (weathered)	3700
76 (2)	Olivine pyroxenite	3748 (?)
21	Poikilitic hornblende norite	3923
60	Olivine pyroxenite	3948
67	Pyroxenite	20,283± 10%

Three of the four sharp, local anomalies near the borders correlate with known bodies of emery, and the four coincide with the areas of high susceptibility shown on Figure 12. Therefore the fourth anomaly, which is over 800 gammas and is in the northwestern corner of the complex, is considered to have the same origin. Rough computations indicate that the emery bodies must be as deep as they are wide, assuming a polarization contrast of .002 cgs.

from the gravity data. The magnetic susceptibility of a central slab, 0.35 mile thick, would have to be $17,000(10)^{-6}$ cgs to produce the magnetic anomaly. Since the measured susceptibilities in the central region average less than $500(10)^{-6}$ cgs, these assumptions are untenable. If the assumption is made that very highly polarized rocks (*i.e.*, $20,000(10)^{-6}$ cgs) exist as a marginal feature along the lower boundary as they do along the outer boundaries,

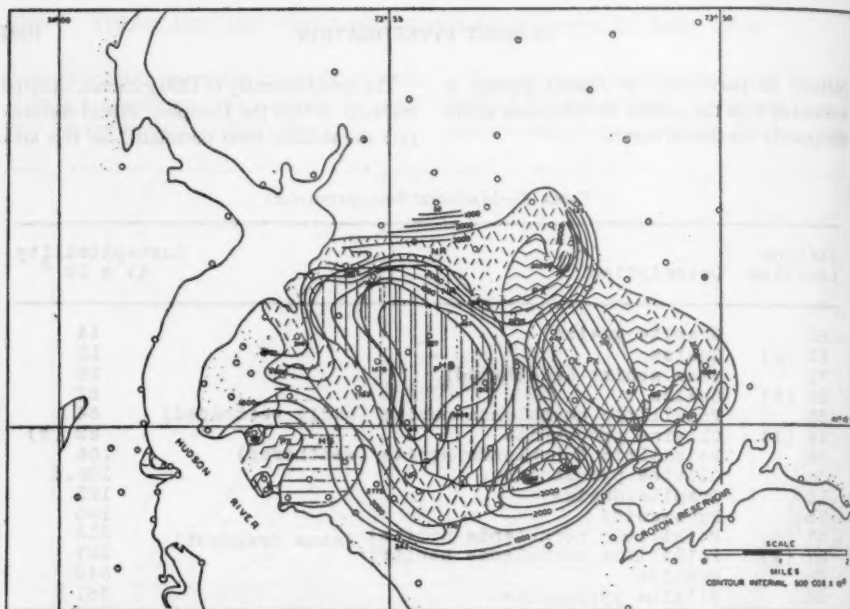


FIGURE 12.—MAGNETIC SUSCEPTIBILITY OF ROCKS IN THE CORTLANDT COMPLEX

TABLE 4.—PRINCIPAL CONCLUSIONS

Geologic Structure (Balk)	Petrologic (Shand)	Geophysical
<ol style="list-style-type: none"> 1. Entire Complex funnel-shaped 2. Three interior funnel-shaped foliation structures, central funnel in central poikilitic hornblende area and flanking funnels in pyroxenitic areas 3. Inner funnel shapes due to crystal settling of early crystallized aggregates 4. Maximum depth of Complex, 3.5 to 6.5 miles 5. Pyroxene-rich rocks are early differentiates from a parent noritic magma. 6. Strong foliation caused by proximity to stationary cold surface, <i>i.e.</i>, host rock. Such foliation found in (a) border zones, and (b) central internal funnel. 7. Foliation in central internal funnel decreases in dip as center is approached. 	<ol style="list-style-type: none"> 1. Norite is the parent magma. 2. Magma source is single pipe located in Balk's central internal funnel. 3. Pyroxenitic and noritic rock contemporaneous 4. Pyroxenites and peridotites result from settling in sinks. 5. Settling produced the parallel banding. 6. Poikilitic hornblende resulted from hot solutions from feeder pipe after crystallization of parent magma. 7. Iron-ore concentrates are result of same hot solutions. 8. Iron-ore concentrates occur only in boundary area of Complex. 	<ol style="list-style-type: none"> 1. Cylindrical feeder pipe, 2.4 miles in diameter, at least 5 miles deep, underlies Balk's eastern funnel (olivine pyroxenitic area). Fig. 13B, Sec. 2. 2. Cylindrical feeder pipe, 1.2 miles in diameter, at least 5 miles deep, near Balk's western funnel. Fig. 13B, Sec. 2. 3. Small feeder pipes underlie Stony Point and Rosetown extensions west of Hudson River. 4. Thickness of central area, 0.35 mile from gravity data, confirmed by magnetic data. 5. Pipe material indicated to be pyroxenite by gravity analyses. 6. Magnetic susceptibilities confirm Shand's distribution of ore minerals. Fig. 13A, Sec. 1, 2. 7. Susceptibility and density values suggest extreme thinning of Complex between Balk's central and eastern internal funnels. Fig. 13A, Secs. 2 and 3. Fig. 13B, Sec. 1. 8. All magnetic anomalies, except the one in the central area, associated with border rocks. Exception considered to originate beneath the Complex. Fig. 13A, Secs. 1 and 2.

still only a fraction of the observed anomaly can be accounted for. Unless the polarization of the slab is dependent upon permanent magnetic effects, the anomaly must originate from below the Complex and must be related to an anomalous concentration of magnetite in the host rock. This feature could be of the same origin as the large anomalies of several thousand gammas found outside the Complex. An estimation of the depth to the top of the anomalous body, using the one-half slope method (Peters, 1949) along a north-south profile through the center of the anomaly, is 0.3 mile, thus corroborating the gravimetric estimate of 0.35 mile. This magnetic estimate should, however, be construed only as confirming the order of magnitude of the thickness. The paucity of the data and the nature of the assumptions involved in making this estimate prohibit the placing of great reliability on any single estimate.

RECAPITULATION OF GEOLOGICAL AND GEOPHYSICAL RESULTS

The authors fully realize the ambiguity of gravity and magnetic data. Nevertheless, as they are in the most favorable position to review and consider all the data, it is their responsibility to synthesize the geophysical and geological results. The conclusions, although presented uniquely, are not necessarily so. However, the distinctiveness of the gravity and magnetic anomalies, especially when abetted by the determination of densities and susceptibilities, does significantly facilitate the problem of interpretation.

The principal results of Balk's structural investigations, Shand's petrological studies, and the authors' geophysical surveys are summarized in Table 4.

On the whole, the geological and geophysical data correlate, with one marked exception. There is no geophysical evidence for a magma pipe in the area of Balk's central funnel, which Shand believes is the primary source of the rocks forming the Complex. It is paradoxical that the two less well-developed structural funnels described by Balk's lineation studies should be characterized by pronounced gravity anomalies which suggest the presence of feeder

pipes, but the most perfectly outlined funnel has no marked geophysical counterpart.

The dips mapped in the funnels by Balk appear to hold a clue as to why the central funnel area has no vertical extent. From the structural map (Fig. 13B) and section (Fig. 13B, Sec. 1) it is seen that, whereas in the central funnel the angles of dip get progressively less toward the center, those in the eastern funnel are much steeper and show no tendency to flatten in the center. To show this point in detail, the dips of the lineations from Balk's original structural map are plotted and contoured (Fig. 14). Over the central area the contours change in dip from 60° to 20° toward the center of the structure. In other areas such perfectly systematically arranged contours can be constructed only locally. It does appear significant, though, that at the center of the primary gravity "high" in the eastern olivine pyroxenitic zone, there is a suggestion of a reversed relationship, with dips increasing from 60° to 90° as the center is approached. Also, between this area and the central area there is a belt in which the foliation is essentially vertical. The data are confused, and no specific relationship is evident over the secondary pipe in the western area.

This difference in the funnel structure of the olivine pyroxenitic area and the poikilitic hornblende area is regarded as most significant. In discussing basic intrusives in general, Balk (1937) regards the increase in dip toward the center of the intrusive as a characteristic structural feature. The structural pattern in the central poikilitic hornblende area of the Cortlandt Complex is the reverse of this and is, in fact, an inverted picture of the foliation pattern associated with domelike intrusives where dips are outward rather than inward toward the center, with the lowest dips of foliation in the central area. Since flow structures within igneous rocks are the result of viscous drag and reflect the presence of boundaries between materials of different viscosity, this structural pattern of an inverted dome indicates that the central portion of the Cortlandt Complex was emplaced downward rather than upward. Therefore, it presumably has no great thickness.

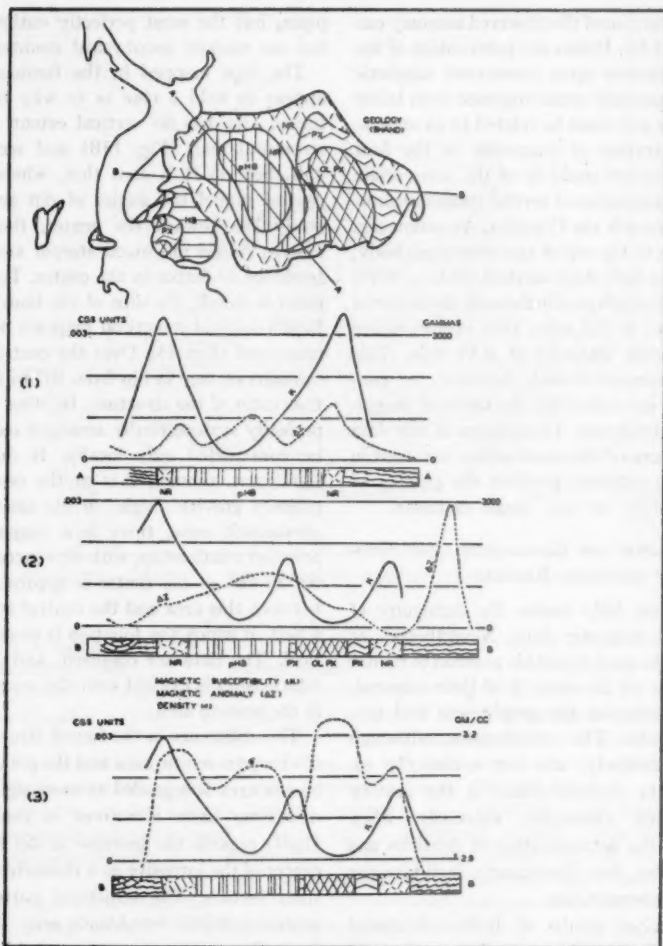


FIG. 13A

FIGURE 13.—COMPARATIVE GEOLOGIC AND GEOPHYSICAL PROFILES

CONCLUSIONS

From a consideration of all the evidence on hand it appears that:

(1) A series of magmatic pipes are located along a line from Rosetown to Dickerson Hill (Fig. 15). This line probably marks an ancient tensional fracture trending approximately east-west.

(2) The pipes increase in size from a 0.1 mile diameter at Rosetown to 2.4 miles at Dickerson Hill.

(3) The material in all the pipes is basic, probably pyroxenite, because a density of 3.1 is required to explain the gravity anomalies.

(4) A relatively thin sheet of igneous rocks is located between the two principal pipes and consists of norite with poikilitic hornblende.

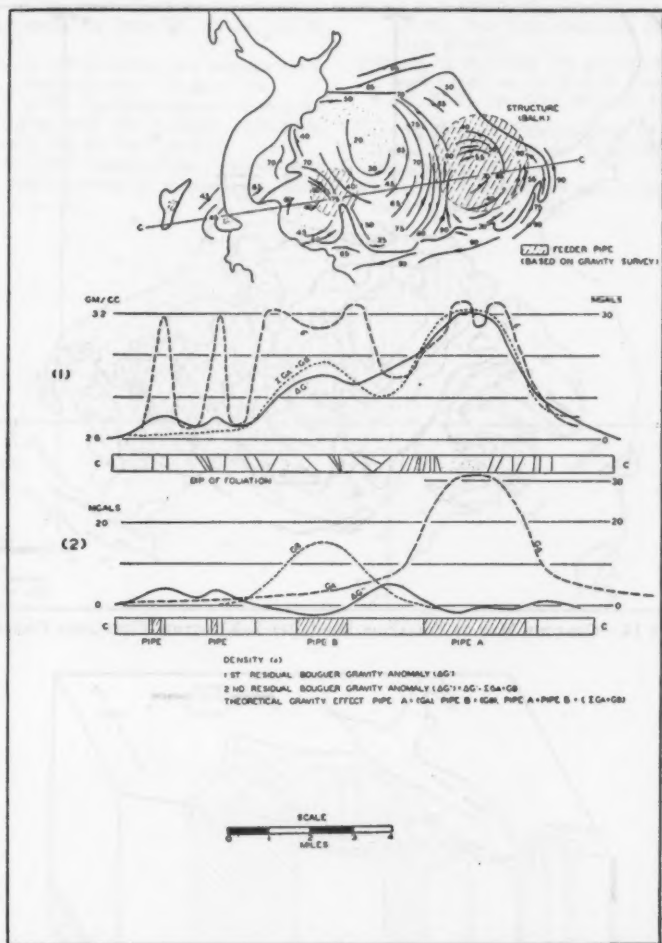


FIG. 13B

Its structure shows that it was emplaced downward. This could have resulted from:

- Subsidence during emplacement resulting from the removal of magmatic material at depth,
- Subsidence during emplacement resulting from regional tectonic forces (Bucher, 1948), or,
- Gravity filling of pre-existent surface depressions by extruded material.

REFERENCES CITED

- Balk, R. (1927) *Die primäre struktur des noritmassivs von Peekskill am Hudson, nördlich New York*, Neues Jahrb. Min., Beilageband 57, pp. 249-303.
- (1937) *Structural behavior of igneous rocks*, Geol. Soc. Am., Mem. 5.
- Bucher, W. H. (1948) *Guidebook of excursions*, Geol. Soc. Am., 61st Ann. meeting, p. 33-50.
- Butler, J. W. (1936) *Origin of the emery deposits near Peekskill, New York*, Am. Mineral., vol. 21, p. 537-574.

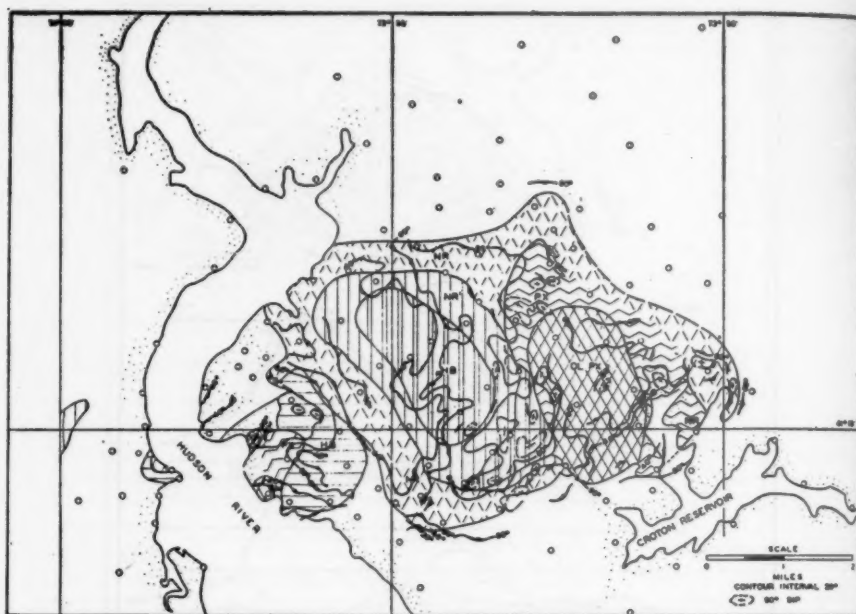


FIGURE 14.—CONTOUR MAP OF FOLIATION DIP (after Balk) WITHIN CORTLANDT COMPLEX

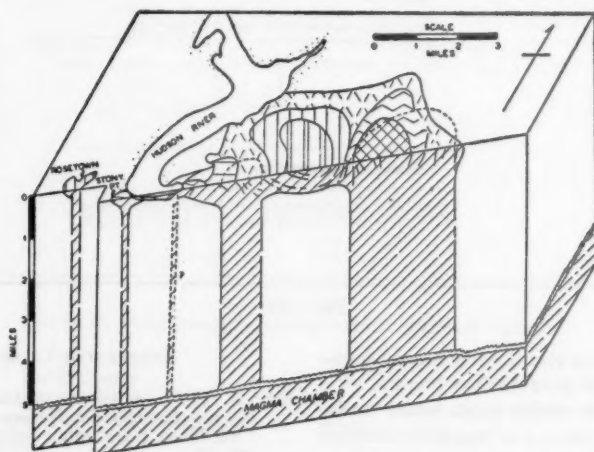


FIGURE 15.—BLOCK DIAGRAM SHOWING PROPOSED SUBSURFACE STRUCTURE OF CORTLANDT COMPLEX

Dana, J. D. (1880) *On the geological relations of the limestone belts of Westchester Co., N. Y.*, (4). *Hornblende, Augitic, and other associated rocks . . .*, *Am. Jour. Sci.*, 3d ser., vol. 20, p. 194-220. (Reprinted under different title in

Geol. Mag., 2d ser., vol. 8, p. 59-65, 110-119, 162-171).

Geyer, R. A. (1951) *Geomagnetic survey of a portion of southeastern New York*, *Geophysics*, vol. 16, no. 2, p. 252-257.

- Kemp, J. F. (1888) *On the Rosetown extension of the Cortlandt series*, Am. Jour. Sci., 3d ser., vol. 36, p. 247-53.
- Nettleton, L. L. (1942) *Gravity and magnetic calculations*, Geophysics, vol. 7, no. 3, p. 115.
- Peters, L. J. (1949) *The direct approach to magnetic interpretation and its practical application*, Geophysics, vol. 14, no. 3, p. 310.
- Rogers, G. S. (1911) *Geology of the Cortlandt series and its emery deposits*, N. Y. Acad. Sci., Ann., vol. 21, p. 11-86.
- Shand, S. J. (1942) *Phase petrology in the Cortlandt complex, New York*, Geol. Soc. Am., Bull., vol. 53, p. 409-428.
- Williams, G. H. (1886) *The peridotites of the "Cortlandt series" on the Hudson River near Peekskill, N. Y.*, Am. Jour. Sci., vol. 31, p. 26-41.
- GRAVITY METER EXPLORATION CO., HOUSTON, TEXAS; UNIVERSITY OF WISCONSIN, MADISON, WISCONSIN
- MANUSCRIPT RECEIVED BY THE SECRETARY OF THE SOCIETY, MARCH 9, 1951

APPENDIX 1.—BOUGUER REDUCTION OF GRAVITY OBSERVATIONS

Area: Cortlandt		State: New York		Inst.: Humble		Obs.: Woollard		Comp.: Woollard Steenland	
Sta.	Lat., N.	Long., W.	Elevation (1)	Obs. G. 980.†	Theo. G. (2) 980.†	El. & Boug. Cor.	Comp. G. 980.†	Boug. Anomaly Mgals.	
(16 June 1946)									
1	41-07.8	73-55.5	165	.2638	.2812	.0098	.2714	-7.6	
2	41-10.4	73-59.85	122	.2624	.2851	.0073	.2778	-15.4	
3	41-12.13	73-59.56	206	.2509	.2877	.0124	.2753	-24.4	
4	41-10.75	74-02.0	496	.2305	.2855	.0298	.2557	-25.2	
5	41-13.35	73-59.12	88	.2597	.2895	.0053	.2842	-24.5	
6	41-14.73	73-58.8	94	.2659	.2916	.0056	.2860	-20.1	
7	41-13.9	74-06.7	822	.2146	.2903	.0493	.2410	-26.4	
8	41-18.0	73-59.18	29	.2704	.2964	.0017	.2947	-24.3	
9	41-16.83	73-57.73	28	.2693	.2946	.0017	.2929	-23.6	
10	41-19.07	73-55.85	172	.2663	.2979	.0103	.2876	-21.3	
11	41-17.49	73-53.32	355	.2675	.2956	.0213	.2743	-6.8	
12	41-18.83	73-52.0	316	.2689	.2976	.0190	.2786	-9.7	
13	41-19.60	73-50.30	434	.2627	.2988	.0260	.2728	-10.1	
14	41-20.22	73-47.50	435	.2689	.2997	.0261	.2736	-4.7	
15	41-18.20	73-48.52	548	.2588	.2967	.0329	.2638	-5.0	
16	41-16.75	73-47.33	507	.2661	.2945	.0304	.2641	+2.0	
17	41-17.48	73-49.98	305	.2705	.2956	.0183	.2773	-6.8	
18	41-17.54	73-52.10	400	.2629	.2957	.0240	.2717	-8.8	
(17 June 1946)									
19	41-17.89	73-56.18	6	.2753	.2962	.0004	.2958	-20.5	
20	41-16.28	73-55.75	110	.2785	.2939	.0065	.2873	-8.9	
21	41-16.82	73-55.73	144	.2735	.2948	.0066	.2862	-12.7	
22	41-16.03	73-56.47	10	.2778	.2935	.0005	.2929	-15.1	
23	41-15.80	73-56.93	134	.2689	.2932	.0080	.2852	-16.3	
24	41-15.33	73-57.45	62	.2720	.2925	.0037	.2888	-16.8	
25	41-14.95	73-57.83	15	.2758	.2919	.0009	.2910	-15.2	
26	41-14.93	73-57.17	24	.2831	.2919	.0014	.2905	-7.4	
27	41-15.30	73-56.57	106	.2776	.2924	.0064	.2860	-8.4	
28	41-14.95	73-55.90	108	.2836	.2919	.0065	.2854	-1.5	
29	41-16.50	73-55.48	136	.2819	.2927	.0082	.2845	-2.6	
30	41-16.68	73-55.17	166	.2810	.2929	.0100	.2829	-1.9	

- 7.2

-0100

2945

2845

2845

2845

2845

2845

2845

2845

2845

2845

2845

28 41-14.95 73-55.90 108 .2836 .2919 .0065
 29 41-16.50 73-55.48 136 .2819 .2927 .0068
 30 41-15.88 73-55.17 166 .2810 .2969 .0100

31	41-16.69	73-55.28	167	.2773	.2945	.0100	.2845	- 7.2
32	41-17.25	73-55.20	201	.2702	.2953	.0121	.2832	- 8.9
33	41-17.10	73-54.70	353	.2650	.2951	.0212	.2739	- 2.4
34	41-16.80	73-54.20	296	.2744	.2946	.0178	.2768	+ 4.0
35	41-16.48	73-53.70	329	.2785	.2942	.0197	.2745	+ 5.7
36	41-16.20	73-53.85	395	.2757	.2937	.0237	.2700	+ 3.9
37	41-16.97	73-54.45	385	.2742	.2934	.0231	.2703	+ 0.7
38	41-15.80	73-54.75	335	.2737	.2931	.0201	.2730	+ 0.2
39	41-15.12	73-54.69	219	.2804	.2921	.0131	.2790	+ 8.7
40	41-14.60	73-54.45	234	.2776	.2914	.0140	.2774	+ 10.1
41	41-15.45	73-53.58	265	.2854	.2926	.0159	.2767	+ 20.2
42	41-15.65	73-53.04	264	.2872	.2929	.0158	.2771	+ 14.4
43	41-16.07	73-52.48	312	.2951	.2936	.0187	.2749	+ 2.5
44	41-16.60	73-51.92	454	.2815	.2943	.0272	.2671	
45	41-17.13	73-52.18	467	.2896	.2951	.0280	.2671	

(18 June 1946)

46	41-14.15	73-54.9	141	.2762	.2907	.0085	.2822	- 6.0
47	41-14.0	73-55.5	95	.2753	.2905	.0057	.2848	- 9.5
48	41-14.15	73-55.93	100	.2751	.2907	.0060	.2847	- 9.6
49	41-14.38	73-56.25	106	.2771	.2910	.0064	.2846	- 7.5
50	41-14.20	73-56.58	10	.2783	.2908	.0006	.2902	- 11.9
51	41-14.66	73-56.65	87	.2792	.2914	.0052	.2862	- 7.0
52	41-14.39	73-56.92	86	.2778	.2910	.0052	.2858	- 8.0
53	41-14.29	73-56.90	108	.2744	.2909	.0065	.2844	- 10.0
54	41-14.57	73-55.68	85	.2817	.2913	.0051	.2862	- 4.6
55	41-14.34	73-55.20	80	.2794	.2910	.0048	.2862	- 6.8
56	41-14.23	73-54.60	143	.2792	.2908	.0086	.2852	- 3.0
57	41-14.85	73-54.25	238	.2815	.2917	.0139	.2778	+ 3.7
58	41-15.20	73-53.98	255	.2834	.2922	.0153	.2769	+ 6.5

.0654
 .0665
 .0688
 .0695
 .0685

.2836
 .2819
 .2810

28
 29
 30

Sta.	Lat., N. ° ' "	Long., W. ° ' "	Eleva- tion (1)	Obs., G. 980.†	Theo. G. (2) 980.†	El. & Boug. Cor.	Comp. G. 980.†	Boug. Anamol. Mgal.
59	41-16.03	73-51.71	360	.2942	.2935	.0216	.2719	+22.3
60	41-16.03	73-51.20	340	.2951	.2935	.0204	.2731	+22.0
61	41-16.68	73-51.40	524	.2742	.2945	.0314	.2631	+11.1
62	41-17.50	73-54.40	354	.2627	.2957	.0212	.2745	-11.8
63	41-17.00	73-53.72	414	.2659	.2950	.0248	.2702	-4.3
64	41-17.80	73-53.35	361	.2640	.2961	.0217	.2744	-10.4
65	41-17.53	73-52.78	380	.2681	.2957	.0228	.2729	-4.8
66	41-17.32	73-52.54	495	.2649	.2954	.0296	.2658	-0.9
67	41-16.92	73-52.57	551	.2682	.2948	.0331	.2617	+6.5
68	41-17.28	73-51.09	336	.2675	.2953	.0202	.2751	-7.6
69	41-16.90	73-50.70	488	.2675	.2948	.0293	.2655	+2.0
70	41-16.70	73-50.20	280	.2808	.2945	.0168	.2777	+3.1
71	41-16.68	73-49.28	491	.2666	.2945	.0295	.2650	+1.6
72	41-15.47	73-48.78	446	.2741	.2926	.0268	.2658	+8.3
73	41-15.50	73-48.65	408	.2782	.2927	.0245	.2682	+10.0
74	41-15.62	73-50.27	252	.2939	.2929	.0151	.2778	+16.1
75	41-15.46	73-50.92	217	.3056	.2926	.0130	.2796	+26.0
76	41-15.50	73-51.30	270	.3036	.2927	.0162	.2765	+27.1
77	41-14.53	73-51.00	225	.2932	.2912	.0135	.2777	+15.5
78	41-14.27	73-51.16	295	.2854	.2909	.0177	.2732	+12.2
79	41-12.72	73-53.84	120	.2739	.2886	.0072	.2614	-7.5
(19 June 1946)								
80	41-10.50	73-52.12	65	.2729	.2853	.0051	.2802	-7.4
81	41-22.46	73-49.12	523	.2634	.2882	.0314	.2568	+6.6
82	41-13.65	73-45.95	207	.2835	.2899	.0124	.2775	+6.3
83	41-14.05	73-47.35	208	.2870	.2905	.0125	.2780	+9.7
84	41-14.87	73-49.22	215	.2875	.2917	.0129	.2788	+2.2
85	41-14.68	73-50.43	253	.2862	.2912	.0168	.2760	+2.2

83	41-14.05	73-47.35	208	.2870	.2905	.0125	.2780	+ 9.0
84	41-14.87	73-49.22	215	.2875	.2917	.0129	.2788	+ 9.7
85	41-14.53	73-50.43	253	.2882	.2912	.0152	.2768	+ 8.2
86	41-14.95	73-50.41	219	.2963	.2919	.0131	.2788	+ 17.4
87	41-15.04	73-51.30	204	.3033	.2920	.0122	.2798	+ 23.5
88	41-14.15	73-51.75	226	.2977	.2907	.0136	.2771	+ 10.6
89	41-14.60	73-52.35	283	.2902	.2914	.0170	.2744	+ 15.8
90	41-14.10	73-53.28	218	.2797	.2906	.0131	.2775	+ 2.2
91	41-14.48	73-52.88	268	.2856	.2912	.0161	.2751	+ 10.5
92	41-13.65	73-52.60	488	.2829	.2899	.0293	.0606	+ 2.3
93	41-13.95	73-54.20	141	.2788	.2904	.0085	.2819	- 3.1
94	41-13.75	73-54.87	120	.2737	.2901	.0072	.2829	- 9.2
95	41-16.7	73-56.3	21	.2792	.2945	.0013	.2932	- 14.0
96	41-16.22	73-53.10	297	.2869	.2938	.0178	.2760	+ 10.9
97	41-15.29	73-52.27	300	.2869	.2924	.0180	.2744	+ 22.9
98	41-14.95	73-53.20	273	.2870	.2919	.0164	.2755	+ 11.5
99	41-14.37	73-53.90	186	.2824	.2910	.0112	.2798	+ 2.6
100	41-14.75	73-53.45	246	.2852	.2916	10148	.2768	+ 8.4
(16 Sept. 1947)	(Use Frost Meter)							
101	41-21.26	73-40.30	220	.2974	.3013	.0132	.2881	+ 9.3
102	41-19.69	73-41.62	245	.2926	.2988	.0147	.2841	+ 8.5
103	41-19.20	73-44.80	416	.2771	.2980	.0250	.2730	+ 4.1
104	41-18.27	73-46.43	533	.2651	.2967	.0320	.2647	+ 0.4
105	41-17.18	73-46.22	400	.2742	.2951	.0240	.2711	+ 3.1
106	41-17.57	73-47.91	506	.2622	.2957	.0304	.2653	- 3.1
107	41-18.98	73-47.55	625	.2574	.2978	.0375	.2603	- 2.9
108	41-19.99	73-48.70	436	.2663	.2994	.0262	.2732	- 6.9
109	41-18.70	73-50.00	550	.2518	.2974	.0331	.2644	- 12.6
110	41-20.27	73-50.58	396	.2670	.2998	.0232	.2766	- 9.6
111	41-19.54	73-51.63	464	.2589	.2987	.0278	.2709	- 12.0
112	41-18.27	73-51.43	452	.2587	.2968	.0271	.2697	- 11.0
113	41-19.49	73-53.00	139	.2748	.2986	.0083	.2903	- 15.5

Sta.	Lat., N. O ° ' "	Long., W. O ° ' "	Eleva- tion (1)	Obs., G. 980. +	Theo., G. (2) 980. +	El., & Boug. Cor.	Comp., G. 980. +	Boug. Anomaly Mgal.
114	41-18.33	73-53.42	440	.2576	.2969	.0264	.2705	-12.9
115	41-18.67	73-54.46	125	.2705	.2974	.0275	.2899	-19.4
116	41-17.89	73-54.37	359	.2601	.2963	.0215	.2748	-14.7
117	41-16.20	73-57.04	70	.2705	.2937	.0042	.2895	-19.0
118	41-15.88	73-57.39	112	.2682	.2933	.0067	.2866	-18.4
119	41-15.66	73-57.50	100	.2896	.2929	.0060	.2869	-17.3
120	41-15.67	73-57.22	108	.2699	.2928	.0065	.2863	-16.4
121	41-15.50	73-57.93	25	.2723	.2927	.0015	.2912	-18.9
122	41-15.06	73-57.46	35	.2759	.2920	.0021	.2899	-14.0
123	41-15.45	73-56.98	23	.2775	.2926	.0014	.2912	-13.7
124	41-15.70	73-56.35	43	.2806	.2930	.0026	.2904	-9.8
125	41-15.40	73-56.09	102	.2821	.2925	.0061	.2864	-4.3
126	41-14.95	73-56.25	100	.2814	.2919	.0060	.2859	-4.5
127	41-13.20	73-54.65	141	.2719	.2893	.0085	.2808	-8.9
128	41-12.11	73-51.93	360	.2643	.2876	.0216	.2660	-1.7
129	41-12.86	73-51.48	312	.2719	.2888	.0187	.2701	+1.8
130	41-8.45	73-50.75	246	.2794	.2896	.0148	.2748	+4.6
131	41-13.93	73-49.86	210	.2839	.2904	.0126	.2778	+6.1
132	41-14.35	73-48.80	249	.2829	.2910	.0149	.2761	+5.8
133	41-14.06	73-48.02	220	.2843	.2905	.0132	.2773	+7.0
134	41-14.92	73-47.34	387	.2773	.2917	.0232	.2695	+8.8
(17 Sept. 1947)		(Use Kumble)						
135	41-01.75	73-57.40	195	.2558	.2722	.0117	.2605	-4.7
136	41-12.04	73-57.88	18	.2640	.2875	.0011	.2864	-22.4
137	41-12.85	73-58.03	10	.2657	.2887	.0006	.2881	-22.4
138	41-13.44	73-57.61	8	.2672	.2896	.0005	.2891	-21.9
139	41-13.93	73-56.67	15	.2675	.2904	.0009	.2895	-22.0
140	41-14.23	73-58.58	11	.2707	.2904	.0007	.2903	-19.4
141	41-14.43	73-58.21	70	.2691	.2911	.0042	.2895	-17.6

APPENDIX

1099

139 41-13.93 73-59.67 15
 140 41-14.23 73-59.59 11
 141 41-14.43 73-59.21 70

142	41-14.45	73-59.44	115	.2652	.2911	.0069	.2842	-19.0
143	41-14.52	73-59.34	135	.2641	.2912	.0081	.2831	-19.0
144	41-14.27	73-59.09	65	.2645	.2909	.0039	.2870	-22.5
145	41-14.23	73-59.81	243	.2656	.2908	.0146	.2762	-20.6
146	41-14.79	71-00.06	255	.2664	.2916	.0159	.2757	-19.3
147	41-14.79	73-59.28	150	.2622	.2916	.0090	.2826	-20.4
148	41-15.06	73-59.70	8	.2707	.2920	.0005	.2915	-20.8
149	41-15.52	73-58.70	12	.2702	.2927	.0007	.2920	-21.8
150	41-16.80	73-58.50	35	.2686	.2937	.0021	.2916	-23.0
151	41-17.60	73-57.65	120	.2657	.2958	.0072	.2886	-22.9
152	41-17.81	73-57.02	14	.2735	.2961	.0008	.2953	-21.8
153	41-18.35	73-55.49	22	.2767	.2969	.0013	.2956	-18.9
154	41-13.73	73-51.65	245	.2815	.2901	.0147	.2754	+ 6.1
155	41-13.20	73-49.93	295	.2762	.2893	.0177	.2716	+ 4.6
156	41-12.72	73-49.50	362	.2718	.2886	.0217	.2689	+ 4.9
157	41-11.84	73-50.70	357	.2664	.2872	.0214	.2658	+ 0.6
158	41-12.01	73-49.69	459	.2647	.2875	.0276	.2600	+ 4.7
159	41-12.97	73-48.32	460	.2700	.2889	.0276	.2613	+ 8.7
160	41-13.27	73-47.50	292	.2624	.2894	.0175	.2719	+10.5
161	41-13.10	73-46.31	221	.2672	.2891	.0133	.2768	+11.4
162	41-15.62	73-47.86	495	.2700	.2929	.0297	.2632	+ 6.8

(26 Oct. 1947) (Use Frost)

163	41-08.37	73-49.28	238	.2765	.2819	.0143	.2676	+ 6.9
164	41-09.63	73-50.24	376	.2641	.2838	.0226	.2612	+ 2.9
165	41-11.00	73-51.22	339	.2662	.2859	.0203	.2656	+ 0.6

Sta.	Lat., N. o ' "	Long., W. o ' "	Eleva- tion (1)	Obs. G. 980.†	Theo. G. (2) 980.†	El. & Boug. Cor.	Comp. G. 980.†	Boug. Anomaly Mgal.
166	41-10.52	73-49.80	497	.2601	.2852	.0292	.2560	+ 4.1
167	41-11.18	73-48.40	335	.2740	.2862	.0201	.2661	+ 7.9
168	41-11.52	73-47.10	487	.2684	.2867	.0292	.2575	+10.9
169	41-12.19	73-46.58	383	.2767	.2877	.0230	.2647	+12.0
170	41-12.33	73-45.27	455	.2751	.2879	.0273	.2606	+14.5
171	41-14.51	73-45.34	240	.2883	.2912	.0144	.2769	+11.5
172	41-15.20	74-44.50	295	.2902	.2922	.0135	.2787	+11.5
173	41-15.57	73-45.43	505	.2742	.2928	.0303	.2625	+11.7
174	41-16.20	73-45.11	379	.2813	.2938	.0227	.2711	+10.2
175	41-16.08	73-46.50	505	.2699	.2936	.0303	.2633	+ 6.6
176	41-15.24	73-46.39	638	.2641	.2923	.0380	.2540	+10.1
177	41-13.54	73-47.78	300	.2804	.2897	.0180	.2717	+ 8.7
178	41-11.97	73-48.41	497	.2662	.2874	.0298	.2576	+ 8.6
179	41-10.83	73-45.97	450	.2736	.2857	.0270	.2587	+14.9
180	41-12.75	73-42.85	397	.2804	.2886	.0238	.2648	+15.6
181	41-13.20	73-41.05	398	.2831	.2892	.0239	.2653	+17.8
182	41-11.68	73-40.65	480	.2786	.2872	.0288	.2584	+20.2
183	41-11.40	73-43.85	360	.2827	.2865	.0216	.2649	+17.8
184	41-10.17	73-45.49	421	.2761	.2847	.0253	.2594	+16.7
185	41-08.91	73-46.58	424	.2736	.2828	.0254	.2574	+16.2

(1) In feet above Mean Sea Level.

(2) From International Formula.

Area
Sta.1
2
3
4
5
6
7
8
9
10
11
12
13
14
15
16
17
18
1919
20
21
22
23
24
25
26
27
28
29
30
31
32
33
34
35
36
37
38
39
40
41
42

APPENDIX 2.—REDUCTION OF MAGNETIC OBSERVATIONS

Area: Cortland State: New York Inst.: Askania Obs.: Steenland
Comp.:

Sta.	Obs. scale	Obs. Gamma	Temp. Corr.	Diurnal Corr.	Base Corr.	Tare	Rel. Sta. 1	Lat. Corr.	Magnetic Anomaly
16 June 1946, Mgr. #1, S. V. = 30 gammas/scale div.									
1	13.25	398	14	-78	0	--	334		
2	29.65	890	26	-75	-1	--	840		
3	7.7	231	46	-77	-2	--	198	-42	156
4	-2.0	-60	50	-79	-3	--	-92		
5	14.0	420	58	-84	-4	--	390	-47	343
6	13.0	390	62	-85	-5	--	362	-56	306
7	53.0	1590	69	-93	-6	--	1560		
8	17.1	513	70	-107	-7	--	469	-79	390
9	6.0	180	65	-114	-8	--	123	-66	57
10	21.6	648	65	-133	-9	--	571	-74	497
11	1.05	32	58	-141	-10	--	-61	-55	-116
12	13.7	411	49	-150	-11	--	299	-58	241
13	19.8	594	46	-147	-11	--	482	-58	424
14	18.5	555	42	-142	-12	--	443	-51	392
15	11.5	345	41	-142	-13	--	231	-41	190
16	7.7	231	38	-144	-13	--	112	-27	85
17	10.2	306	38	-149	-14	--	181	-42	139
18	4.7	141	32	-150	-15	--	8	-50	-42
18	16.3	489	22	-161	-16	--	334		
17 June 1946, Mgr. #1, S. V. = 30 gammas/scale div.									
19	12.75	382	-24	-125	0	-1	232	-57	165
20	23.2	696	-6	-122	-1	-1	564	-55	509
21	31.6	948	-2	-120	-2	-1	823	-58	765
22	27.9	837	2	-118	-3	-1	717	-56	661
23	7.0	210	11	-115	-3	-1	102	-56	46
24	6.1	243	23	-111	-4	-1	150	-54	96
25	4.9	147	30	-106	-5	-1	65	-53	12
26	16.0	480	40	-98	-6	-1	415	-51	364
27	16.3	489	49	-91	-7	-1	439	-52	387
28	-1.0	-30	48	-89	-7	-1	-79	-46	-125
29	2.0	60	46	-87	-8	-1	10	-48	-38
30	33.4	1002	48	-86	-9	-1	954	-49	905
31	17.4	522	52	-91	-12	-1	470	-56	414
33	13.55	406	52	-88	-14	-1	365	-57	298
34	23.2	696	50	-88	-14	-1	643	-53	590
35	42.15	1264	54	-87	-15	-1	1215	-49	1166
36	46.5	1395	57	-89	-16	-1	1346	-47	1299
37	28.5	855	61	-90	-16	-1	809	-48	761
38	35.8	1074	57	-91	-17	-1	1022	-48	974
39	14.0	420	54	-82	-17	-1	364	-43	321
40	28.8	864	50	-97	-18	-1	798	-39	759
41	34.1	1023	49	-100	-20	-1	951	-41	910

Sta.	Obs. scale	Obs. gamma	Temp. Corr.	Diurnal Corr.	Base Corr.	Tare	Rel. Sta. 1	Lat. Corr.	Magnetic Anomaly
42	43.9	1317	48	-103	-20	-1	1241	-42	1199
43	37.1	1113	47	-103	-21	-1	1035	-42	993
44	22.6	678	45	-102	-22	-1	598	-43	555
45	57.1	1713	40	-102	-22	-1	1628	-45	1583
11*	1.0	30	38	-105	-23	-1	-61		
19*	11.0	330	33	-106	-24	-1	232		
18 June 1946, Mgr. #1, S. V. = 30 gammas/scale div.									
46	6.3	189	26	-112	0	-2	101	-38	63
47	7.15	214	32	-116	-1	-2	127	-39	88
48	7.6	228	35	-116	-1	-2	144	-42	102
49	56.6	1098	38	-116	-1	-2	1017	-44	973
50	12.8	384	38	-115	-1	-2	304	-44	260
51	26.15	784	38	-115	-1	-2	704	-47	657
52	21.2	636	39	-115	-2	-2	556	-47	509
53	27.4	822	38	-114	-2	-2	792	-46	696
54	47.65	1430	38	-114	-2	-2	1350	-44	1306
55	0.2	6	40	-114	-2	-2	-72	-40	-112
56	21.4	642	40	-113	-2	-2	565	-37	528
57	29.9	897	41	-113	-2	-2	821	-40	781
58	23.6	708	46	-113	-3	-2	636	-41	595
59	12.3	369	42	-111	-3	-2	295	-38	257
60	17.7	531	44	-109	-3	-2	461	-37	424
61	19.8	594	46	-107	-3	-2	528	-42	486
11*	0.1	3	47	-106	-3	-2	-61		
62	4.8	144	46	-110	-4	-2	74	-58	16
63	9.6	288	45	-109	-4	-2	218	-53	165
64	3.8	114	45	-110	-4	-2	43	-57	-14
65	27.9	834	40	-111	-4	-2	757	-53	704
66	42.2	1266	25	-113	-4	-2	1172	-50	1122
67	16.9	507	10	-116	-4	-2	395	-48	347
68	7.45	224	2	-121	-5	-2	98	-45	53
69	10.0	300	3	-120	-5	-2	176	-41	135
70	-2.0	-60	3	-123	-5	-2	-187	-37	-224
71	9.8	294	5	-131	-5	-2	161	-34	127
72	approximately 3000								
73	3.1	93	5	-145	-5	-2	-54	-27	-81
74	-0.2	-6	8	-148	-5	-2	-53	-31	-184
75	20.55	616	18	-152	-6	-2	474	-33	341
76	26.4	792	22	-156	-6	-2	650	-34	616
77	18.3	549	17	-158	-6	-2	400	-26	374
78	13.7	411	16	-159	-6	-2	260	-24	236
79	11.0	330	19	-163	-7	-2	177	-25	152
46*	8.55	256	19	-165	-7	-2	101		
19 June 1946, Mgr. #1, Scale value = 30 gammas/scale div.									
80	23.15	694	-31	-111	0	4	556	-16	540
81	9.6	288	-26	-111	-2	4	153	-6	147
82	5.8	174	-14	-113	-3	4	48	-2	46
83	4.65	140	1	-113	-4	4	28	-9	19
84	58.3	1749	1	-114	-5	4	1635	-22	1613
85	9.0	270	9	-112	-7	4	164	-24	140
86	18.5	555	15	-112	-0	4	454	-27	427
87	11.6	348	14	-107	-10	4	249	-31	218

Sta.	Obs. scale	Obs. gamma	Temp. Corr.	Diurnal Corr.	Base Corr.	Tare	Rel. Sta. 1	Lat. Corr.	Magnetic Anomaly
88	23.5	705	24	-102	-12	4	619	-27	592
89	37.7	1131	21	-99	-13	4	1044	-31	1013
90	24.5	735	18	-102	-14	4	641	-32	609
91	61.1	1833	16	-102	-16	4	1735	-33	1702
92	11.2	336	18	-104	-17	4	237	-26	211
93	36.6	1098	19	-106	-18	4	997	-34	963
94	17.8	534	26	-107	-19	4	438	-35	403
95	22.1	683	33	-108	-23	4	569	-59	510
11*	1.2	36	33	-109	-25	4	-61		
96	33.4	1002	39	-112	-27	4	906	-45	861
97	27.0	810	42	-129	-28	4	699	-35	664
98	22.4	672	40	-129	-30	4	557	-37	520
99	17.45	524	42	-128	-32	4	410	-36	374
100	33.3	999	40	-131	-33	4	879	-36	843
80*	23.1	693	41	-144	-38	4	556		
18 Sept. 1947, Mgr. #1, S. V. = 33.5 gammas/scale Div.									
101	77.0	2580	-54	-65	6	-2328	139		
102	77.3	2590	-54	-69	4	-2328	143		
103	app.	2850							
104	app.	3000							
105	77.9	2610	-17	-69	2	-2328	198	-36	162
16*	75.1	2517	-6	-72	1	-2328	112		
Reset latitude adjustment									
16*	25.7	861	-1	-74	0	-674	112		
106	30.2	1011	0	-76	-1	-674	260	-45	215
107	34.6	1159	2	-75	-1	-674	411	-53	358
108	34.3	1149	9	-76	-2	-674	406	-64	342
109	22.4	750	14	-77	-3	-674	10	-61	-51
110	41.1	1376	17	-77	-3	-674	639	-72	567
111	32.7	1095	21	-77	-4	-674	361	-71	290
112	29.0	971	24	-78	-5	-674	238	-63	175
113	32.9	1102	32	-79	-6	-674	375	-76	299
114	29.2	978	41	-81	-6	-674	258	-70	188
115	20.1	673	41	-81	-7	-674	-48	-78	-126
116	22.9	767	42	-81	-8	-674	46	-71	-25
117	27.8	931	50	-90	-12	-674	215	-69	146
118	29.0	971	50	-98	-13	-674	236	-68	168
119	24.3	808	55	-100	-14	-674	75	-67	8
120	26.6	898	64	-98	-15	-674	175	-66	109
121	14.6	489	70	-98	-16	-674	-228	-67	-395
122	20.4	683	78	-105	-17	-674	-35	-63	-98
123	21.3	714	78	-104	-18	-674	-4	-64	-68
124	35.2	1179	80	-101	-18	-674	466	-64	402
125	32.1	1075	81	-105	-19	-674	358	-60	298
126	79.2	2652	74	-106	-20	-674	1926	-58	1868
51*	42.4	1420	72	-110	-21	-674	687		
127	35.2	1213	65	-121	-22	-674	461	-40	421
128	25.8	864	58	-121	-23	-674	104	-24	80
129	11.5	385	56	-122	-23	-674	-378	-27	-405
130	21.8	730	51	-120	-24	-674	-17	-28	-45
131	80.0	2680	48	-117	-24	-674	1913	-28	1885
133	38.2	1280	46	-109	-25	-674	518	-27	491
134	38.7	1296	45	-106	-25	-674	536	-22	514
16*	26.2	878	40	-106	-26	-674	112		

Sta.	Obs. scale	Obs. gamma	Temp. Corr.	Diurnal Corr.	Base Corr.	Tare	Rel. Sta. 1	Lat. Corr.	Magnetic Anomaly
19 Sept. 1947, Mgr. #1, S. V. = 33.5 gammas/scale div.									
135	32.55	1091	-27	-70	8	-628	374		
136	26.0	871	-8	-68	7	-628	174	-44	130
137	34.1	1142	0	-68	7	-628	453	-51	402
138	32.2	1079	2	-68	7	-628	392	-54	338
139	23.1	774	10	-67	6	-628	95	-60	35
140	30.8	1032	16	-66	6	-628	358	-62	296
141	28.6	958	28	-69	6	-628	295	-62	233
142	30.1	1009	42	-69	5	-628	359	-62	297
143	23.0	770	42	-70	5	-628	119	-63	56
144	28.2	944	47	-70	5	-628	298	-64	234
145	40.8	1367	55	-72	4	-628	726	-66	660
146	45.5	1525	56	-73	4	-628	884	-70	814
147	26.4	884	62	-74	4	-628	248	-68	180
148	25.8	864	66	-73	4	-628	233	-67	166
149	27.5	921	74	-73	4	-628	298	-70	228
150	26.9	901	87	-80	2	-628	282	-74	208
151	31.4	1152	88	-80	2	-628	534	-79	455
152	31.5	1055	87	-85	1	-628	430	-80	350
153	10.8	362	89	-86	1	-628	-262	-77	-339
51*	39.4	1320	97	-85	0	-628	704		
154	25.0	838	90	-95	-1	-628	204	-53	171
155	24.1	807	87	-96	-2	-628	168	-24	144
156	18.8	630	88	-99	-2	-628	-11	-19	-30
157	18.9	633	87	-103	-2	-628	-13	-18	-31
158	66.1	2215	82	-103	-3	-628	1663	-15	1548
159	19.0	636	80	-101	-3	-628	-16	-16	-32
160	34.5	1156	74	-99	-3	-628	500	-14	486
161	50.1	1678	72	-98	-3	-628	1021	-10	1011
162	14.6	489	58	-98	-4	-628	-183	-31	214
16*	23.9	800	45	-101	-4	-628	112		
26 Oct. 1947, Mgr. #2, S. V. = 31.6 gammas/scale div.									
163	36.0	1138	-33	-61		-860	183		
164	36.4	1150	-16	-60		-860	214		
165	37.5	1185	1	-60		-860	266	-15	251
166	35.0	1106	7	-58		-860	195	-8	187
167	1.0	32	13	-57		-860	-872	-6	-878
168	63.8	2017	16	-57		-860	1116	-1	1115
169	34.6	1094	22	-57		-860	199	-4	195
170	37.4	1182	26	-58		-860	280	-1	289
171	36.0	1138	30	-59		-860	249	-16	233
172	38.7	1223	33	-59		-860	337	-17	320
173	39.0	1232	38	-60		-860	350	-23	327
174	54.8	1731	40	-62		-860	849	-27	822
175	27.0	853	41	-64		-860	-30	-30	-60
177	37.3	1179	49	-69		-860	299	-19	280
178	33.3	1052	49	-70		-860	171	-10	161
179	22.8	720	53	-72		-860	-199	4	195
180	25.9	818	56	-74		-860	-60		
184	34.1	1078	54	-77		-860	195	10	205
135*	40.0	1264	48	-78		-860	374		

*Reoccupation

CONTINENTAL SHELF SEDIMENTS OF SOUTHERN CALIFORNIA

BY K. O. EMERY

ABSTRACT

Sediments of the continental shelf near the cities of Santa Monica, San Pedro, and San Diego, California, were classified and charted in groups composed of authigenic, organic, residual, relict, and detrital types. Representatives of the first four groups occur only where they are not masked by the generally more rapidly deposited detrital sediments. The latter, taken alone, present a relatively simple gradation from coarse- to fine-grained in a seaward direction.

CONTENTS

TEXT	Page	ILLUSTRATIONS	Facing page
Introduction.....	1105	1. Sediment chart of three areas in California.....	1106
Results.....	1106		
Geological significance.....	1106		
References cited.....	1107		

INTRODUCTION

The shore line of southern California is bordered by a continental shelf whose width ranges between a quarter of a mile and 15 miles and averages 4 miles. The depth of its outer edge is 180 to 420 feet. Beyond the shelf is a succession of deep basins and troughs separated by islands and shallow banks. This irregular area, known as the continental borderland, is limited on the west by the continental slope, located 40 to 150 miles beyond the mainland shore line.

Studies have been made of the sediments in three of the widest zones of the shelf: Santa Monica Bay (Shepard and Macdonald, 1938), San Pedro Bay (Moore, 1951) and off San Diego (Emery, Butcher, Gould, and Shepard, 1952). The work was based on 200, 160, and 1660 samples, respectively, supplemented by 25 to 50 chart notations of bottom materials.

These and most other studies reveal a complex distribution of continental-shelf sediments in which there is a notable absence of progressive decrease of grain size with distance from shore. In a summary of the sediments on the East Asiatic continental shelf Shepard, Emery, and Gould (1949) showed that some of the

environmental factors responsible for irregular distribution of grain size are: bottom currents, exposure to large waves, near-by large river mouths, contiguous sand beaches, submarine basins and hills, abundance of calcareous organisms, recent explosive vulcanism, and presence of lag materials. Some of these factors cannot easily be determined for ancient sediments.

A different and perhaps sometimes more useful basis for examination of distribution of grain size is the type of sediment. In general, any shelf sediment belongs to one or more of five main groups: authigenic (glauconite and phosphorite), organic (Foraminifera and shells), residual (weathered from underlying rocks), relict (remnant from a different earlier environment—such as a now-submerged beach or dune), and detrital (presently supplied chiefly from adjacent river mouths, beaches, or sea cliffs). A variety of detrital sediment, rafted, is of only local significance. A new sediment chart of each of the three well-studied areas off California (Pl. 1) indicates in color each of the five groups of sediment. In most places small patches of sediment occupy spaces between the rocks and the cobbles.

RESULTS

At Santa Monica Bay several areas of rock bottom mark outcrops of Miocene shales and limestones. Organic sediment (shelly sand) was found at the edge of the shelf, in a rocky area atop the shelf, and in the bottom of a submarine canyon. The first two sites are typical for shells because in such places detrital sediments are either not deposited or are deposited so slowly that they do not mask the shell debris. All the other surface sediments appear to belong to the detrital group. A narrow belt of coarse sand borders the mountainous coast west of Santa Monica and possibly also the sea cliffs at the south end of the bay. This is followed by a broad belt of fine sand whose outer boundary is irregular because of topographic control on the south and possibly because of currents on the north. The next zone is one of sand-and-mud that in turn grades into mud beyond the edge of the shelf. Thus, taken by themselves, the detrital sediments exhibit a good gradation from coarse to fine in an offshore direction.

San Pedro Bay is characterized by a central area of Miocene shales and sandstones with smaller outcrops of Pliocene shales near the western shore and along the outer edge of the shelf. In patches between the Miocene rocks and in a peripheral area is a medium-grained brown sand that contains Early Pleistocene Foraminifera. This sand is believed to be derived from slight weathering of a poorly consolidated bed that elsewhere is buried beneath later sediments; thus, it belongs to the residual group. An olive-gray medium-grained sand surrounds the residual sand and also forms a large patch on the northeastern side of the shelf. Its location and its coarseness suggest that it was deposited as a beach or a blanket during a time of slightly lower sea level. It is termed a relict sediment. The remaining surface sediments are detrital, ranging from fine sand on most of the surface of the shelf, through sand-and-mud, to mud in the deeper and quieter water beyond the shelf. A similar gradation to mud exists in the protected water behind the breakwater east of San Pedro in the lee of the hills farther west.

The bottom topography and sediments off San Diego are more complex. Cretaceous sandstones and shales crop out along the west side

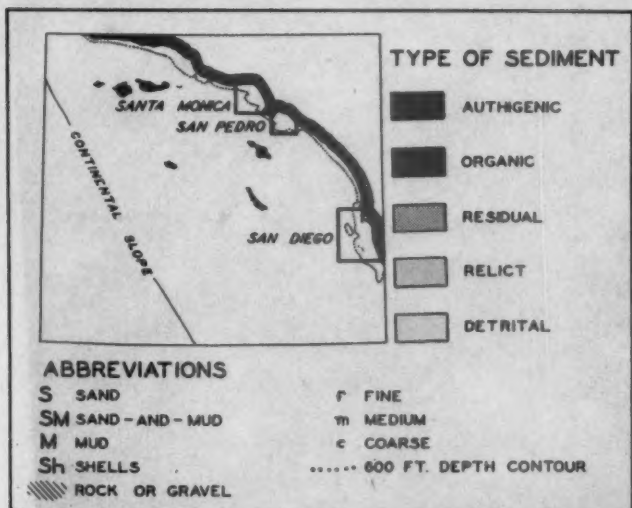
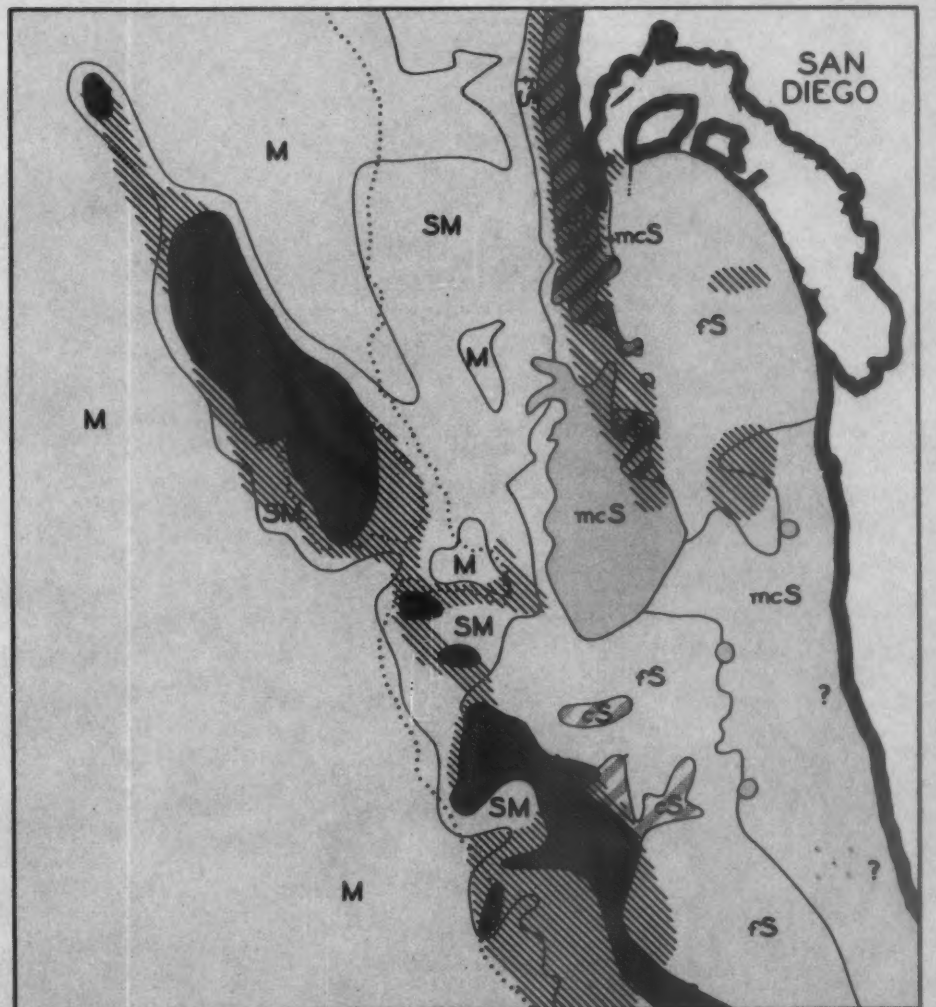
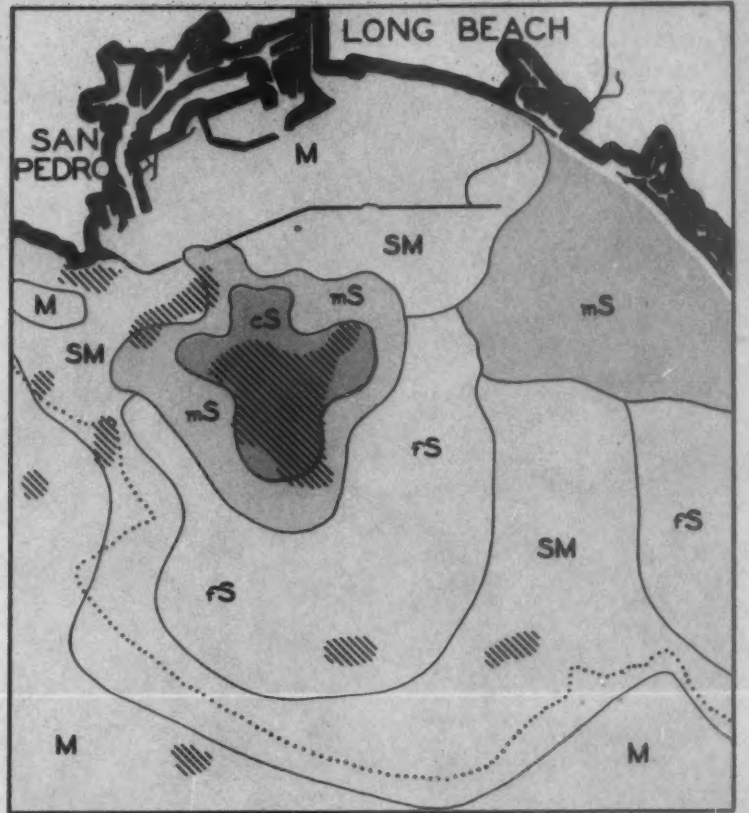
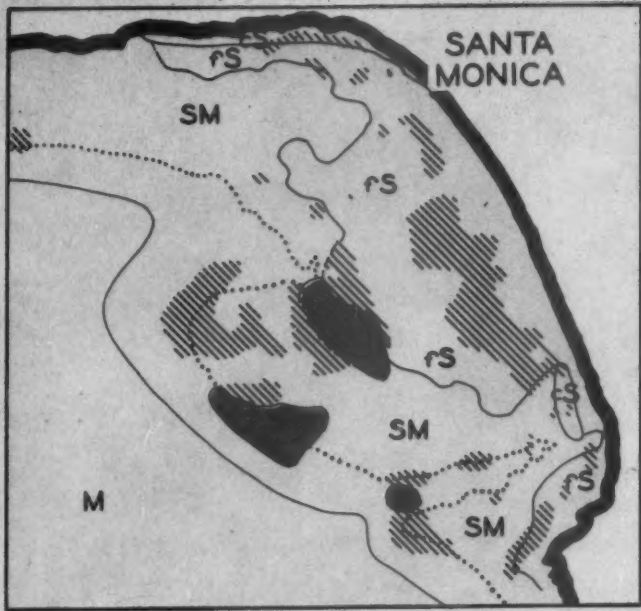
of the peninsula at the north end of the area. Miocene sandstones occur around the islands farther south, and Pliocene shales are abundant on the top of the bank west of the true shelf. Mixed authigenic sediments (glauconite and phosphorite) and organic sediments (Foraminifera) thinly blanket the top of the bank and other areas of nondeposition of detrital sediments near the edge of the shelf. Organic shell sand occurs in a similar area of detrital nondeposition near the islands. Shells mixed with sediment probably of residual origin occur among the rocks that border the peninsula. A large area in the middle of the map and several other much smaller areas contain a medium- to coarse-grained brown sand that is iron-stained and coarser than most of the other sediments. This is believed to be a partially exposed blanketing sand of Late Pleistocene age. It is considered here as a relict sediment, though in a sense it is residual. Adjoining the large area of relict sand is a patch of coarse sand mixed with shells—a mixture of the relict and the organic groups. The remainder of the area is covered with present-day detrital sediment that ranges from medium and coarse sand (possibly partly residual) near the southern cliffed shore and the islands, through fine sand, sand-and-mud, to mud. The outer boundary of the sand-and-mud area is markedly influenced by the topography; there is a large indentation in the deep water between the bank and the true shelf and a smaller one in the submarine canyon south of the bank. A small isolated area of mud occurs on the floor of the canyon, and another one of unknown origin is on the shelf east of the bank. In general, however, with sediments of other origin excluded, the detrital sediments grade outward to finer grain sizes as in the other two shelf areas.

GEOLOGICAL SIGNIFICANCE

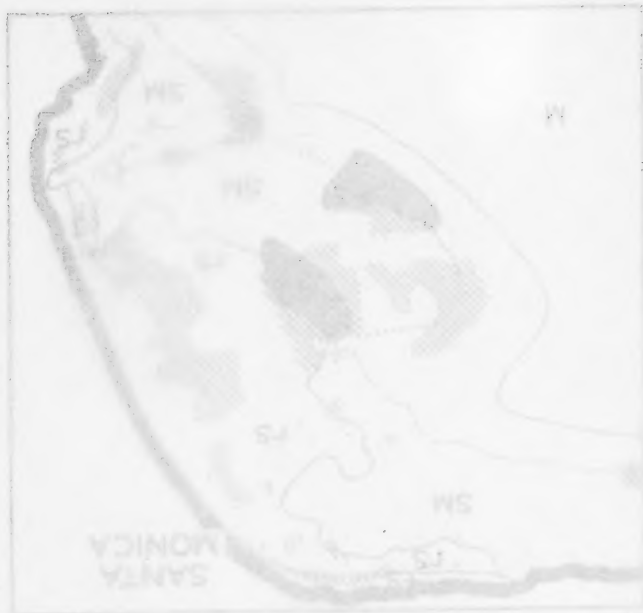
Prior to about 1935 the sediments of the continental shelves were generally believed to be gradational from coarse-grained near shore to fine-grained off shore. Subsequent investigations of the continental shelves of Europe, the United States, and East Asia have shown that the sediments are patchy and irregular in their grain-size distribution. The sediment charts,

e area
islands
ndant
shelf.
e and
(Fom-
bank
etrital
rganic
etrital
mixed
occur
insula.
p and
tain a
that is
e other
rtially
tocene
iment,
ng the
course
relict
of the
l sedi-
e sand
uthem
sand,
ary of
enced
tation
d the
marine
d area
n, and
e shelf
, with
etrital
izes as

of the
ved to
shore
estiga-
pe, the
n that
n their
charts,



SEDIMENT CHART OF THREE AREAS IN CALIFORNIA



SEDIMENT CHARTS OF THE BAY

howe
prese
out th
transp
When
and ro
maini
detrit
decrea
the s
from
topog
from
season
of gra
beddin
sedim
ondar
sedim
Sed
occur
luted
banks
The p
the re
rise of

however, show all the sediments that are present on the shelf, with no attempt to single out the detrital sediment which alone is being transported from shore and deposited there. When sediments of authigenic, organic, residual, and relict origin are recognized and only the remaining detrital sediments are considered, the detrital sediments present a general trend of decreasing grain size in a seaward direction for the shelf off southern California. Variations from this trend result from irregularities in topography, from local currents, and probably from occasional inadequate samples. Storm, seasonal, or longer-period shifting of the zones of grain-size gradation may result in some interbedding or mixing of coarse- and fine-grained sediments, but this appears to be of only secondary importance in the zonation of detrital sediments on the shelves.

Sediments belonging to the first four groups occur only where they are not covered or diluted by detrital sediment, in such places as banks, hills, and the outer edge of the shelf. The present patchy distribution is evidently the result of insufficient time since postglacial rise of sea level for the present supply of detrital

sediment to bury completely the irregular topography. The generally simpler distribution of sediments that were deposited in ancient epicontinental seas suggests that the floors of those seas had a less complex topography than the present floor of the continental shelves.

REFERENCES CITED

- Emery, K. O.; Butcher, W. S.; Gould, H. R.; and Shepard, F. P. (1952) *Submarine geology off San Diego, California*, Jour. Geol., vol. 60, (in press).
- Moore, D. G. (1951) *The marine geology of San Pedro shelf*, Univ. Southern Calif., Master's Thesis, 48 p.
- Shepard, F. P.; Emery, K. O.; and Gould, H. R. (1949) *Distribution of sediments on east Asiatic continental shelf*, Allan Hancock Foundation Pub., Occ. Paper no. 9, 64 pp.
- Shepard, F. P., and Macdonald, G. A. (1938) *Sediments of Santa Monica Bay, California* Am. Assoc. Petrol. Geol., Bull., vol. 22, p. 201-216.

UNIVERSITY OF SOUTHERN CALIFORNIA, LOS ANGELES 7, CALIF.

MANUSCRIPT RECEIVED BY THE SECRETARY OF THE SOCIETY, APRIL 9, 1952

CONTRIBUTION OF ALLAN HANCOCK FOUNDATION No. 98

Faint, illegible text in the left column of the page.

Faint, illegible text in the right column of the page.

The
other
and t
be lar
rocks
east-f
plates
The o
Two
correl
sets. I
outlet
rock
glacia

Intro
Physi
Geolo
Str
Str
Glaci
Gla
Mo
Date
Drain
Refer

M
the
(Fig
(188
occup
erosi
verse
that
tend
Valle
when

GLACIATION AND DRAINAGE CHANGES IN THE FISH LAKE PLATEAU, UTAH

BY CLYDE T. HARDY AND SIEGFRIED MUESSIG

ABSTRACT

The Fish Lake Plateau, nearly centrally located among the High Plateaus of Utah, exhibits glacial and other geomorphic features of regional significance. The plateau is divided into two areas by Fish Lake and the wide valley of Sevenmile Creek. The Fish Lake trough is a structural basin; Sevenmile Valley may be largely erosional. Volcanic rocks of Tertiary age underlie most of the plateau; early Tertiary sedimentary rocks are also present. Glaciated canyons with well-developed cirques are especially prominent along the east-facing sides of the Fish Lake trough and Sevenmile Valley. Ice-eroded features occur over much of the plateau top. Near the mouths of several of the glaciated canyons are two conspicuous sets of moraines. The older set is more extensive and less rugged than the younger and occurs at somewhat lower elevations. Two substages of glaciation thus recognized are correlated with Wisconsin I and II of Ray; probable correlatives of Wisconsin III, IV, and V are represented by moraines which are younger than these two sets. Fish Lake drains north into Fremont River, a tributary of the Colorado River. An abandoned southern outlet and waterfall, the latter at a higher elevation than the present elevation of the original northern bedrock divide, indicate drainage reversal. Evidence is presented which suggests that this reversal was preglacial and probably the result of fault-block tilting.

TEXT

ILLUSTRATIONS

	Page	Figure	Page
Introduction.....	1109	1. Index map of central Utah.....	1110
Physiographic setting.....	1110	2. Map of Fish Lake Plateau, Utah, and vicinity.....	1111
Geologic setting.....	1111		
Stratigraphy.....	1111		
Structure.....	1112		
Glacial features.....	1113		
Glaciated valleys.....	1113		
Moraines.....	1113		
Date of glaciations.....	1114		
Drainage changes related to Fish Lake.....	1115		
References cited.....	1116		

	Facing Page
Plate	
1. Glaciated valleys and moraines.....	1112
2. Fish Lake.....	1113
3. Map of part of the Fish Lake Plateau, Utah, showing glacial and geomorphic features.....	1114

INTRODUCTION

Many prominent features of glaciation in the Fish Lake Plateau of south-central Utah (Fig. 1) were first described by C. E. Dutton (1880). He concluded that Fish Lake (Fig. 2) occupies a valley produced by normal stream erosion previous to regional tilting which reversed the drainage of the lake. He thought that the abandoned outlet channel which extends southward from Fish Lake reached Grass Valley, within the interior Sevier Lake basin, whereas it joins the valley of the Fremont

River, a tributary of the Colorado River. Gilbert, as cited by Dutton, apparently regarded the Fish Lake basin as a structural depression which resulted from faulting.

During preliminary reconnaissance of the Fish Lake Plateau in 1950, the authors recognized evidence for at least two substages of glaciation. Gould (1939), in the eastern part of the Aquarius Plateau, and Spieker and Billings (1940), in the Wasatch Plateau, recognized only one substage. These facts together with the problems alluded to in the above paragraph, suggested that a field study might reveal evi-

dence for some conclusions regarding the glacial history of the area and the history of Fish Lake. Furthermore, it appeared from this reconnaissance that a glacial chronology of the Fish

PHYSIOGRAPHIC SETTING

The Fish Lake Plateau is nearly centrally located among the High Plateaus of Utah (Fig.

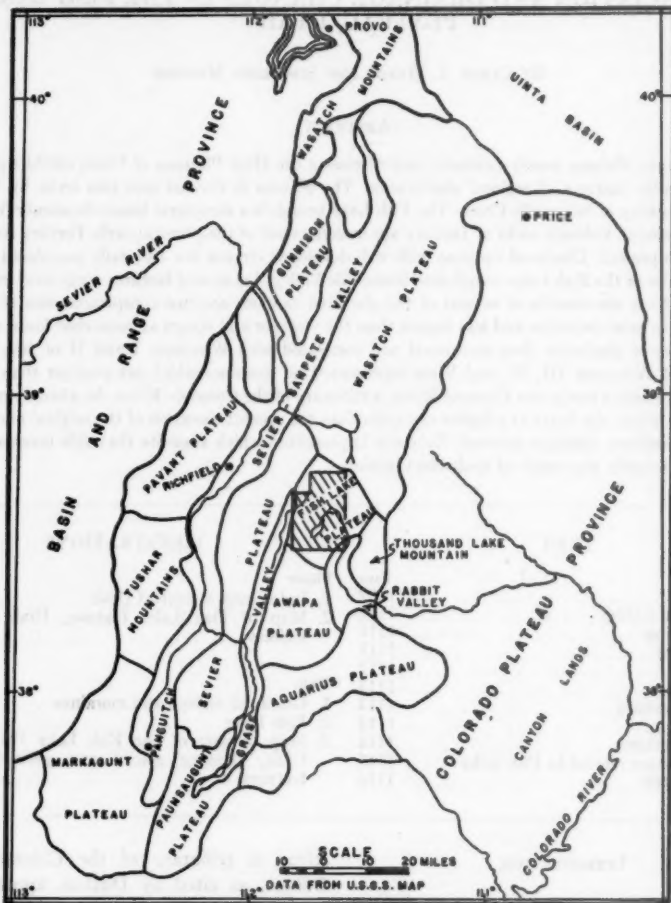


FIGURE 1.—INDEX MAP OF CENTRAL UTAH

Lake Plateau, when based on additional data, might correspond rather closely to that established by Ray (1940) for the Southern Rocky Mountains.

Aerial photographs were used in the field and the data were subsequently plotted on a large-scale base map obtained from the U. S. Forest Service. A plane-table traverse was made in order to obtain elevations for all points which are critical in the history of Fish Lake.

1). It rises above the southern extremity of the Wasatch Plateau and is directly east of the northern part of the Sevier Plateau. From the southern margin of the Fish Lake Plateau the Awapa Plateau slopes gently toward the southeast; however, the two plateaus are not distinctly separated. To the south the Awapa Plateau joins the Aquarius Plateau. Rabbit Valley and Thousand Lake Mountain are to the east, with the Canyon Lands of the Colo-

ndo I
Mount
part of
Two
the Fis

Lake
the ea
rated
Lake
Moun
least
of a o
gener
tween
west
River

Colorado River basin beyond. Thousand Lake Mountain is considered an outlier of the eastern part of the Aquarius Plateau.

Two distinct topographic units are found in the Fish Lake Plateau (Fig. 2): (1) the Fish

sect the eastern flank of the mountains. Seven-mile Valley separates the Fish Lake Mountains from the area to the northeast which includes Mt. Terrill and Mt. Marvine, both of which rise above 11,000 feet. Fish Lake paral-

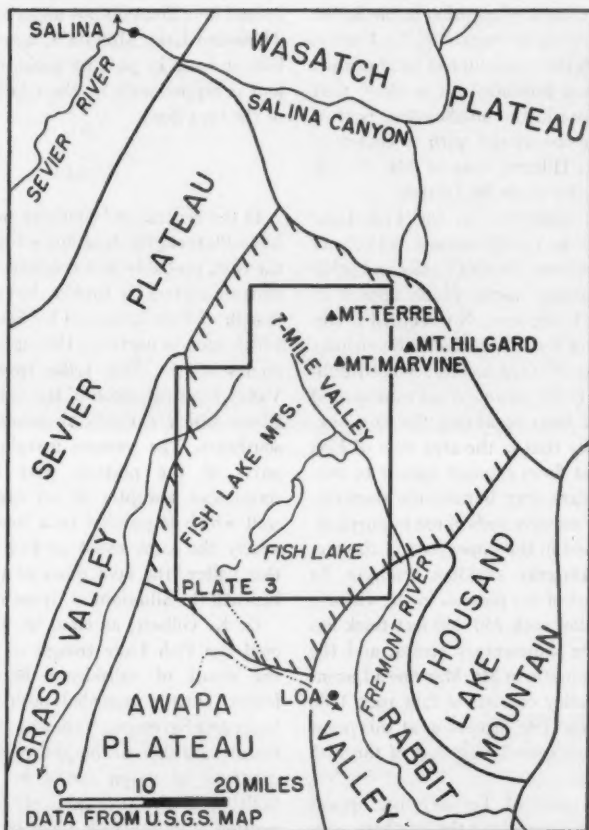


FIGURE 2.—MAP OF FISH LAKE PLATEAU, UTAH, AND VICINITY

Lake Mountains in the western part, and (2) the eastern part of the plateau, which is separated from the Fish Lake Mountains by Fish Lake and Sevenmile Valley. The Fish Lake Mountains, which attain an elevation of at least 10,000 feet, are the flat-topped remnants of a once more extensive plateau which slope in general toward the east and form a divide between the interior Sevier Lake basin to the west and the drainage basin of the Colorado River to the east. Several glaciated valleys dis-

sects the eastern flank of the mountains. Seven-mile Valley separates the Fish Lake Mountains from the area to the northeast which includes Mt. Terrill and Mt. Marvine, both of which rise above 11,000 feet. Fish Lake paral-

GEOLOGIC SETTING

Stratigraphy

The Fish Lake Plateau is extensively underlain by thick series of lava flows that are probably correlative with the volcanic rocks of

middle or late Tertiary age described by Callaghan (1939) in the vicinity of Marysvale, Utah. These flows are unusually well exposed in the glaciated valleys of the Fish Lake Mountains and also along the eastern edge of the Fish Lake trough. In all probability the lava emanated from centers of eruption in the Sevier Plateau to the west, as suggested by Dutton (1880), although the possibility of local centers of eruption is not precluded. It is likely that many of the flows in the northeastern part of the plateau are associated with a center of eruption at Mt. Hilgard, east of Mt. Terrill, an observation also made by Dutton.

The volcanic succession in the Fish Lake Plateau appears to consist almost entirely of volcanic flows without the thick tuffs and other volcanic sedimentary rocks which appear in the Marysvale, Utah, area. No detailed petrographic studies of the flow rocks in the vicinity of the Fish Lake Plateau have ever been published. Dutton (1880), however, has summarized a few pertinent facts regarding the flow succession, especially that in the area west of Fish Lake. The oldest flows exposed appear to consist largely of dark-gray hornblende trachyte. Above these are massive beds of red to purplish-red trachytes, and in the upper part of the succession is a light-gray sanidine trachyte. In the northern part of the plateau in the vicinity of Mt. Terrill, flow rock 250-450 feet thick lies directly over the sedimentary strata, and the ridge which culminates in Mt. Marvine adjacent to Sevenmile Valley consists of flow rock 1200 to 1800 feet thick. The succession at this point is in many respects similar to that of the Fish Lake Mountains.

Sedimentary rocks of Tertiary age appear beneath the lava flows along the northern edge of the Fish Lake Plateau and along the eastern margin of Sevenmile Valley near Mt. Terrill. They probably represent the Green River formation of Eocene age, which occurs extensively in the southern part of the Wasatch

Plateau. Sedimentary rocks are not exposed along the major part of the western margin of the plateau because the lava flows dip westward beneath the alluvium of Grass Valley. Likewise, the sedimentary rocks are obscured by alluvium in Rabbit Valley to the east, if indeed lava flows do not underlie the alluvium. Thousand Lake Mountain, however, is underlain at least in part by rocks of Jurassic age and is capped only by the relatively thin edge of the lava flows.

Structure

In the central and southern parts of the Fish Lake Plateau, the lava flows dip gently toward the east, probably as a result of initial dip. The plateau surface is broken by the steep-sided trough of Fish Lake and by Sevenmile Valley, which trends north-northwest nearly at right angles to the Fish Lake trough. Sevenmile Valley is an extension of the valley of Fremont River which extends in general toward the southeast. The western margin of the higher parts of the plateau west of Fish Lake terminates abruptly in an exceedingly steep wall which is parallel to a linear valley with nearly the same trend as Fish Lake. Beyond this valley, the lava flows of the plateau dip beneath the alluvium of Grass Valley.

G. K. Gilbert, as cited by Dutton, considered the Fish Lake trough to be dominantly the result of subsidence between marginal faults. Dutton regarded both the Fish Lake basin and Sevenmile Valley as strictly erosional features, although he did not question the existence of major faults in the area. That faulting is of topographic significance in connection with the Fish Lake basin is indicated by the linear aspect of the eastern margin of the basin and also by the parallelism of this cliff with similar features in the area. Moreover, the conspicuous saddles along the cliff east of Fish Lake seem to represent truncated valleys

PLATE 1.—GLACIATED VALLEYS AND MORAINES

FIGURE 1. VIEW TOWARD THE WEST SHOWING MORAINES ASSOCIATED WITH A GLACIATED CANYON BETWEEN PELICAN AND ROCK SPRINGS CANYONS

Wisconsin I moraine forms the low hills in the foreground; Wisconsin II moraine occurs at the mouth of the canyon.

FIGURE 2. VIEW TOWARD THE NORTHWEST SHOWING PELICAN CANYON

Wisconsin II moraine seen in foreground.



FIGURE 1



FIGURE 2

GLACIATED VALLEYS AND MORAINES



FIGURE 1



FIGURE 2
FISH LAKE

(Pl. 2
pears
in res
the s
struct

The
easter
and v
nearly
Spring
most
tacula
inter

We
in the
erode
tend
the w
indica
must
gener
mover
surface
On t
Moun
ley, F
there

Com
that h
Marvi
of the
do not
Alth
Valley
glacier
cupied

Mon
glaciat

The
bedrock
beyond

Wisc
is in th

(Pl. 2, fig. 1). Sevenmile Valley, however, appears to be the result of normal stream erosion in response to the dip of the lava flows toward the southeast, although there may be some structural control due to faulting.

GLACIAL FEATURES

Glaciated Valleys

The glaciated canyons which dissect the eastern flank of the Fish Lake Mountains north and west of Fish Lake are characterized by nearly vertical walls 300-800 feet high. Rock Springs Canyon and Pelican Canyon are the most prominent, although several less spectacular canyons exhibit features of special interest.

Well-defined intersecting cirques are found in the upper parts of the canyons, and ice-eroded features found on the plateau top extend nearly to the escarpment which bounds the western margin of the plateau. This clearly indicates that virtually the entire plateau top must have been covered by ice which had a general eastward motion. The direction of movement followed the slope of the plateau surface as well as pre-existing drainage lines. On the western flank of the Fish Lake Mountains, only one important glaciated valley, Praeton Canyon, is found. In this area there are also several relatively small cirques.

Conspicuous cirques and extensive areas that have been eroded by ice exist east of Mt. Marvine and Mt. Terrill, but glaciated canyons of the type found in the Fish Lake Mountains do not occur.

Although the Fish Lake basin and Sevenmile Valley contain extensive moraines deposited by glaciers from side valleys, they were never occupied by trunk glaciers.

Moraines

Moraines of two substages of Wisconsin glaciation are readily distinguished in the Fish

Lake Plateau. The older moraine underlies and is locally more extensive than the younger; however, both moraines commonly extend into the broad valleys (chiefly Sevenmile Valley and the Fish Lake trough) adjacent to the glaciated canyons. The surface of the older moraine is considerably less rugged than that of the younger and is characterized by rather smooth hummocks. In one striking occurrence, immediately north of Fish Lake, the older moraine forms an expansive loop in the Fish Lake basin directly east of a small canyon and the younger moraine obstructs the mouth of the canyon at a considerably greater elevation (Pl. 1, fig. 1). Generally, however, the difference in elevation between the older and the younger moraines is about 150-200 feet. The older loop moraine mentioned above is breached by a relatively broad channel; all the younger moraines are cut by deep youthful channels. The older moraine contains pieces of coarse-grained flow rocks with perceptibly thicker weathering rims than similar pieces in the younger moraine. These observations suggest a distinct age difference between the two sets of moraines. This age difference, however, is probably not so great as to require the recognition of two stages of glaciation in this area; rather, it seems likely that the older and younger moraines represent glacial substages (Flint, 1947, p. 209). No evidence for pre-Wisconsin glaciation has been observed in the Fish Lake Plateau.

Moraines of both substages are clearly evident immediately north of Fish Lake and east of the small glaciated valley described above (Pl. 3). The expansive loop of the older moraine is nearly a mile wide, and the elevation of the top surface is about 8455 feet. The elevation of the younger moraine at the mouth of the canyon is about 8960 feet. In the Sevenmile Valley at Rock Springs Canyon, the older moraine extends from beneath the southern margin of

PLATE 2.—FISH LAKE

FIGURE 1. VIEW TOWARD THE EAST SHOWING THE EARLY SOUTH OUTLET OF FISH LAKE

The abandoned channel extends toward the lower right of the picture; the abandoned waterfall on a bedrock divide is hidden by trees in the left center. Valleys, apparently truncated by faulting, are seen beyond the lake.

FIGURE 2. VIEW TOWARD THE NORTHEAST SHOWING THE NORTH OUTLET OF FISH LAKE

Wisconsin I moraine seen in left foreground and bedrock in right foreground. The breached divide (8,413') is in the middle distance to the right of the center of the picture, beyond which is Sevenmile Valley.

a lobe of the younger moraine that spreads nearly across the valley. Here the top surface of the older moraine has an elevation of about 8535 feet and the top surface of the younger moraine about 8670 feet. Extensive moraine of the later substage is also found north of Rock Springs Canyon in Sevenmile Valley opposite three prominent cirques in the Fish Lake Mountains. A lobate moraine in Praeton Canyon on the western side of the Fish Lake Mountains is of the later substage, although some moraine marginal to this lobe may be older.

The conspicuous moraine at Pelican Canyon near the northern end of Fish Lake represents the later glaciation (Pl. 1, fig. 2). Here the top surface has an elevation of about 8797 feet, which is 392 feet above the present level of Fish Lake. Probably a loop moraine of the earlier substage of glaciation existed transverse to the valley of Fish Lake opposite Pelican Creek, although the restriction of Fish Lake at this point may be due to outwash.

East of Mt. Terrill and Mt. Marvine in the northeastern part of the Fish Lake Plateau, two prominent cirques are associated with the moraines of the late substage. The elongate cirque immediately southeast of Mt. Terrill is related to a younger moraine which extends up, as well as down, the adjoining valley, and in this respect is similar to moraines described by Spieker and Billings (1940) in Joe's Valley in the Wasatch Plateau.

Other moraines, possibly recessional, are prominent only in Rock Springs Canyon at an intermediate elevation between the younger of the two extensive moraines and the cirques at the head of the canyon. A low moraine ridge is found near the lip of the elongate cirque southeast of Mt. Terrill and is evidently earlier than the protalus rampart which parallels the wall of the cirque. Protalus ramparts are also found along the north-facing walls of the cirques north of Rock Springs Canyon and elsewhere.

DATE OF GLACIATIONS

The recognition of at least two substages of glaciation in the Fish Lake Plateau, which correspond in all essential details to substages recognized in the Southern Rocky Mountains and perhaps elsewhere in the western United

States (Ray, 1940), suggests a correlation with other areas and indirectly permits a dating of the glaciations.

The younger moraine, which is found adjacent to or overlying the older moraine, rises about 300 feet above the latter, although the difference in elevation observed in Sevenmile Valley at Rock Springs Canyon is only about 150-200 feet. The top surface of the older moraine is generally at an elevation of about 8500 feet and that of the younger moraine here referred to is at about 8800 feet. This younger moraine is distinguished from those farther up the canyons solely on the basis of topographic position; there is no definite evidence to exclude the possibility that the moraines at higher elevations are recessional and therefore should not be assigned to substages. The remarkable preservation of all of these moraines, however, necessitates that they be related to the Wisconsin stage. Likewise, the small moraines found near the lips of cirques, notably east of Mt. Terrill, may in reality be recessional moraines, although Matthes (1941) has regarded similar occurrences in the Sierra Nevada as indicative of a rebirth of glaciers during late post-Pleistocene time.



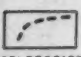
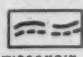
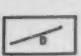
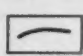


The correspondence of the various moraines in the Fish Lake Plateau with the moraine succession described by Ray in the Southern Rocky Mountains is indeed remarkable, although no evidence of warm interstadial periods has been found in the Fish Lake Plateau. The correspondence, based largely on topographic position, is supported by the distinct age difference in the two older moraines in the Fish Lake area. Thus, in the Medicine Bow Mountains, Ray (1940) found moraine of the earliest known Wisconsin substage at an elevation of 8100 feet and those of successively younger substages at 8500 feet, 10,000 feet, and 10,500 feet. The difference in elevations between moraines of the two earlier substages seems to correspond in a general way throughout the Rocky Mountain area, and this difference is not greatly different from that observed in the Fish Lake Plateau (100-300 feet).

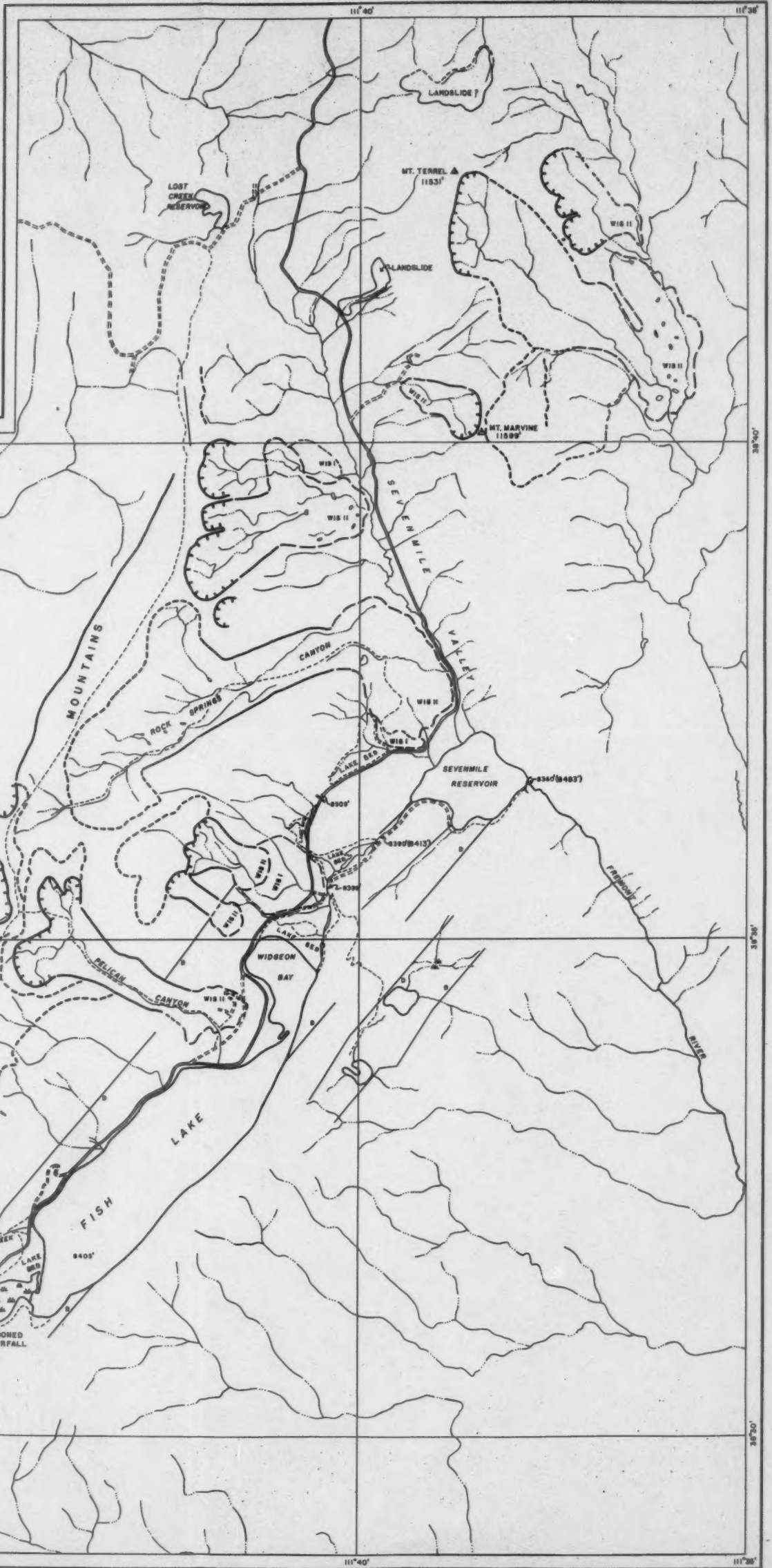
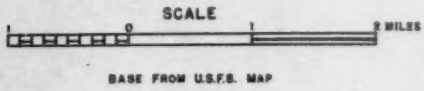
In view of these considerations, the nomenclature of Ray (1940), which was proposed and utilized for correlational purposes, is tentatively adopted for the Fish Lake Plateau. Thus Wis-

with
g of
lja-
ises
the
mile
out
no-
out
ere
ger
up
hic
ex-
at
ore
re-
nes,
to
nall
bly
anal
re-
erra
iers
mes
ine
ern
al-
ods
The
hic
dif-
ish
un-
iest
ion
ger
500
no-
to
the
not
the
en-
and
ely
/is-

co

EXPLANATION

-  CIRQUE
-  WISCONSIN I MORAINE
-  ICE EROSION
-  WISCONSIN II MORAINE
-  INFERRED FAULT
-  CLIFF OR SCARP
-  DIVIDE
-  TRAIL



MAP OF PART OF THE FISH LAKE PLATEAU, UTAH, SHOWING GLACIAL AND GEOMORPHIC FEATURES

consin
morain
Wiscon
within
interm
viously
rains
only a
corresp
found
the pr
Wiscon
tains.

DRAIN

Fish
trends
faults.
the ne
rises a
east si
near th
wide

stream
the lak
by the
Lake
within
just n
depth
easter

Dut
and w
southe
believ
Grass
basin.

Frem
Colora
less, t
age re
posite
region
explai
aband
40 fee

The
end of
rock
betwe
voir.

moraine I and II represent respectively the older moraine and the adjacent younger moraine. Wisconsin III may be represented by moraines within the canyons in the Fish Lake area at an intermediate elevation between those previously described and the cirques. These moraines are not mapped and the elevations are only approximately known. Wisconsin IV may correspond to the small moraines sometimes found near the outer edges of the cirques, and the protalus ramparts may be associated with Wisconsin V as in the Southern Rocky Mountains.

DRAINAGE CHANGES RELATED TO FISH LAKE

Fish Lake occupies a structural trough which trends northeast-southwest between marginal faults. Several small creeks enter the lake on the northwest side, and a steep linear cliff rises abruptly from the shoreline on the southeast side (Pl. 2, fig. 1). Including Widgeon Bay near the northern end, the lake is about 1 mile wide and 5 miles long. The present outlet stream extends from the northeastern point of the lake to Sevenmile Reservoir which is drained by the Fremont River. The elevation of Fish Lake is about 8405 feet; this is maintained within a few feet by a gate in the outlet stream just north of Widgeon Bay. Maximum known depth near the steep cliff which parallels the eastern shore is about 120 feet.

Dutton found an abandoned outlet channel and waterfall over a bedrock divide near the southern end of Fish Lake (Pl. 2, fig. 1). He believed that this channel extends westward to Grass Valley, which is within the Sevier Lake basin. In reality it extends southeast to the Fremont River which ultimately joins the Colorado River. Dutton recognized, nevertheless, that these features clearly indicate drainage reversal, as the present outlet is at the opposite end of Fish Lake. He postulated a slight regional tilt downward toward the northeast to explain this reversal. The elevation of the abandoned waterfall is about 8445 feet or about 40 feet above the present lake level.

The present outlet stream at the northern end of Fish Lake flows through a breached bedrock divide about two-thirds of the distance between Widgeon Bay and Sevenmile Reservoir. The elevation of the stream bed at this

point is about 8390 feet, and the projected level of the original bedrock divide is about 8413 feet, only 32 feet lower than the present elevation of the abandoned south outlet channel (8445 feet). The only other divide which might have been breached near the northern end of the lake is at an elevation of 8509 feet, about 96 feet higher than the probable level of the lower divide (8413 feet) which was breached. It is presumed, in the absence of evidence pointing to another conclusion, that the original northern divide (projected level about 8413 feet) was breached either as a result of the regional tilting toward the northeast postulated by Dutton or, more likely, as a result of the tilting of a fault block.

The possibility must be considered, however, that the present outlet channel through the original bedrock divide (projected level about 8413 feet) was initiated or eroded in part by northward diversion of original southward drainage as the consequence of a dam formed against bedrock by the older loop moraine which is just north of Widgeon Bay at the northern end of Fish Lake (present elevation of the top surface of this moraine is about 8455 feet). In this event, the ponded lake formed north of the moraine would have reached an elevation of about 8413 feet, the projected level of the original bedrock divide to the north, and would then have breached this divide. This suggestion is considered unlikely because a south-flowing stream probably existed between the moraine and the bedrock cliff immediately to the east (Pl. 2, fig. 2). Therefore, the moraine could not have formed an effective dam as high as 8413 feet; indeed, it probably formed no dam at all. Thus, the bedrock divide (8413 feet) could not have been breached by northward drainage prior to tilting. For the same reason, it is unlikely that this moraine ever dammed a north-flowing stream from Fish Lake to the extent that drainage could have been diverted southward over a divide at the north end of Fish Lake, which is now at an elevation of 8445 feet.

It is also unlikely that southward drainage from Sevenmile Valley to Fish Lake initiated the channel across the divide (projected level about 8413 feet) before fault-block tilting or regional tilting. Although the projected level

(8483 feet) of the divide which may have existed at the lower end of Sevenmile Reservoir is 70 feet higher than the original elevation of the breached divide (8413 feet) between Sevenmile Valley and Fish Lake, there is no evidence for a lake at this elevation (8413 feet) in Sevenmile Valley. Probably, as elsewhere in the vicinity of the Fish Lake Plateau (Dutton, 1880, p. 163), drainage from Sevenmile Valley was maintained through the valley of the upper part of the Fremont River as the faulting occurred over a protracted period in the late Tertiary and early Quaternary. Indeed, the youthful channel of the upper part of the Fremont River appears to be cut within a more mature valley, presumably an extension of Sevenmile Valley.

From these considerations it seems evident that the older moraine at the northern end of Fish Lake, immediately north of Widgeon Bay, played no part in the drainage reversal and that fault-block tilting must have effected the reversal, inasmuch as the abandoned waterfall (8445 feet) at the southern end of Fish Lake is higher than the former bedrock divide (8413 feet) between Fish Lake and Sevenmile Valley. Consequently, before tilting, the Fish Lake basin had a south outlet, whereas Sevenmile Valley was drained by the Fremont River. The only effect that this moraine now has on the drainage in the area is that the moraine and associated outwash now dam Fish Lake to a higher level than the present channel (8390 feet) to the north at the site of the original bedrock divide (8413 feet). Hence the older moraine, which now dams Fish Lake at the north end, is probably younger than the tilting, or this dam would have been removed by stream erosion long ago. The possibility exists, however, that the tilting occurred soon after the deposition of this moraine and that sufficient time has not elapsed for the removal of this moraine dam.

The history of Fish Lake may be briefly summarized as follows. As a consequence of the formation of the Fish Lake basin as a

structural depression, a lake was ponded therein. Eventually the bedrock divide at the southern end was topped, and all drainage into the basin, south of the two divides (8413 and 8509 feet) near the northern end, was to the south and east where it joined the Fremont River. Drainage in Sevenmile Valley flowed south to the upper part of the Fremont River, which at this time probably had no connection with the Fish Lake basin. Fault-block tilting, downward to the northeast, effected a drainage reversal so that the lower bedrock divide (8413 feet) near the northern end of the lake was breached; and drainage from Fish Lake thenceforth reached the upper part of the Fremont River through Sevenmile Valley. The glacial features in the area played no important part in these drainage changes, although moraine of the earlier substage now dams Fish Lake to a slightly higher level than would otherwise exist. The outlet at the east end of Sevenmile Reservoir north of Fish Lake is antecedent, having been maintained throughout tilting.

REFERENCES CITED

- Callaghan, Eugene (1939) *Volcanic sequence in the Marysvale region in southwest-central Utah*, Am. Geophys. Union, Tr., 20th Ann. Mtg., pt. 3, p. 438-452.
- Dutton, C. E. (1880) *Report on the geology of the High Plateaus of Utah*, U. S. Geogr. and Geol. Survey of Rocky Mountain Region, p. 260-277.
- Flint, Richard Foster (1947) *Glacial geology and the Pleistocene epoch*, John Wiley and Sons, Inc., p. 209.
- Gould, L. M. (1939) *Glacial geology of Bonanza Mountain, Utah*, Geol. Soc. Am., Bull., vol. 50, p. 1371-1380.
- Matthes, F. E. (1941) *Rebirth of the glaciers of the Sierra Nevada during late post-Pleistocene time*, Geol. Soc. Am., Bull., vol. 52, p. 2030.
- Ray, Louis L. (1940) *Glacial chronology of the Southern Rocky Mountains*, Geol. Soc. Am., Bull., vol. 51, p. 1851-1918.
- Spieker, E. M., and Billings, M. P. (1940) *Glaciation in the Wasatch Plateau, Utah*, Geol. Soc. Am., Bull., vol. 51, p. 1173-1198.

UTAH STATE AGRICULTURAL COLLEGE, LOGAN, UTAH; U. S. GEOLOGICAL SURVEY, JOPLIN, MISSOURI.

MANUSCRIPT RECEIVED BY THE SECRETARY OF THE SOCIETY, MARCH 25, 1952

herein
Southern
basin,
9 feet
th and
Drain-
to the
at this
th the
vnward
ersal so
) near
eached;
ceforth
River
eatures
n these
of the
e to a
erwise
renmile
cedent,
ing.

e in the
Utah,
Mtg.

y of the
d Geol.
60-272
and the
s, Inc.

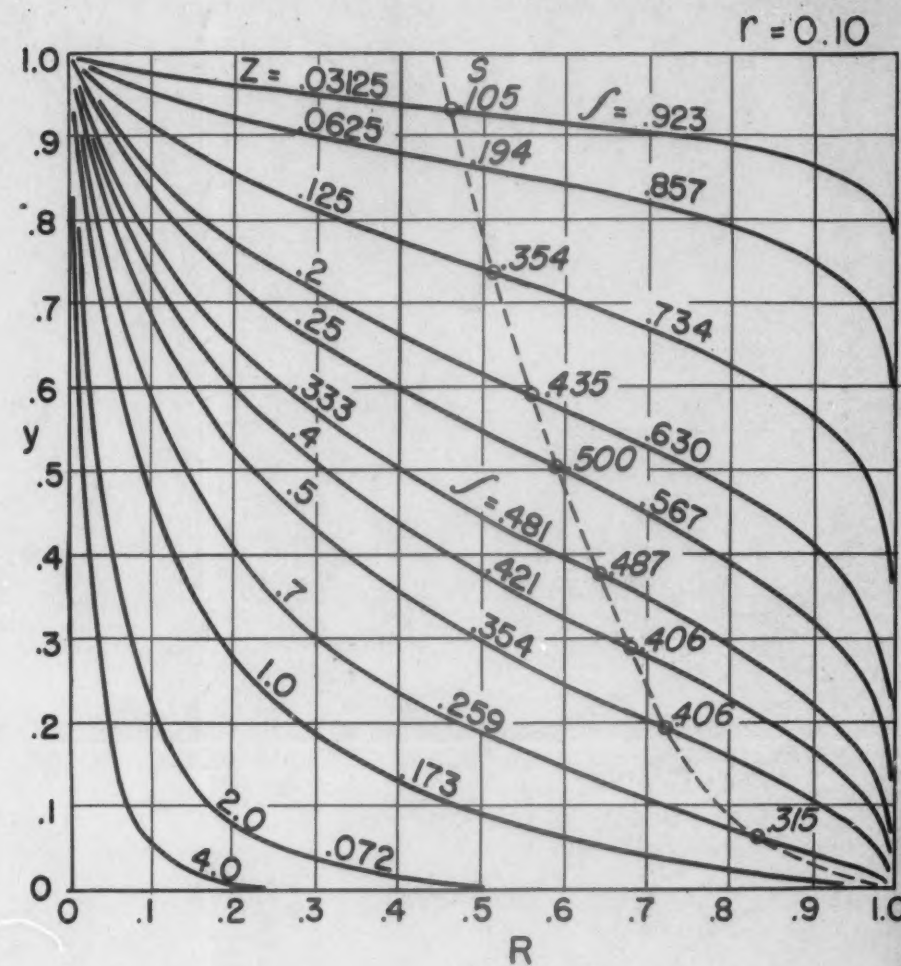
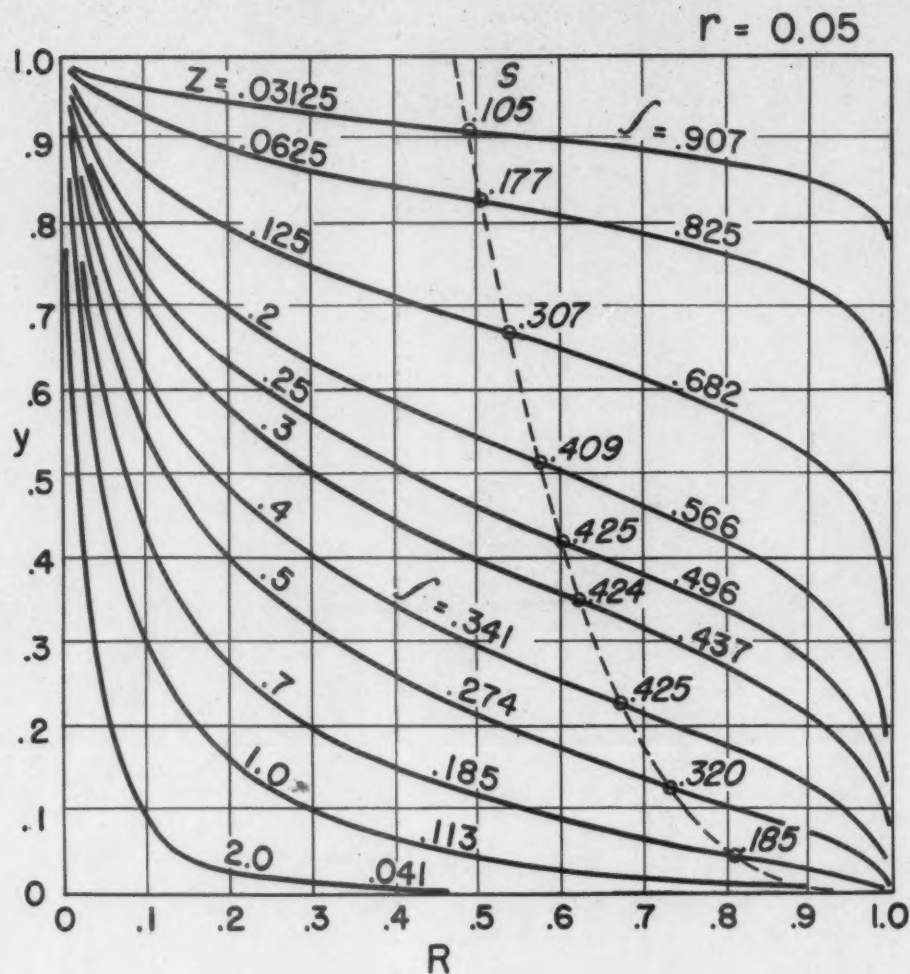
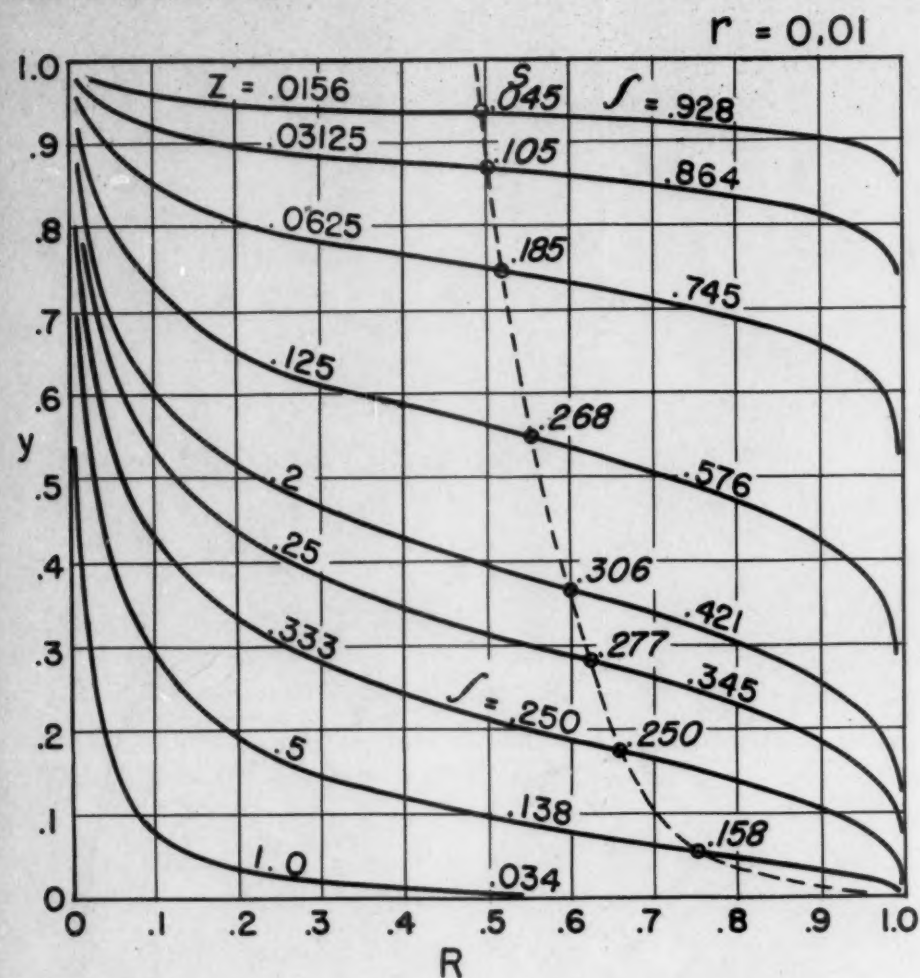
Boulder
ll., vol.

s of the
ne time,
South-
Ball.

Glacis-
ol. Soc.

LOGAN,
JOPLEN,

OF THE



MODEL HYPOMETRIC FUNCTION FOR DRAINAGE BASINS

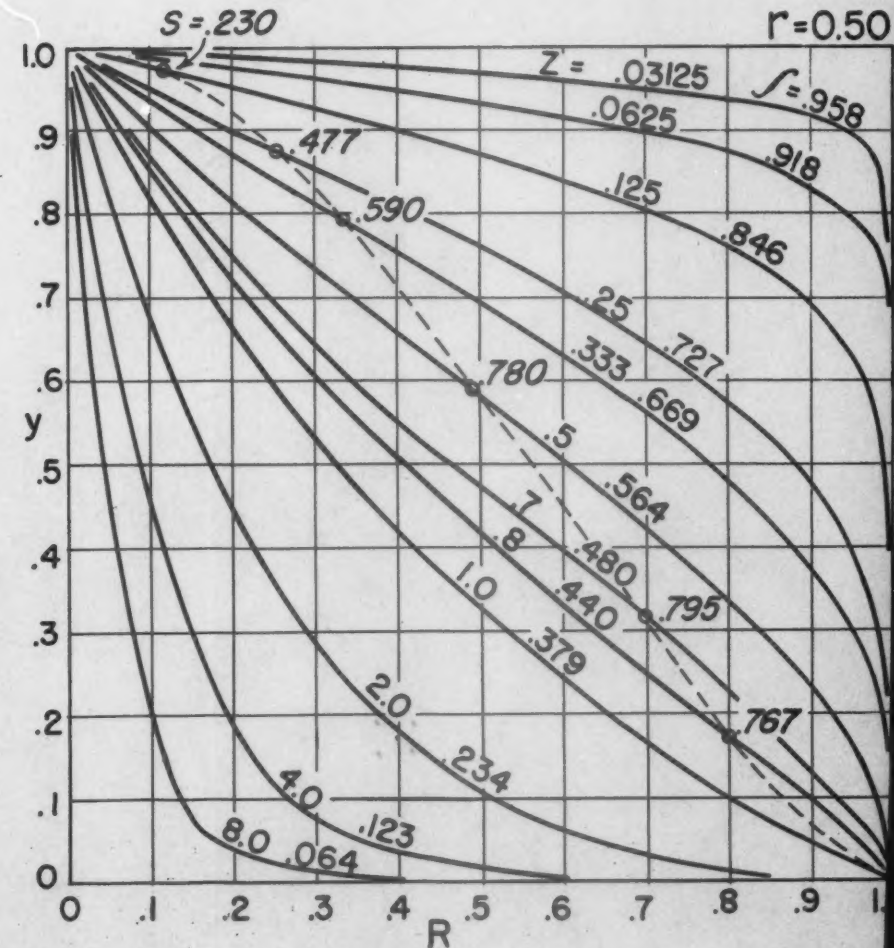
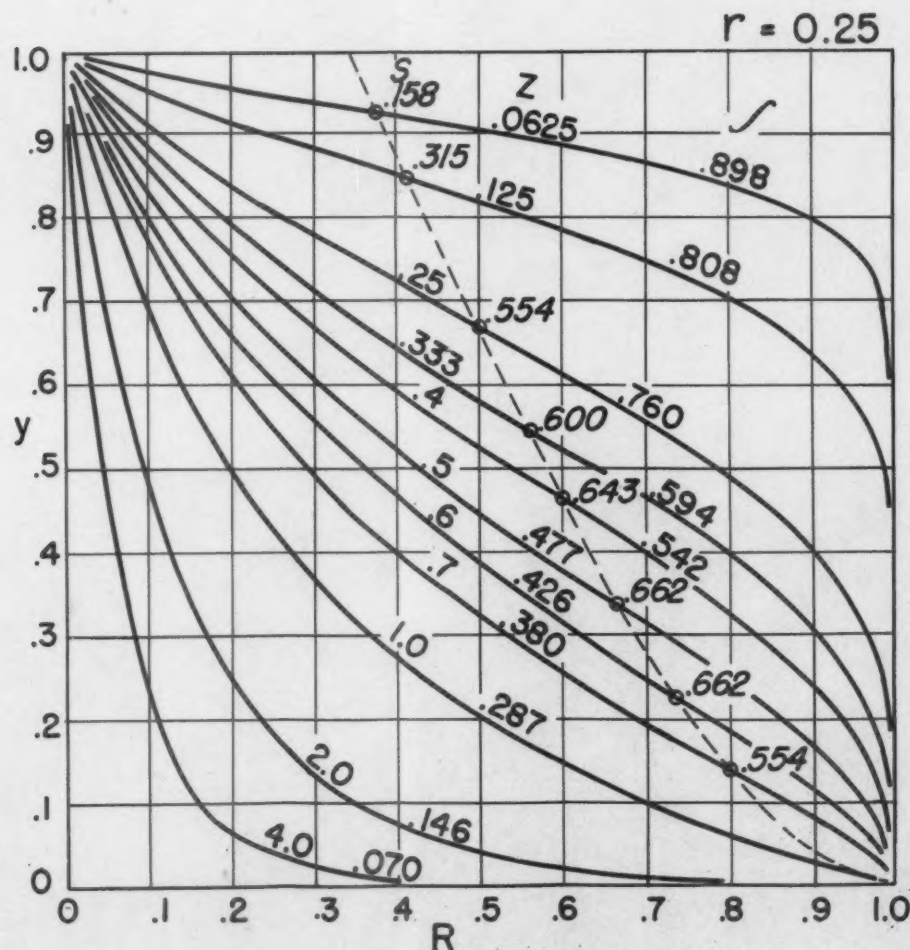
$$y = \left[\frac{d-x}{x} \cdot \frac{a}{d-a} \right]^Z$$

Representative curves of five families, each family produced by a different value of r , where $r = \frac{a}{d}$.

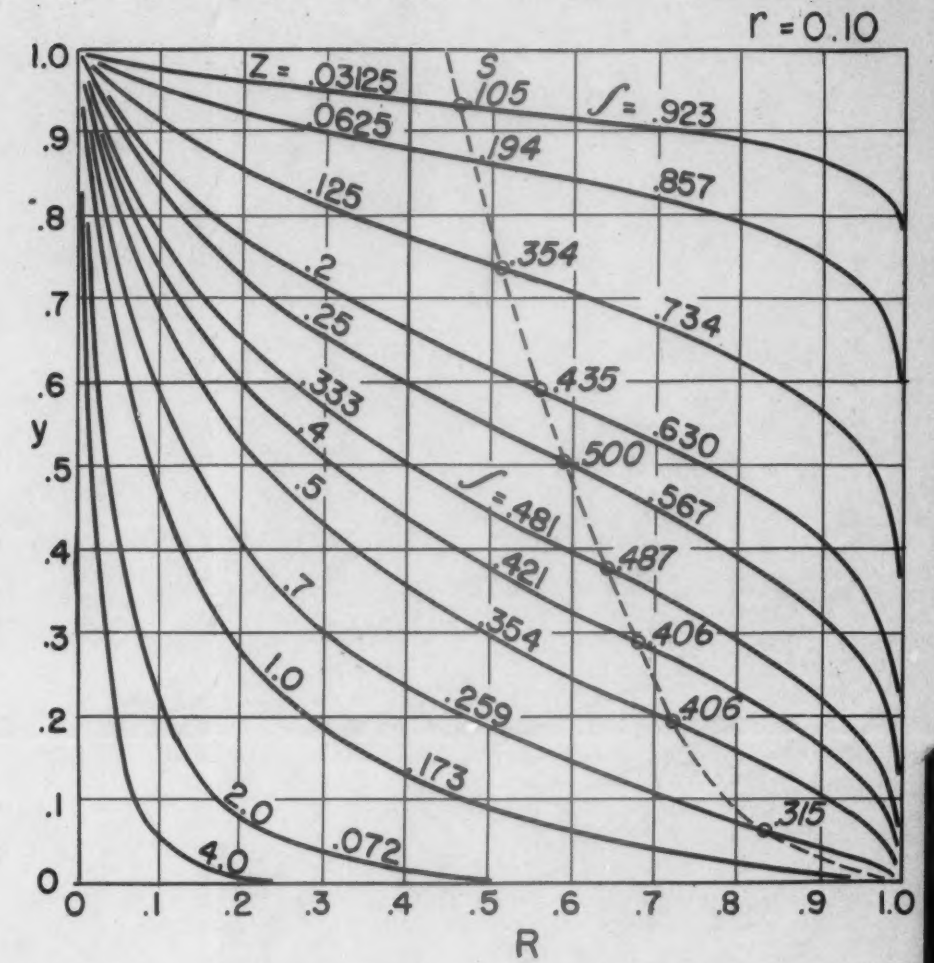
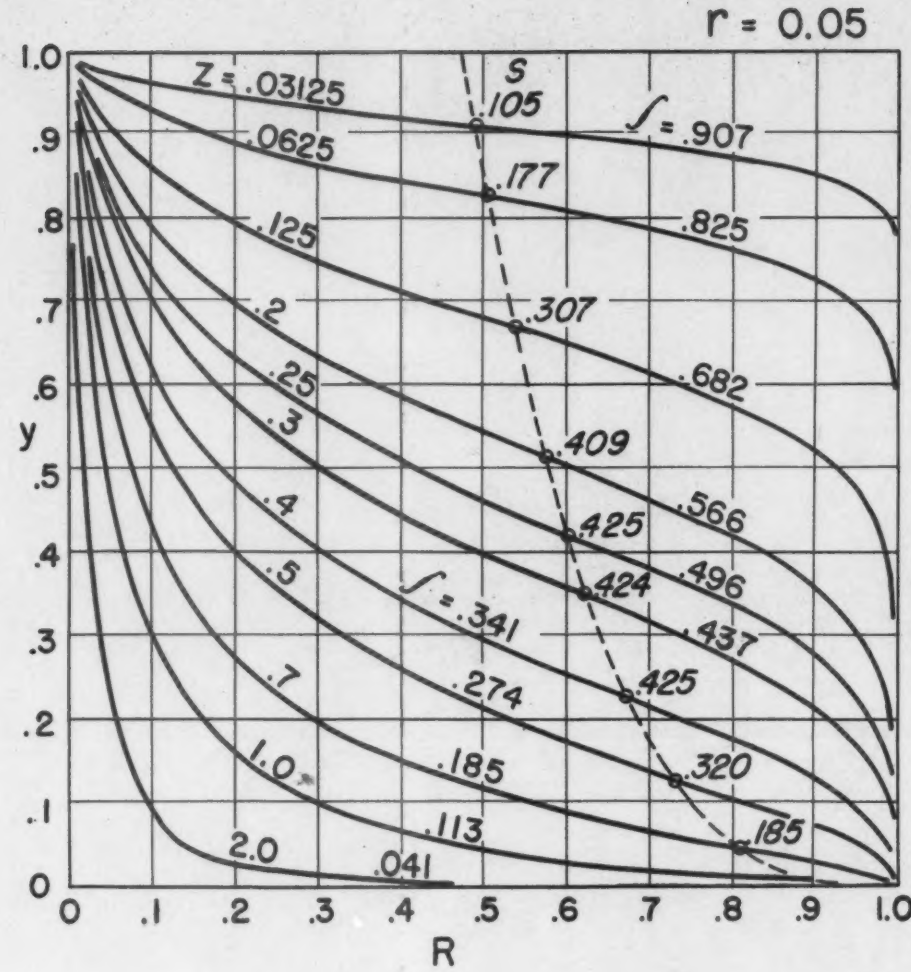
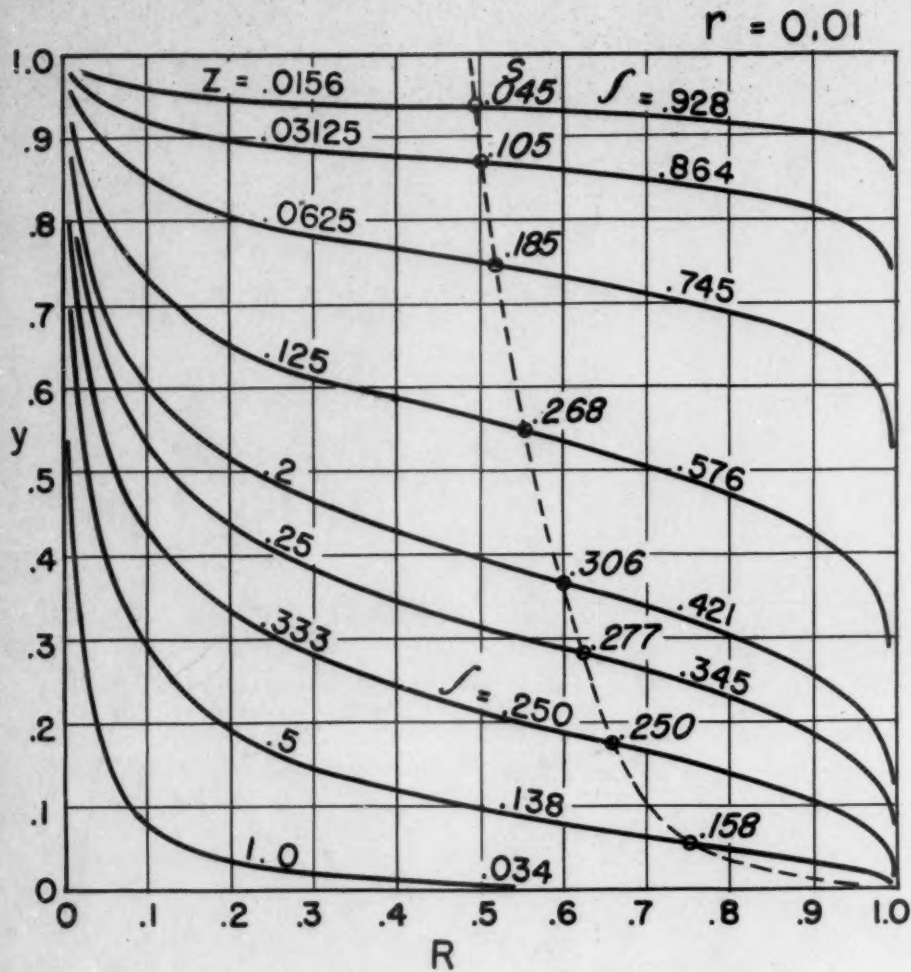
Abscissa scaled in terms of percent, R , where $R = \frac{x-a}{d-a}$

S = Slope of curve at inflection point

\int = Hypsometric integral



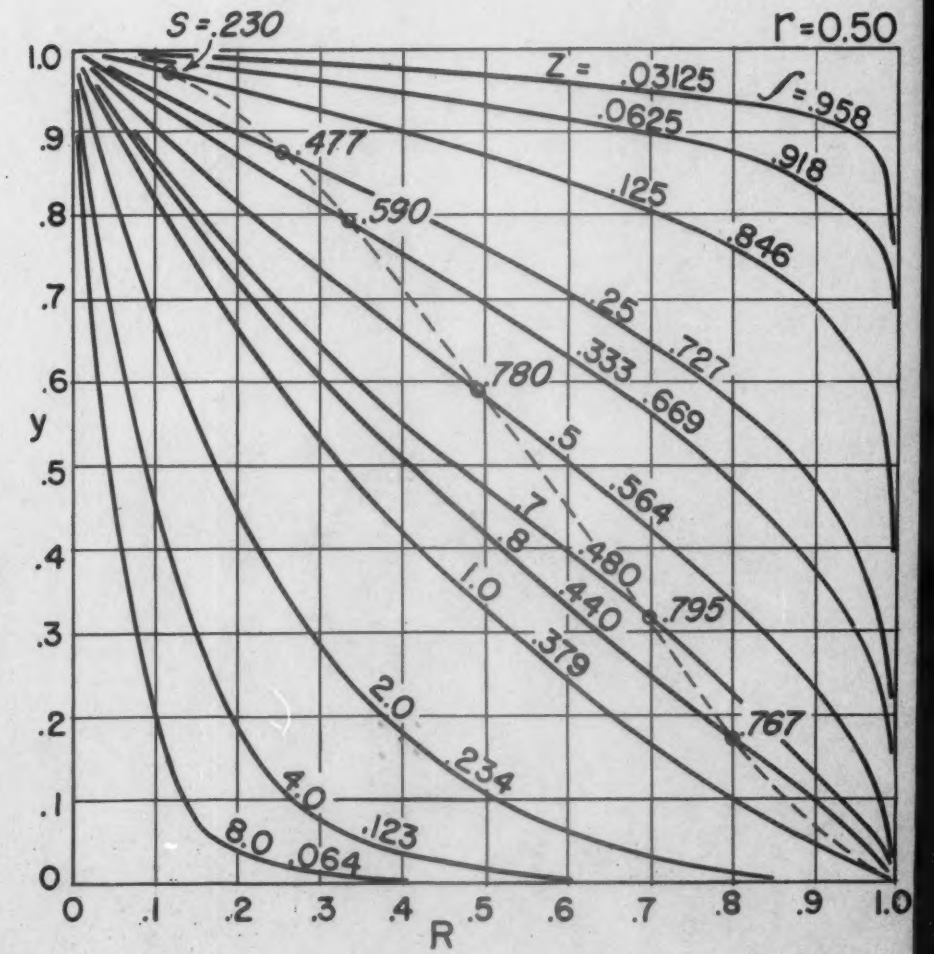
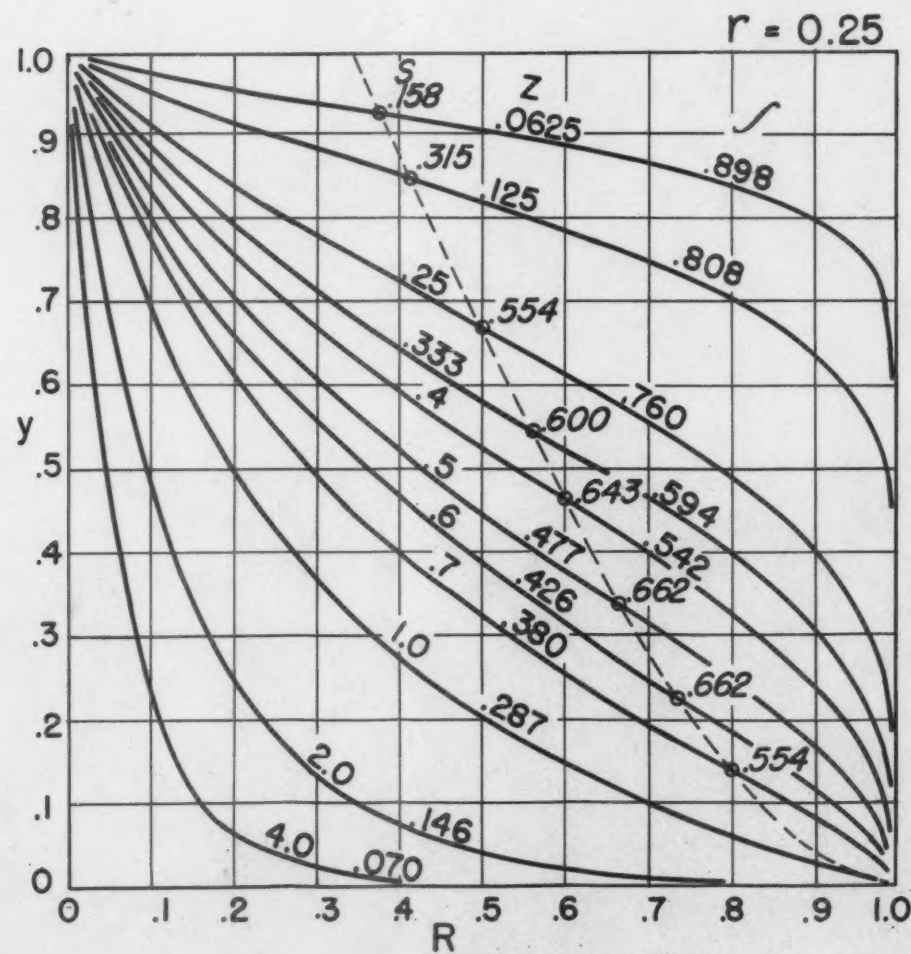
MODEL HYPOMETRIC CURVES FOR FIVE VALUES OF r



MODEL HYPSONETRIC FUNCTION FOR DRAINAGE BASINS

$$y = \left[\frac{d-x}{x} \cdot \frac{a}{d-a} \right]^Z$$

Representative curves of five families, each family produced by a different value of r , where $r = \frac{a}{d}$.
 Abscissa scaled in terms of percent, R , where $R = \frac{x-a}{d-a}$
 S = Slope of curve at inflection point
 \int = Hypsometric integral



MODEL HYPSONETRIC CURVES FOR FIVE VALUES OF r

HY

The
age be
scribe
and in
uncti
itted
taken
Sta
omet
theres
rium
De
thoug
steep
integ
curve
curve
Pr
tion

Intro
Princ
Hy
Pe
M
In
A
In
Ro

Geog

TI
Cl
Ro

G
In
Frac
Ref

Fig
1.

HYSOMETRIC (AREA-ALTITUDE) ANALYSIS OF EROSIONAL TOPOGRAPHY

BY ARTHUR N. STRAHLER

ABSTRACT

The percentage hypsometric curve (area-altitude curve) relates horizontal cross-sectional area of a drainage basin to relative elevation above basin mouth. By use of dimensionless parameters, curves can be described and compared irrespective of true scale. Curves show distinctive differences both in sinuosity of form and in proportionate area below the curve, here termed the hypsometric integral. A simple three-variable function provides a satisfactory series of model curves to which most natural hypsometric curves can be fitted. The hypsometric curve can be equated to a mean ground-slope curve if length of contour belt is taken into account.

Stages of youth, maturity, and old age in regions of homogeneous rock give a distinctive series of hypsometric forms, but mature and old stages give identical curves unless monadnock masses are present. It is therefore proposed that this terminology be replaced by one consisting of an inequilibrium stage, an equilibrium stage, and a monadnock phase.

Detailed morphometric analysis of basins in five sample areas in the equilibrium stage show distinctive, though small, differences in hypsometric integrals and curve forms. In general, drainage basin height, slope steepness, stream channel gradient, and drainage density show a good negative correlation with mean integrals. Lithologic and structural differences between areas or recent minor uplifts may account for certain curve differences. Regions of strong horizontal structural benching give a modified series of hypsometric curves.

Practical applications of hypsometric analysis are foreseen in hydrology, soil erosion and sedimentation studies, and military science.

CONTENTS

TEXT			
	Page		Page
Introduction	1118	2. The percentage hypsometric function	1120
Principles of hypsometric analysis	1118	3. Integration of the hypsometric function	1121
Hypsometric curve in absolute units	1118	4. Model hypsometric function	1122
Percentage hypsometric curve	1119	5. Family of curves for the value $r = 0.1$	1122
Method of obtaining hypsometric data	1119	6. Comparison of several curve families	1123
Integration of the hypsometric function	1120	7. Graphic solution of integrals and exponents	1124
A model hypsometric function	1121	8. Small drainage basin in badlands, Perth Amboy, New Jersey	1125
Inflection points and slopes	1123	9. Hypsometric curve of basin shown in Figure 8	1126
Relation of hypsometric curve to ground slopes	1125	10. Hypothetical drainage basin	1126
Geomorphic applications of hypsometric analysis	1128	11. Contour belt	1126
The geomorphic cycle	1128	12. Correlation of mean ground slopes and adjusted slopes of hypsometric curve segments	1127
Characteristics of the equilibrium stage	1130	13. True mean-slope curve of basin shown in Figure 8	1128
Relation of hypsometric forms to drainage forms	1136	14. Inequilibrium (youthful) stage	1129
Geologic factors affecting equilibrium forms	1136	15. Equilibrium (mature) stage	1130
Influence of horizontal structure	1139	16. Monadnock phase	1131
Practical applications of hypsometric analysis	1140	17. Mean hypsometric curves of five areas in the equilibrium stage	1132
References cited	1141	18. Representative basins from five sample areas	1133
		19. Stream numbers and bifurcation ratios for five sample areas	1137
ILLUSTRATIONS			
	Page		
Figure 1. Figure of reference in percentage hypsometric analysis	1119		

	Page	Plate	Facing page
20. Stream lengths and length ratios for five sample areas.....	1137	1. Model hypsometric curves for five values of r	1117
21. Hypsometric curves of three basins in Mesa Verde Region.....	1139	TABLES	
22. Hypsometric curves of three basins near Soissons, France.....	1140	1. Morphometric data for five sample areas..	1134
23. Hypsometric curves of large drainage basins.....	1140	2. Statistical data for mean integrals of five areas.....	1138

INTRODUCTION

Topography produced by stream-channel erosion and associated processes of weathering, mass movement, and sheet runoff is extremely complex, both in the geometry of the forms themselves and in the interrelations of the processes which produce the forms. Although the fluvial-erosional landforms constitute the largest proportion of the earth's land surfaces and therefore deserve intensive study, only in recent years have investigations moved from the rather limited phase of simple visual observation and generalized verbal descriptions to the more productive but vastly more refractory phase of quantitative description and dynamic analysis.

Dynamic-quantitative studies require, first, a thorough morphological analysis in order that the form elements of a landscape may be separated, quantitatively described, and compared from region to region. Drainage network characteristics and channel gradients, slope profile forms, declivities and lengths, drainage densities, and hypsometric properties are among the general classes of morphological information for which standardized measures must be set up so that the essential differences and similarities between regions can be understood. Second, the topographic forms must be related quantitatively to the rates and intensities of the denudational processes. These relationships may take the form of empirical equations derived by methods of mathematical statistics from the observational data, or deduced mathematical models whose validity is sustained by observed values.

The material in the present paper is merely one very small part of the morphological analysis. It concerns the investigation of hypsometric properties of small drainage basins—that is, area-altitude relationships and the

manner in which mass is distributed within a drainage basin.

Some parts of this paper represent work supported by the Penrose Bequest, Project Grant 525-48; but the greater part of the investigation was supported by the Office of Naval Research under Contract N6 ONR 271, Task Order 30, Project No. NR 089-042.

The writer is greatly indebted to Dr. W. W. Rubey, Chairman of the National Research Council, and Dr. Luna B. Leopold, Water Resources Division of the U. S. Geological Survey, for critically reading the manuscript and making many suggestions for its clarification. Mr. James L. Lubkin of the Columbia School of Engineering developed the model hypsometric function; Professor Robert Bechhofer and his staff of the Statistical Consulting Service of Columbia University advised the author on testing procedures.

PRINCIPLES OF HYPOMETRIC ANALYSIS

Hypsometric Curve in Absolute Units

Hypsometric analysis is the study of the distribution of ground surface area, or horizontal cross-sectional area, of a landmass with respect to elevation. The simplest form of hypsometric curve (hypsographic curve) is that in absolute units of measure. On the ordinate is plotted elevation in feet or meters; on the abscissa the area in square miles or kilometers lying above a contour of given elevation. The areas used are therefore those of horizontal slices of the topography at any given level. This method produces a cumulative curve, any point on which expresses the total area (reduced to horizontal projection) lying above that plane.

The absolute hypsometric curve has been used in regional geomorphic studies to show the presence of extensive summit flatness or terrac-

ing, where the surfaces lies approximately horizontal. Where these surfaces have a pronounced regional slope, they may not appear on the curve. Because a good topographic map, from which the hypsonetric curve was prepared, will usually show these features, the justification for an elaborate hypsonetric process for interpreting geomorphic history is doubtful.

For analysis of the form quality of erosional topography, use of absolute units is unsatisfactory because areas of different size and relief cannot be compared, and the slope of the curve depends on the arbitrary selection of scales. To overcome these difficulties, it is desirable to use dimensionless parameters independent of absolute scale of topographic features.

Percentage Hypsonetric Curve

Hypsonetric analysis, in general use for calculation of hydrologic information (Langbein *et al.*, 1947), takes a complete drainage basin above a selected point on a main stream as the area of study. The present study of form qualities of erosional topography likewise uses natural drainage basins, whether single or composite, on the assumption that the form of each drainage basin results from the interaction of slope-wasting and channel-deepening processes within the limits of the drainage divide, and hence that each basin should be treated as a unit.

Most drainage basins in homogeneous materials are pear-shaped in outline, with lateral divides converging to a clearly defined constriction, or mouth (Horton, 1941, p. 303). For hypsonetric study, a geometric unit of reference consists of a solid bounded on the sides by the vertical projection of the basin perimeter and on the top and base by parallel planes passing through the summit and mouth respectively (Fig. 1). Although both of these reference planes may be expected to change as the basin is denuded, they are real points which can always be determined.

The percentage hypsonetric method used in this investigation relates the area enclosed between a given contour and the upper (headward) segment of the basin perimeter to the height of that contour above the basal plane.

The method has been used by Langbein (1947) for hydrologic investigations. Two ratios are involved (Fig. 1): (1) ratio of area between the contour and the upper perimeter (Area *a*) to total drainage basin area (Area *A*), repre-

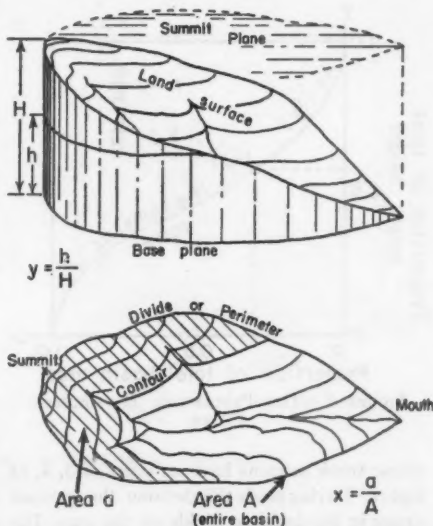


FIGURE 1.—FIGURE OF REFERENCE IN PERCENTAGE HYPSONETRIC ANALYSIS
Showing derivation of the dimensionless parameters used in Figure 2.

sented by the abscissa on the coordinate system. (2) Ratio of height of contour above base (*h*) to total height of basin (*H*), represented by values of the ordinate.

The resulting hypsonetric curve (Fig. 2) permits the comparison of forms of basins of different sizes and elevations. It expresses simply the manner in which the volume lying beneath the ground surface is distributed from base to top. The curve must always originate in the upper left-hand corner of the square ($x = 0, y = 1$) and reach the lower right-hand corner ($x = 1, y = 0$). It may, however, take any one of a variety of paths between these points, depending upon the distribution of the landmass from base to top.

Method of Obtaining Hypsonetric Data

Actual measurement and calculation of hypsonetric data have been done by the writer in

the following steps: First, the drainage basin is selected and outlined. Selection of the basin is influenced by the purpose of the investigation, which may call for a study of the first-order drainage basins or of composite basins

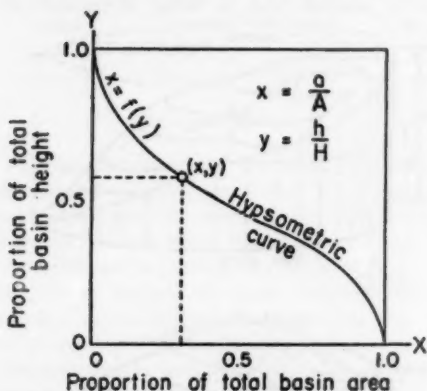


FIGURE 2.—THE PERCENTAGE HYPSEMERIC CURVE

whose trunk streams have an order of 3, 4, or higher.¹ Having made this decision, the operator draws in the drainage divide on the map. The divide is carried down to the stream at its point of junction with a stream of the same or higher order.

With a polar planimeter, the operator measures first the area of the entire basin, then the areas enclosed between each contour and the upper perimeter. Ratios are computed and will range from 1.0 to 0.0. Where relief is strong and contours closely crowded, every second or fifth contour is used, except near the summit where all available contours are used. Obviously the value of hypsometric analysis depends on use of sufficiently accurate and large-scale maps for the drainage basins involved. Where texture is fine and unit basins very small,

¹ Stream orders have been defined by Horton (1945, p. 281-283), but the writer has followed a somewhat different system of determining orders: The smallest, or "finger-tip", channels constitute the first-order segments. For the most part these carry wet-weather streams and are normally dry. A second-order segment is formed by the junction of any two first-order streams; a third-order segment is formed by the joining of any two second-order streams, etc. This method avoids the necessity of subjective decisions, inherent in Horton's method, and assures that there will be only one stream bearing the highest order number.

special field maps on a large scale must first be surveyed.

Height ratios are obtained by first determining the total range between basin mouth and summit point. The height of each measured contour above the mouth elevation is then determined and ratios to total basin height computed. These will range from 0.0 to 1.0 in inverse series to the area ratios.

The ratios are plotted on any convenient cross-section paper and the curve drawn smoothly with the aid of a draftsman's curve. For purposes of comparison with model curves illustrated in Plate 1, cross-section paper of 10 divisions per $\frac{1}{4}$ inch should be used, allotting a square 5 inches wide to the hypsometric graph.

Integration of the Hypsometric Function

In order to calculate the volume of earth material contained between the ground surface and the bottom and sides of the figure of reference (Fig. 1), the landmass may be thought of as consisting of horizontal slabs (Fig. 3). The total volume, V , consists of the sum of all slabs. The volume of one slab, ΔV , is obtained by multiplying the area of the slab, a , by its thickness, Δh . Following the mathematical principle of integration, the entire volume may be stated by the expression

$$V = \int_{\text{base el}}^{\text{summit el}} a \, dh.$$

If we now divide both sides of this equation by H and A , which are constant terms,

$$\frac{V}{HA} = \frac{1}{HA} \int_{\text{base el}}^{\text{summit el}} a \, dh$$

or

$$\frac{V}{HA} = \int_{\text{base el}}^{\text{summit el}} \frac{a}{A} d\left(\frac{h}{H}\right)$$

This expresses the ratio of volume lying beneath the surface, V , to the entire volume of the reference figure, HA . Because $\frac{a}{A} = x$, and $\frac{h}{H} = y$, by our definition, then

$$\frac{V}{HA} = \int_0^{1.0} xy \, dy.$$

Thus, if the hypsometric function, $x = f(y)$, is integrated between the limits of $x = 0$ and $x = 1.0$, a measure of landmass volume remaining with respect to volume of the entire

performed to obtain information useful in hydrologic and other applications.

Inspection of a large number of hypsometric curves has shown that the majority are s-

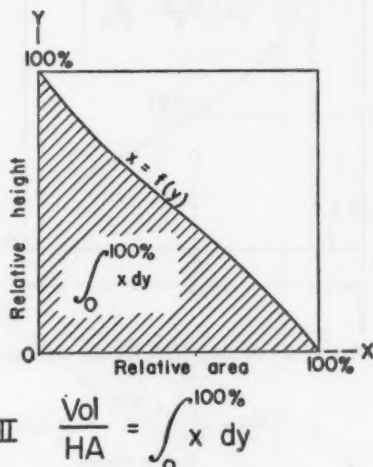
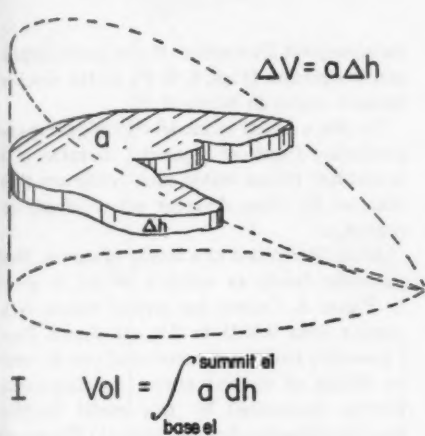


FIGURE 3.—INTEGRATION OF THE HYSOMETRIC FUNCTION
And meaning of hypsometric integral.

reference solid is obtained. This integral is here designated the hypsometric integral and is equivalent to the ratio of area under the hypsometric curve to the area of the entire square. It is expressed in percentage units and can be obtained from any percentage hypsometric curve by measuring the area under the curve with a planimeter. Whether the integration is of the function $y = f(x)$ or $x = f(y)$ is of no consequence. The latter function was used in this explanation because the unit slabs of volume are thought of as being horizontal, rather than vertical.

As discussed elsewhere in this paper, both the form of the hypsometric curve and the value of the integral are important elements in topographic form and show marked variations in regions differing in stage of development and geologic structure.

A Model Hypsometric Function

It is desirable to find a relatively simple, yet flexible function which may be fitted to any natural hypsometric curve. This is necessary so that certain mathematical operations can be

shaped. An up-concavity is commonly present in the upper part; a convexity in the lower part. Sinuosity varies greatly so that the slopes of the curves at their inflection points have a wide range. It is therefore necessary to use an equation having two parameters, one to vary the hypsometric integral, the other to control the sinuosity.

A function² which meets these requirements fairly well is

III $y = \left[\frac{d-x}{x} \cdot \frac{a}{d-a} \right]^r$

where a and d are constants, d always greater than a , and the exponent x , positive or zero (Fig. 4). All curves pass through A and B . The slope of the curve at its inflection point depends on the ratio $\frac{a}{d}$, hereinafter designated r . The general location of the curve depends upon the exponent x .

²The writer is indebted to Mr. James Leigh Lubkin of the School of Engineering of Columbia University for developing this equation. It was adapted from a somewhat similar equation used by Hunter Rouse (1937, p. 536) to describe the distribution of suspended load in a stream.

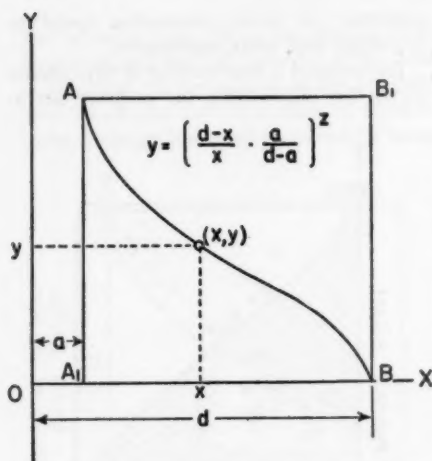


FIGURE 4.—MODEL HYPSEMERIC FUNCTION

abscissa as shown in Figure 4 should range from 0 at $x = a$ to 1.0 at $x = d$. This percentage, R is therefore expressed as

$$R = \frac{x - a}{d - a}$$

In subsequent illustrations of the model hypsometric equation (Figs. 5, 6; Pl. 1) the abscissa appears scaled in terms of R .

To plot a family of model curves having one particular degree of sinuosity, a value of r is selected; curves within each family are then obtained by using different values of the exponent, z .

As an illustration of a family of curves, that particular family in which $r = 0.1$ is given in Figure 5. Curves for several values of z , ranging from 0.0625 to 2.0, are shown. Plate 1 gives five families of curves and can be used for fitting of natural curves by inspection. Curves represented by this model function have the following characteristics (1) The curves are s-shaped where $z < 1$, but are of simple concave-up form where $z > 1$. (2) Where $z < 1$, curves entering at A have a slope, whereas they are tangent to the vertical through the point B.

Decreasing the value of r increases the degree of sinuosity of the curve, thereby reducing the slope of the curve in the region of inflection. This effect may be seen by studying individual curves for the families $r = 0.01, 0.05, 0.1, 0.25,$ and 0.5 (Fig. 6). For comparison, five curves were selected whose integral is approximately the same.

It is not practical to obtain the hypsometric integrals of theoretical curves by mathematical procedures, hence these were obtained by the writer by planimeter measurement for all curves plotted. On each model curve (Pl. 1), the integral is given. The values are only approximate, being subject to errors in measure-

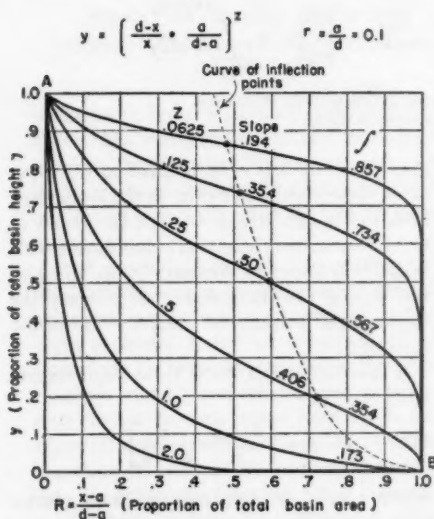


FIGURE 5.—FAMILY OF CURVES FOR THE VALUE, $r = 0.1$

For selected values of z . Given also are the integrals and the slope of each curve at its inflection point. (Other curve families are given in Plate 1.)

In order to have a percentage scale on the abscissa, conforming with the percentage hypsometric function as previously defined, a modification of equation III is introduced. It is desired that the scale of values on the

For plotting, the following form of equation III can be used:

$$IV \quad y = \left[\frac{r}{1-r} \right]^z \left[\frac{1}{(1-r)R+r} - 1 \right]^z$$

where r and R are as defined above. For a given curve, r and z are constants; hence, by substituting a series of values of R ranging from 0 to 1.0, the corresponding values of y may be obtained.

ment as well as errors in plotting the curves from which they were measured.

the second derivative of the function equal to 0. For plotting, it is convenient to find the inflec-

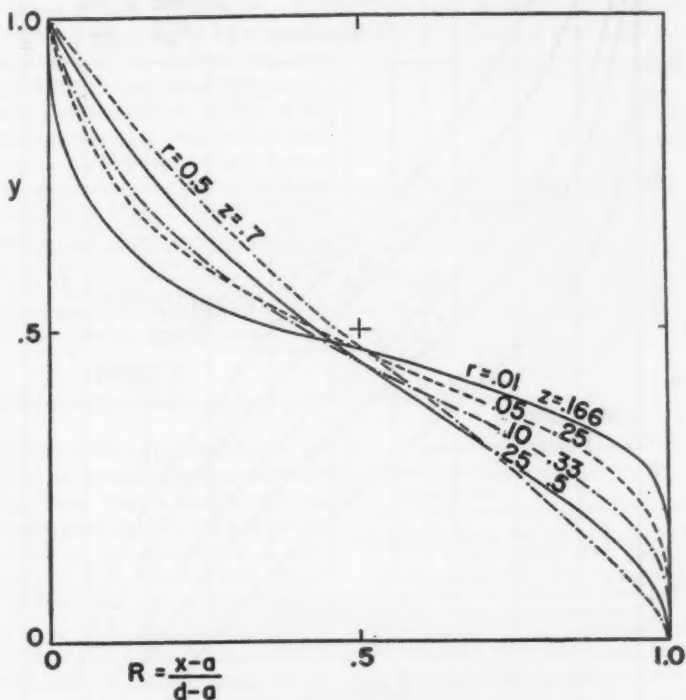


FIGURE 6.—COMPARISON OF SEVERAL CURVE FAMILIES

Showing the effect of varying the value of r in the model hypsometric function. Integrals of these curves are approximately the same.

Because one method of fitting model curves to natural hypsometric curves involves the matching of integrals, it is desirable to have a means of obtaining from a given integral the exponent, z , of a particular model curve which possesses that integral. A graphic solution is shown in Figure 7. Given an integral, measured by planimeter from a natural hypsometric curve, and having selected by inspection the curve family whose value of r gives the closest fit as to shape, one can read the desired value of z .

Inflection Points and Slopes

The point of inflection on any of the model hypsometric curves where z is less than 1.0 may be obtained by the usual method of setting

tion point in terms of R in Equation IV, as the following equation:

$$R_i = \frac{1 + z - 2r}{2(1 - r)}$$

where R_i is the value of R at which the curve inflects. Inflection points and the curves on which they lie are shown on the graphs for the several values of r (Fig. 5; Pl. 1).

Inflection points have morphological significance on hypsometric curves because they mark the level at which the rate of decrease of mass upwards changes from an increasingly rapid rate of decrease to a diminishing rate of decrease. Further investigation may prove this feature to be related to dynamic factors, such as the relative importance of sheet runoff

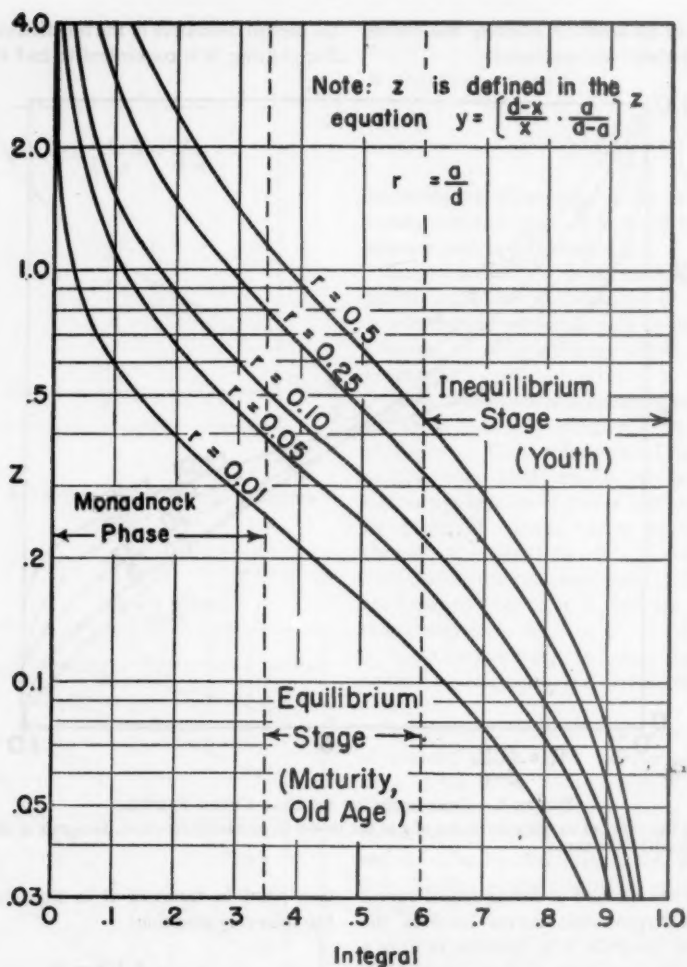


FIGURE 7.—GRAPHIC SOLUTION OF INTEGRALS AND EXPONENTS
For curve families produced by five selected values of r . (See Plate 1 for further data.)

and creep at higher levels compared to channel erosion at lower levels.

While the position of the inflection point on a natural hypsometric curve is greatly affected by chance irregularities of form not significant in the gross aspect of the drainage basin, the slope of the curve in the general region of the inflection can be expected to be a reliable form element. Comparisons of the curve families show that slope at the inflection point is steep where r has high values and diminishes as r

decreases. For the curve family $r = 0.5$, the slopes approach 80 per cent near the center of the diagram, while for the family $r = 0.01$ they are reduced to about 30 per cent.

Hypsometric slope at the inflection point is thus a form characteristic which can be rapidly determined and used as one means of fitting natural to model curves. When the slope of the natural curve in the vicinity of its inflection point has been measured, the curve can be matched to the family having a similar slope.

Then, by matching integrals, the particular value of s can be determined.

Precise values of slope at inflection points can be determined from Equation IV by taking the first derivative of the function and substituting for R the various values of these inflection points already obtained. In view of the labor of calculation involved and the fact that exact values are not required for any uses of hypsometric analysis thus far made, the slopes listed opposite each integral on the graphs were determined by direct angular measurement from the graphs. These are, of course, subject to errors in the use of the protractor on a curve drawn through a number of plotted points.

Relation of Hypsometric Curve to Ground Slope

Characteristics of the hypsometric curve are closely related to ground-slope characteristics of a drainage basin. This is evident from the fact that steepening of slopes in the mid-section of a basin will be accompanied by a more rapid rate of change of elevation with respect to change of horizontal cross-sectional area of the basin. One might, at first thought, suppose that steep parts of the hypsometric curve would coincide with belts of relatively steep slopes, gently sloping parts of the curve with gentle ground slopes. Unfortunately the relationship is not so simple. Figure 8 shows a small drainage basin; Figure 9 is the corresponding hypsometric curve. The curve has a gentle slope in the upper part, corresponding with a broad divide area on the map. The steep intermediate part of the hypsometric curve corresponds with steep valley wall slopes in the mid-section of the basin. But the very lowest part of the curve is steepest of all in the region corresponding to the mouth area of the basin, whereas the contours of the map show that the ground slopes are less here than in the mid-section of the basin. The additional factor is, of course, the length of the belt between successive pairs of contours. ("Length" refers to distance along the contour.) Only if each contour belt is the same length can steepness of ground slope vary directly as steepness of hypsometric curve. In Figure 10, all contours have the same length, and the slope profile is

identical with the hypsometric curve. Obviously a drainage basin cannot fulfill this condition while narrowing to a mouth through which all drainage is discharged by a narrow

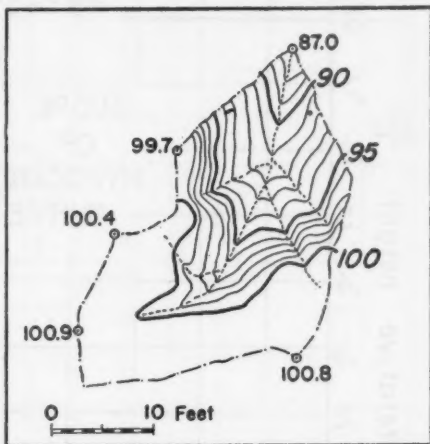


FIGURE 8—SMALL DRAINAGE BASIN IN BADLANDS, PERTH AMBOY, NEW JERSEY
From a special large-scale topographical survey.

channel; a shortening of the length of contours to a minimum approaching zero is required as the drainage basin is followed to its mouth. At the upper end of the drainage basin, the contours can maintain nearly equal length up to the divide (which may be horizontal), but normally the contour length diminishes here, too, to approach zero on the highest peak. Thus the characteristic steepening of hypsometric curves both at the lower and upper ends in mature topography is explained by the diminishing contour lengths.

To relate hypsometric curve to ground slope it is necessary to take contour length into account. First, the length of each contour line is measured. For each belt of ground between two successive contours the lengths of the upper and lower contours are added and the sum divided into two, giving a rough mean length for the contour belt (Fig. 11). Next the area of the contour belt is measured by planimeter. Dividing area of the contour belt by mean length gives a rough mean width (horizontal distance) for the belt. Now, by dividing the contour interval by the mean width we can

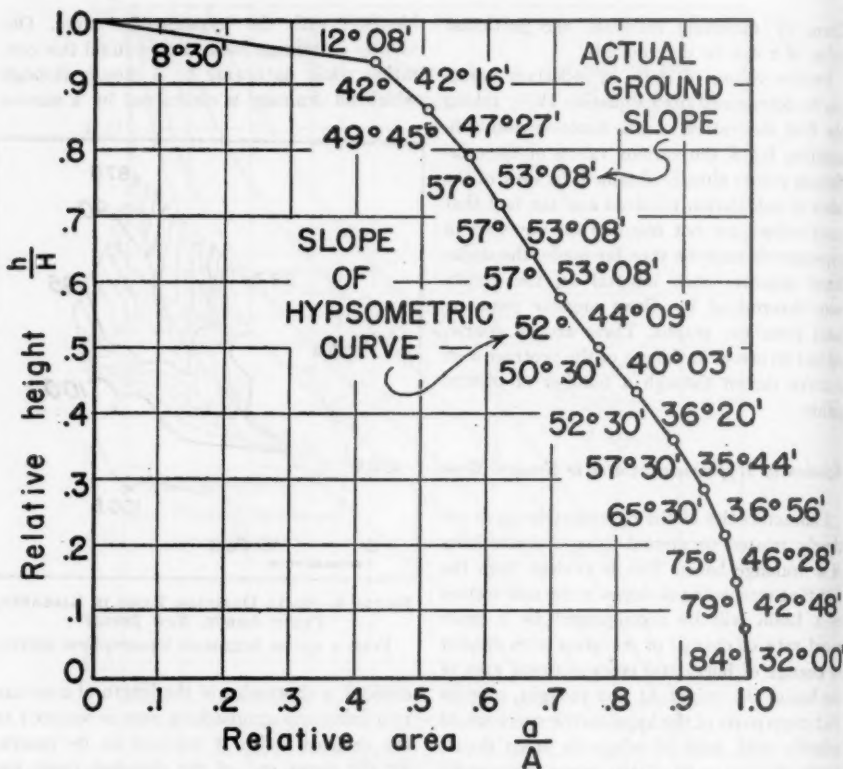


FIGURE 9.—HYPSONETRIC CURVE OF BASIN SHOWN IN FIGURE 8
Showing relation between slope of segments of hypsometric curve and actual mean ground slopes of corresponding segments.

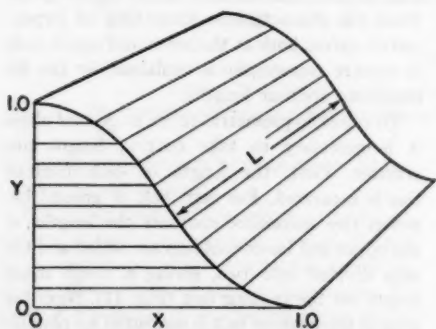


FIGURE 10.—HYPOTHETICAL DRAINAGE BASIN
In which slope of hypsometric curve is identical with ground-slope curve.

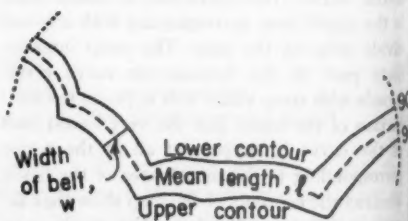


FIGURE 11.—CONTOUR BELT
Showing method of calculating mean length, width, and slope of contour belt.

determine the mean slope of the ground within this particular contour belt, for, $\tan \alpha = \frac{h}{w}$

SLOPE OF HYPSONETRIC CURVE X 1/L

where
 α is
 h is
 w is
 horizon
 Valu
 shown
 hypson
 ticular
 calcula
 the sl
 rough
 If, hor
 slope:
 basin,
 the co
 where
 Rela

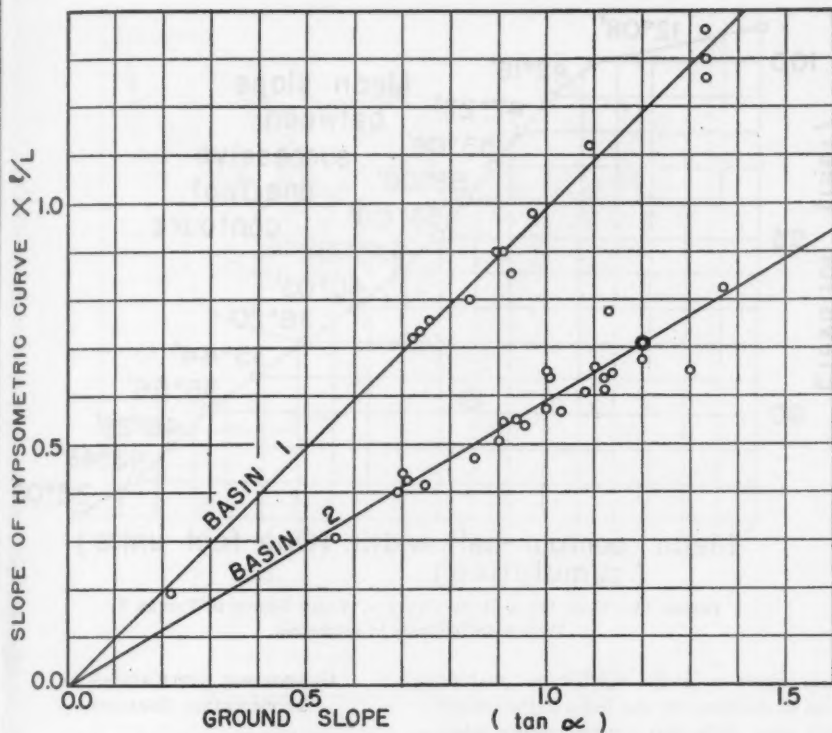


FIGURE 12.—CORRELATION OF MEAN GROUND SLOPES AND ADJUSTED SLOPES OF HYPSONETRIC CURVE SEGMENTS
Basin 1 same as that in Figures 8 and 9.

where

α is angle of ground slope,

h is contour interval

w is mean width of the belt measured in horizontal projection.

Values of mean slope angle for the basin shown in Figure 8 are written directly on the hypsonetric curve (Fig. 9) opposite the particular segments to which they relate. The calculated mean slope figures compared with the slope of the hypsonetric curve shows rough correspondence only in the upper part. If, however, we correlate the mean ground slope figures with the contour map of the basin, the slope angles vary as the spacing of the contours, being highest in the midsection, where slopes up to 53° are found.

Relationship of hypsonetric curve to mean

ground slopes may be summarized by the following equation, which takes into account relative length of each contour belt.

$$VI \quad \frac{l}{L} \tan \theta = \kappa \tan \alpha$$

where θ = slope of hypsonetric curve

α = mean ground slope

l = contour length at given relative height

L = length of longest contour in basin

κ = a constant

To test the usefulness of this equation, the values of ground slope have been plotted against corresponding values of hypsonetric curve slope for each contour interval of the drainage basin (Fig. 12, Basin 1). Also plotted on Figure 12 are corresponding data for a second drainage

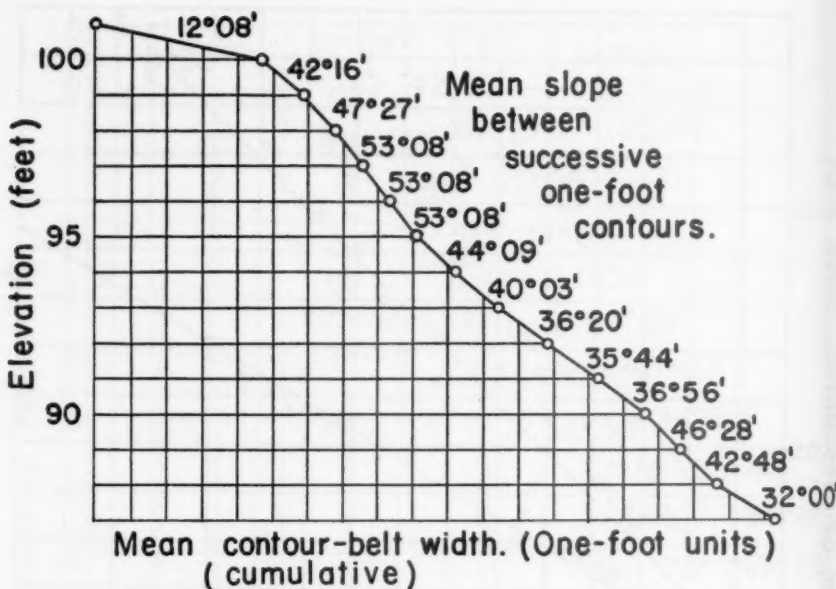


FIGURE 13.—TRUE MEAN-SLOPE CURVE OF BASIN SHOWN IN FIGURE 8
Abscissa and ordinate on same scale.

basin which is in the equilibrium (mature) stage of development and has a narrow divide ridge crest. Note that the two curves, which were fitted by inspection, pass through the origin but have markedly different slopes, which may be attributed to the difference in stage of development of the two basins. The tangent function is extremely sensitive to small errors of horizontal measurement, and, because the range of error in measurement from the map is relatively large, the values are subject to considerable variation. Hence these correlation diagrams should be thought of as only demonstrating the general validity of Equation VI.

A profile of the true mean ground slope (Fig. 13) is a cumulative plot of mean-slope angles for each contour belt. This curve differs from the hypsometric curve of the same basin (Fig. 9) in that the mean-slope curve is plotted with absolute values, the scale of feet being the same on both ordinate and abscissa. By use of this curve, ground slope distribution with respect to height can be depicted for direct visual analysis, inasmuch as the slope of the curve is the actual mean ground slope.

GEOMORPHIC APPLICATIONS OF HYPSOMETRIC ANALYSIS

The Geomorphic Cycle

The hypsometric curve exhibits its widest range of forms in the sequence of drainage basins commencing with early youth (inequilibrium stage), progressing through full maturity (equilibrium stage), and attaining temporarily the monadnock phase of old age.

A drainage basin in youth is shown in Figure 14. It is from the Maryland coastal plain where a large proportion of upland surface has not yet been transformed into valley-wall slopes. The hypsometric curve has a very high integral, 79.5%, indicating that about four-fifths of the landmass of the reference solid remains. Despite the bold convexity of the curve through its central and lower parts, the upper end has the concavity typical of nearly all normal drainage basins, and shows that some relief does exist in the broad divide areas.

Figure 15 represents a small drainage basin in fully mature topography of the Verdugo

Dr
curve
Hills,
narro
surfa
proxi
with
smoo
typic
tively
In
despi

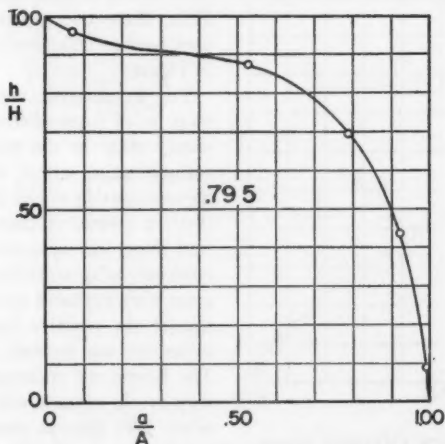
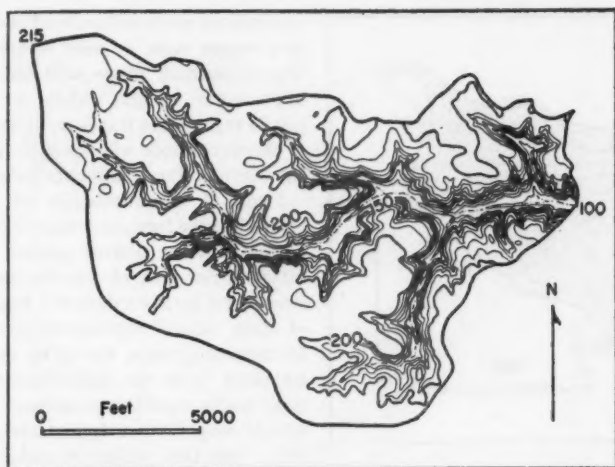


FIGURE 14.—INEQUILIBRIUM (YOUTHFUL) STAGE

Drainage basin of Campbell Creek on the Maryland Coastal Plain (above) with its hypsometric curve (below). From Yellow Tavern Quadrangle, Virginia, U. S. Geological Survey, 1:31,680.

Hills, southern California. Here divides are narrow and no vestiges remain of an original surface. The hypsometric curve passes approximately across the center of the diagram, with a hypsometric integral of 43%, and is smoothly s-shaped. This particular curve is typical of third- or fourth-order basins in relatively homogeneous rocks.

In late mature and old stages of topography, despite the attainment of low relief, the hypso-

metric curve shows no significant variations from the mature form, and a low integral results only where monadnocks remain. For example, a drainage basin in northern Alabama where low relief has developed on weak shales and limestones, but with prominent monadnock masses of sandstone which are outliers of a retreating escarpment, has a strongly concave hypsometric curve; the integral, 17.6%, is unusually low (Fig. 16). After monad-

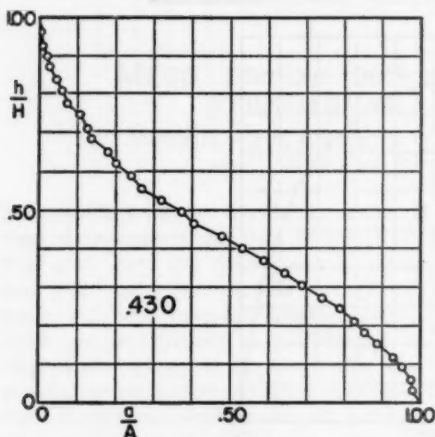
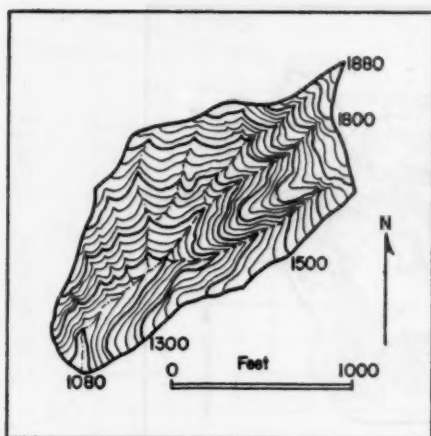


FIGURE 15.—EQUILIBRIUM (MATURE) STAGE. A small drainage basin in the Verdugo Hills, near Burbank, California (above), corresponding hypsometric curve (below). From Sunland Quadrangle, California, U. S. Geological Survey, 1:24,000.

nock masses are removed, the hypsometric curve may be expected to revert to a middle position with integrals in the general range of 40% to 60%.

From the standpoint of hypsometric analysis, the development of the drainage basin in a normal fluvial cycle seems to consist of two major stages only; (1) an inequilibrium stage of early development, in which slope transformations are taking place rapidly as the drainage system is expanded and ramified. (2) An equilibrium stage in which a stable

hypsometric curve is developed and maintained in a steady state as relief slowly diminishes. The monadnock phase with abnormally low hypsometric integral, when it does occur, can be regarded as transitory, because removal of the monadnock will result in restoration of the curve to the equilibrium form.

Figure 7 shows relations of hypsometric integral, curve form, and stage of development. Values of z are plotted against hypsometric integrals for each of five families of curves represented by five values of r . From inspection of many natural hypsometric curves and the corresponding maps, the writer estimates that transition from the inequilibrium (youthful) stage to the equilibrium (mature) stage corresponds roughly to a hypsometric integral of 60%, but that where monadnocks become conspicuous features the integrals drop below 35%. These two percentages have, therefore, been used as tentative boundaries of the stages in Figure 7.

The hypsometric curve of the equilibrium stage is an expression of the attainment of a steady state in the processes of erosion and transportation within the fluvial system and its contributing slopes (Strahler, 1950). In this state, a system of channel slopes and valley-wall slopes has been developed which is most efficiently adapted to the reduction of the land-mass with available erosional forces, balanced against the resistive forces of cohesion maintained by the bedrock, soil, and plant cover. The basins are no longer expanding in area; they are in contact with similar basins on all sides. The general similarity among hypsometric curves of regions in the equilibrium stage, despite great differences in relief, drainage density, climate, vegetation, soils, and lithology, seems to show that the distribution of mass with respect to height normally follows the s-shaped model hypsometric curve with its upper concavity and lower convexity.

Characteristics of the Equilibrium Stage

Five areas were selected which showed a great range of relief, and for which excellent large-scale topographic maps and air photographs were available. Within each area, six basins of the third or fourth order were outlined and the hypsometric curves plotted for each. A mean curve for each area was obtained

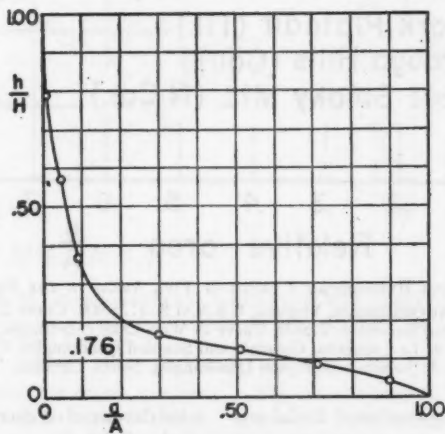
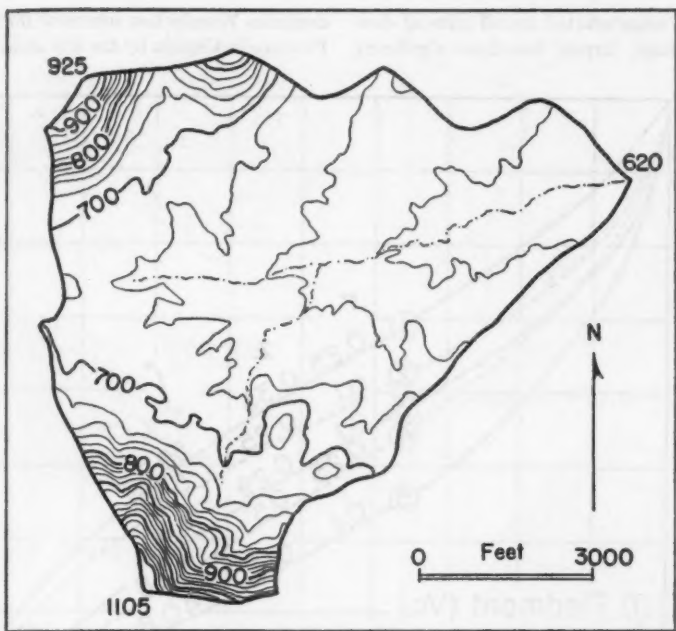


FIGURE 16.—MONADNOCK PHASE

Drainage basin of Atwood Branch, Newburgh Quadrangle, Alabama (above) showing remnants of retreating sandstone escarpment; corresponding hypsometric curve (below).

by plotting the arithmetic means of the ordinates of the six individual basin curves at every ten per cent division on the abscissa (Fig. 17). Figure 18 shows one drainage basin from each of the five areas; that basin was selected whose hypsometric curve most closely

follows the mean curve shown in Figure 17. In this way the reader can visualize the appearance of a drainage basin embodying the characteristics of the mean hypsometric curve. Table 1 gives additional data relating to composition of the drainage systems.

The five areas selected are all areas of denudritic drainage, largely free from significant cambrian Wissahickon schists of the Piedmont Province in Virginia by the first area: moderate

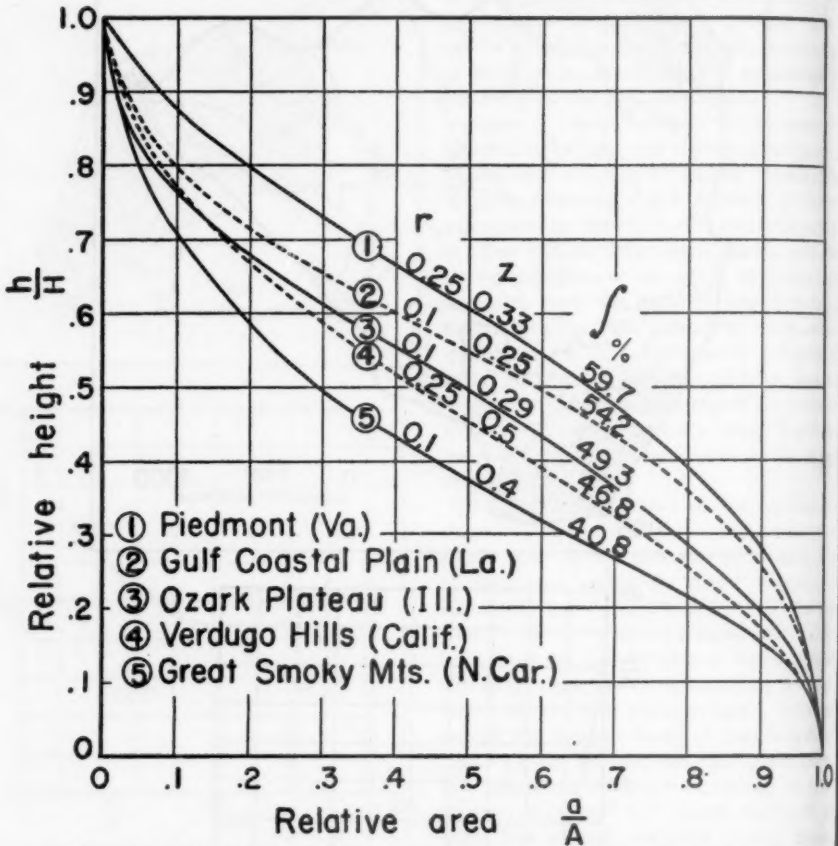


FIGURE 17.—MEAN HYPSEMERIC CURVES OF FIVE AREAS IN THE EQUILIBRIUM STAGE

Curve 1: from Belmont Quadrangle, Virginia, U.S.A.M.S. 1:25,000. Curve 2: from Mittie Quadrangle, Louisiana, U. S. Geological Survey, 1:24,000. Curve 3: Wolf Lake Quadrangle, Illinois, U. S. Geological Survey, 1:24,000. Curve 4: La Crescenta, Glendale and Sunland Quadrangles, California, U. S. Geological Survey, 1:24,000. Curve 5: Judson and Bryson Quadrangles, North Carolina, T.V.A., 1:24,000.

structural control. Long-continued fluvial erosion has removed all traces of flat interstream uplands and it is assumed that the basins are stable in form and that the total regimen of erosion and transportation processes is in a steady state. In relief, lithology and rock structure, vegetation, and climate, however, the five areas differ widely. Extremely low relief on weak Pliocene deposits of the Citronelle formation in western Louisiana is represented by the second area; low relief on Pre-

relief developed on cherts and cherty limestones of the Ozark Plateau province is exemplified by the third area. Extremely rugged terrain of strong relief and steep slopes on deeply weathered metasediments of the lower coastal ranges of the Los Angeles region is seen in the fourth area; great relief with moderately steep slopes on deeply weathered Precambrian Wissahickon schists of the southern flank of the Great Smoky Mountains in the fifth area.

Investigation of the five areas involved

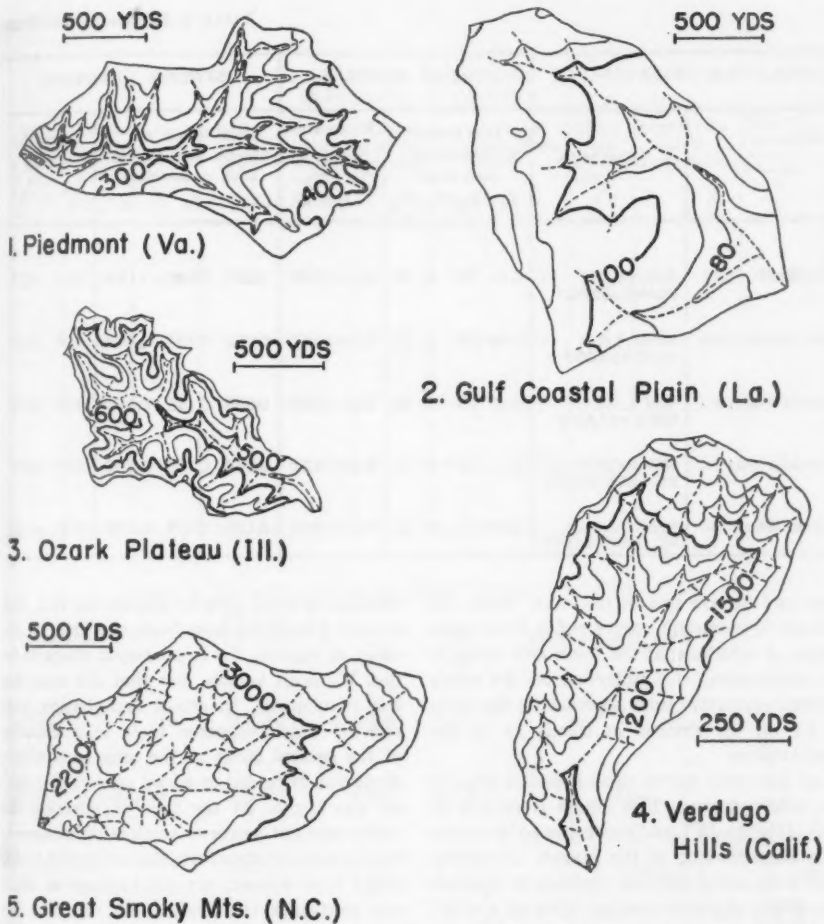


FIGURE 18.—REPRESENTATIVE BASINS FROM FIVE SAMPLE AREAS

[Showing the one drainage basin whose hypsometric curve most closely fits the sample mean curve of Figure 17. Localities as described in Figure 17.]

(1) analysis of the hypsometric curves, similarities and differences, and their degree of resemblance to the model hypsometric function; (2) a comparison of hypsometric data with other categories of data, such as drainage network and slope characteristics. It was hoped that significant differences in the hypsometric curves could be correlated with significant differences in other drainage basin characteristics, and that this might provide clues to causative factors determining the hypsometric properties of mature topography.

The mean curves shown in Figure 17 have appreciable differences both in hypsometric integral and in form. The mean curves were fitted to the theoretical function by inspection, and the apparent best fits are described on the curves and in Table 1 by values of r and s . All five curves were best described by the families having r values 0.1 or 0.25 and we may infer that mature topography in relatively homogeneous materials tends to fall within this general range. Fit was very good for curves 1 and 5, but was good only in the inflection

TABLE 1. MORPHOMETRIC DATA

LOCALITIES INVESTIGATED		STREAM NUMBERS				STREAM LENGTHS						
	Quadrangle	Total number of Streams of each order				Bifurcation Ratio: r_b		Mean length of Stream segments of each order: Miles			Length Ratios	
		Σn_1	Σn_2	Σn_3	Σn_4	$\frac{\Sigma n_1}{\Sigma n_2}$	$\frac{\Sigma n_2}{\Sigma n_3}$	l_1	l_2	l_3	$\frac{l_1}{l_2}$	$\frac{l_2}{l_3}$
1. Piedmont	Belmont, Va. USAMS 1:25,000	141	34	6	0	4.15	5.67	0.234	0.345	1.130	1.47	3.27
2. Gulf Coastal Plain	Middle, La. USGS 1:24,000	96	27	8	(2)	3.55	3.37	0.260	0.427	0.844	1.65	1.97
3. Ozark Plateau	Wolf Lake, Ill. USGS 1:24,000	198	36	10	(4)	5.21	3.80	0.099	0.132	0.368	1.33	2.79
4. Verdugo Hills	Glendale, Surland, Cal. USGS 1:24,000	201	38	9	0	5.29	4.22	0.082	0.116	0.295	1.87	2.54
5. Great Smokies	Bryson, Judson, N.C. USGS 1:24,000	389	87	24	6	4.47	3.62	0.115	0.185	0.269	1.61	1.60

zone and at one end in the other three. All natural hypsometric curves suffer from some degree of misfitness at the lower end owing to the development of a valley-bottom flat which prevents the curve from approaching the value of 1.0 on the abscissa as closely as on the model curves.

All five mean curves show a similar slope in the inflection zone. This ranges from 0.52 to 0.65 ($27\frac{1}{2}^\circ$ to 33°), and may prove to be a common characteristic of the mature or equilibrium form, along with the tendency to resemble the family of curves having values of r of 0.1 to 0.25. Note also that the location of the inflection point of the curve is generally higher for the areas of low relief (Nos. 1-3) than in the areas of great relief (Nos. 4 and 5). Within any one of the families of model curves, the inflection point likewise moves down as the integral diminishes, but in the five mean curves shown here the inflection points all tend to be located higher than in the model curves to which they were fitted.

Because each of the mean curves represents a sample of only six basins, and the differences, while conspicuous on the graph, are not great, it might well prove that the differences between integrals are not statistically significant, but might result from expectable variations

inherent in small samples despite the fact that no real differences exist from one area to the other as regards the hypsometric characteristics. We must assume first that the sampling was randomized. In actual fact, basins were selected which appeared most representative of the general facies of the area as a whole. None was discarded or added after data analysis was begun. At the time of selection the writer was not aware of possible differences in hypsometric or other form characteristics which might later appear, nor did he have in mind any particular trend which he expected the analysis to reveal. The selection, therefore while not mechanically randomized, is thought to be free of conscious prejudice.

Table 2 gives the sample mean, estimated standard deviation of the population (s), and standard error of the mean (s_x) for each sample, consisting of the hypsometric integrals of the six individual basin curves. The table also shows the percentage probabilities of any two samples being drawn from a population with the same mean. The significance test is based upon the t distribution, which is used for small samples. In this instance all tests involved samples of 6 and the table of t is entered under the heading of 10 degrees of freedom. The probability stated is that representing the area

DATA FOR FIVE SAMPLE AREAS

DRAINAGE DENSITY				CHANNEL GRADIENTS		GROUND SLOPES		HYPSONETRIC CURVE				
Total Area of 6 basins in each locality (sq. mi.)	Total Stream Lengths ΣL (miles)	$D_d = \frac{\Sigma L}{A}$	Mean basin height H (feet)	Mean Stream Gradient of 3rd order Streams:		Valley-Wall Slopes, Mean value		Mean Sub-surface integral \int	Best fit to model hypso. function		Slope of hypsonetric curve at inflection point %	
				% (tan)	Degree	Degree	%		r	Z		
327	7.47	51.59	6.90	175.0	0.0113	0° 39'	9.9°	.1745	5968	0.25	.333	.6009
157	9.58	44.40	4.64	61.0	0.0033	0° 10'	3.4°	.0594	5420	0.10	.25	.5317
279	2.26	31.10	13.78	326.0	0.0352	1° 52'	28° 15'	.537	4928	0.10	.29	.5890
254	0.77	20.28	26.17	875.8	0.2246	12° 40'	44.7°	.9896	4684	0.25	.50	.6494
160	5.14	72.71	14.16	1880.2	0.1233	7° 02'	41° 15'	.867	4084	0.10	.40	.5206

TABLE 2. STATISTICAL DATA FOR MEAN INTEGRALS OF FIVE AREAS*

LOCALITY	MEAN INTEGRAL %	S	Sx	PROBABILITY			
1. PIEDMONT, VA.	59.27	6.55	2.67	.16	.016	.005	<001
2. GULF COASTAL PLAIN, LA.	54.01	5.20	2.12				
3. OZARK PLATEAU, ILL.	48.91	5.67	2.31	.14	.026	.004	
4. VERDUGO HILLS, CAL.	46.52	4.58	1.87	.44	.036		
5. GREAT SMOKY N. CAR.	40.61	5.88	2.40	.08			

*Showing means, estimated standard deviation of the population, s, and standard error of the mean, s_x, as estimated from the sample. Probability figures refer to results of t tests of significance of difference in sample means of each pair indicated by bracket. Although integrals are here ranked in descending order, as in Figure 17, the probability figures have no relationship to ranking significance. Probability figure tells only the percentage of times that sample means drawn repeatedly from the same pair of areas will differ by this amount or more through chance variations in sampling alone, assuming that no real difference in the two population means actually exists.

under both tails of the t distribution curve, and hence tells the probability of obtaining differences of sample means as great as, or greater than, the observed differences, with the possibility of either mean being the larger.

Note that, in Table 2, no significant difference is found between means of any two samples whose mean integrals differ by only 5 or 6% or less, but is present when the means differ by 8% or more. While we cannot easily deter-

mine the significance of the ranking, or the probability of rearrangements being likely to occur in the ranking if similar samples of six basins were repeatedly drawn, we can perhaps safely infer that any two consecutive members of the series might readily reverse their order if another set of samples was taken, but that it is most unlikely that one of the last two members of the series could switch places with the first two.

Relation of Hypsometric Forms to Drainage Forms

It is not immediately apparent just why any two integrals of the mean hypsometric curves should differ significantly, or why they should fall into the general sequence which they take. In an effort to obtain clues to this problem, measurement was made of the stream number and length characteristics, drainage density, slopes, relief, and stream gradients. These data are tabulated in Table 1. A number of observations relating to correlation, or lack of correlation, among the various form factors of the topography are as follows:

In general, drainage basin height, slope steepness, stream channel gradients and drainage density show a good but negative correlation with the integral of the hypsometric curve. We may say that mature basins of low relief, gentle slopes, gentle stream gradients, and low drainage density tend to have relatively high integrals; that areas of strong relief, steep slopes, steep stream gradients, and high drainage density tend to give relatively low integrals in the average drainage basin of the third or fourth order. Table 1 bears this out well if over-all trend of the series is considered, but the values of areas 1 and 2 are in reverse order, as are the values of areas 4 and 5. As already stated, however, differences of integral in these two pairs of samples are not significant (see Table 2) and they might easily exchange positions on the list if another sample were taken. What is significant is that Nos. 1 and 2 show very much lower values of drainage density, basin height, slope steepness, and stream gradient than do Nos. 4 and 5, while No. 3 occupies an intermediate position in all cases.

No correlation seems to exist between hypsometric integrals and either bifurcation ratios or

length ratios (Figs. 19, 20). Horton (1945, p. 290) states that bifurcation ratios range from about 2 for flat or rolling country up to 3 or 4 for mountainous regions. The writer's data, based on large-scale maps checked in the field or by stereoscopic study of air photographs, show not only considerably higher ratios, but a complete lack of correlation of ratio with relief. Horton's data were taken from comparatively crude, small-scale maps and he must have omitted a large proportion of the stream channels of first and second order which actually exist.

A positive correlation is evident between the average length of the stream segments of any given order in each area and the corresponding mean hypsometric integrals. Figure 20, in which mean stream lengths are plotted against order numbers, shows progressive decline in stream length from left to right, in the same order as that in which the integrals diminish. Although reversals occur in the trends of the first and second order lengths, the values for areas 1 and 2 are always higher than those of areas 3, 4, and 5.

Because length of stream segments tends to become less as drainage density increases, it is only to be expected that the first two areas, whose texture is coarse, would have longer stream segments than the last three areas, whose texture is much finer. Now, since the mean integrals decrease as drainage density increases, the effect is to give a positive correlation between mean stream segment lengths and mean hypsometric integrals.

Geologic Factors Affecting Equilibrium Forms

Turning from a purely quantitative analysis of the various categories of morphometric data to a qualitative approach, there are several topographic and geologic factors apparent to the investigator to which he can attribute certain of the differences in hypsometric curve forms.

The extreme members of the series (curves 1 and 5, Fig. 17) are developed on essentially similar types of rock, mapped as the Wissahickon schist. A *t* test of significance of difference of sample mean integrals (Table 2) shows a probability less than .001, leading us to discard the hypothesis that both samples have

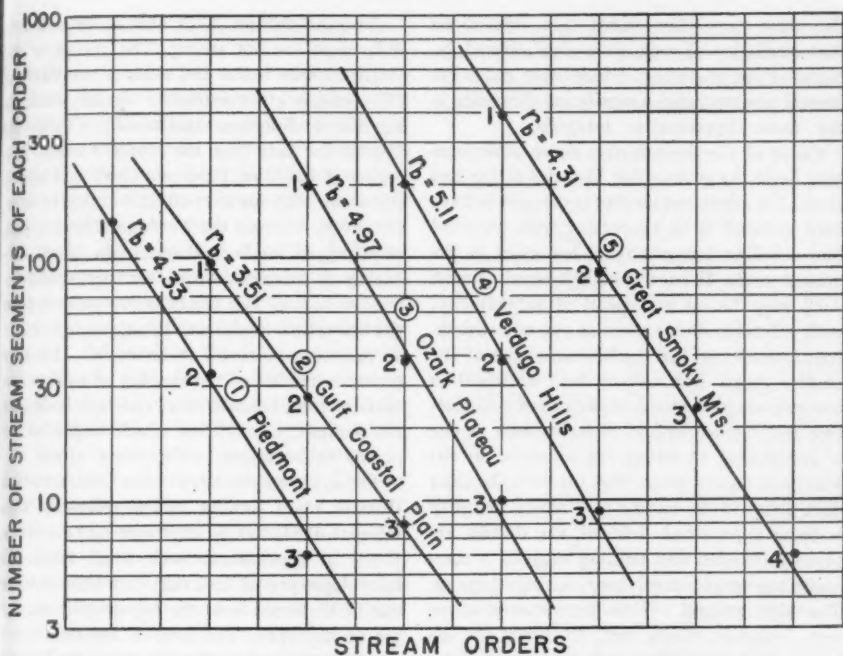


FIGURE 19.—STREAM NUMBERS AND BIFURCATION RATIOS FOR FIVE SAMPLE AREAS

Fitted curve has slope of bifurcation ratio, r_b , whose mean value is given for each area. Number beside each dot is order number.

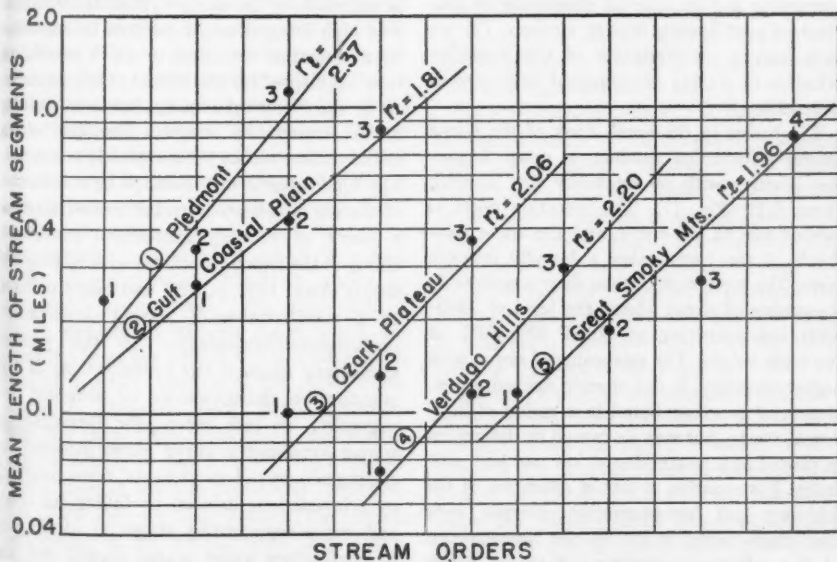


FIGURE 20.—STREAM LENGTHS AND LENGTH RATIOS FOR FIVE SAMPLE AREAS

Fitted curve has slope of length ratio, r_l , averaged for each area. Number beside each dot is order number.

the same population mean. The hypothesis that similarity of rock gives similarity of integral is not sustained. Some other cause (or causes) has produced a significant difference in the mean hypsometric integrals.

Cause of the hypsometric curve differences may lie in the geomorphic histories of the two areas. The Piedmont locality is thought to have been reduced to a peneplain, then dissected into a rolling topography of low relief in the present cycle. If so, the high integral (almost 0.60) may be an expression of submaturity, with extensive divide areas as yet not entirely transformed into the equilibrium slopes of the mature stage. But neither field examination nor map-air photograph study shows a distinctive unconsumed upland element, such as one is accustomed to seeing, for example, on the Maryland coastal plain (Fig. 14) or in the older drift plains of the middle west where maturity is being approached. Instead, the divides are broadly rounded and nothing suggests a composite topography involving two distinct cycles. The high integral of this hypsometric curve may, however, mean that, following the attainment of an equilibrium system, an acceleration of stream corrosion associated with increasing relief set in, perhaps induced by regional upwarping and an over-all steepening of gradient of east-flowing master streams. Do we have here a manifestation of the Penckian principle of waxing development (*aufsteigende Entwicklung*)?

The basins in the south flank of the Great Smoky Mountains produce a mean hypsometric curve with an unusually low integral, about 0.40 (Fig. 17). The inflection point is located low on the curve, and the upper two-thirds of the curve takes a broadly concave form. The topographic maps show a noticeable steepening of slopes above the level of 2800-3000 feet occurring at about 40%-50% of the basin height. The steepening of slopes with higher elevation is not sharply defined, as in structural benching found in a region of horizontal strata, but may be caused by differences in rate of rock weathering at low and high altitudes. For example, if rate of alteration of the feldspars and ferromagnesian minerals were appreciably faster in the warmer temperatures of the valleys, an opening out of the valley bottoms might perhaps be expected.

Among localities 2, 3, and 4, hypsometric differences are not strong. The curves of the Ozark Plateau basins and those of the Verdugo Hills basins are remarkably similar, with no significant difference statistically (Table 2), despite the fact that the Ozark Plateau is a region of flat-lying Paleozoic chert and cherty limestone with an over-all uniformity of summit levels, whereas the Verdugo Hills are part of a rugged, up-faulted mountain block consisting of metamorphosed sediments and intrusive bodies. The Ozark curve departs from the theoretical function at the upper end, where an excessive concavity is developed. This may be an expression of the sapping of weaker formations from beneath more resistant beds near the summit, a condition which might be expected in horizontal sedimentary strata.

The hypsometric curve of the Louisiana Gulf Coastal Plain locality has a relatively high integral, 0.54, but is otherwise quite conventional in appearance. Such small relief and faint slopes prevail here that very little of value can be discerned from the topographic map or air photographs. The area is located within the belt assigned to the Montgomery Terrace of Sangamon age by Fisk (1939, p. 193) at elevations from 120 to 140 feet. The surface is underlain by the sandy Citronelle formation. The high integral might perhaps be explained by a submature condition, in which insufficient time has elapsed for attainment of full maturity. As in the Piedmont locality, however, nothing in the topography suggests remnants of an initial surface not as yet completely consumed. The high integral may perhaps be a reflection of slightly accelerated stream erosion rates as a result of recently accelerated southward tilting of the region associated with epeirogenic uplifts (Fisk, 1939, p. 199) and might perhaps be a manifestation of waxing development (*aufsteigende Entwicklung*). At the present elementary stage of our investigations of the quantitative characteristics of erosional topography, we lack criteria for distinguishing among hypsometric curve forms modified by epeirogenic crustal movements, those modified by rejuvenations induced by falling sea level, and those representing stages in attainment of equilibrium under stable crustal and sea level conditions.

Influence of Horizontal Structure

It is obvious that drainage basins developed in horizontally layered rocks, whether sedimentary strata or lavas, will have strongly modified hypsometric curves if there are marked differences in rock resistance on a scale which is large in proportion to the height of the basin. In the region of cherts and cherty limestones of the Ozark Plateau Province, described above as one of the mature areas in apparently homogeneous materials, structural benching did not seem to produce any conspicuous influence in the hypsometric form. Let us turn, then, to a contrasting example, where structural control is predominant: the regions of cliffs, buttes, and mesas of the southern Mesa Verde, located in northwestern New Mexico, within the Rattlesnake and Chimney Rock quadrangles.

Figure 21 compares three hypsometric curves. The first is of a drainage basin about 4 square miles in extent consisting of a deeply-incised canyon surrounded by a stripped structural surface of low relief. The canyon is cut into the Mesa Verde sandstones and represents a deep re-entrant into the ragged escarpment rising above a broad lowland of weak Mancos shales. As we might expect, the hypsometric curve has a high integral, 68%, and resembles the curve of a youthful region in the inequilibrium stage of development, except for a considerable degree of relief in the upper part of the basin, above the flattened part of the curve which represents the break from canyon walls to stripped surface. In the normal curve of the young basin (Fig. 14), relief on the interstream areas is much less, as we would expect of an initial surface of deposition.

The second curve in Figure 21 shows an abnormally low integral, 33%. This basin is almost entirely in Mancos shale, which extends out from the base of the escarpment but includes a small remnant of the Mesa Verde sandstone, Chimney Rock, rising strikingly from the shale plain. This basin represents a stage in retreat of a cliff line in which the resistant bed is all but completely removed. It is in virtually the same phase as the monadnock phase of the normal cycle (Fig. 16).

The third curve, intermediate between the first and second, represents a basin entirely

underlain by the Mancos shale, well out beyond the limits of the escarpment. Here no vestiges remain of the overlying resistant formation and the basin is in a virtually homogeneous

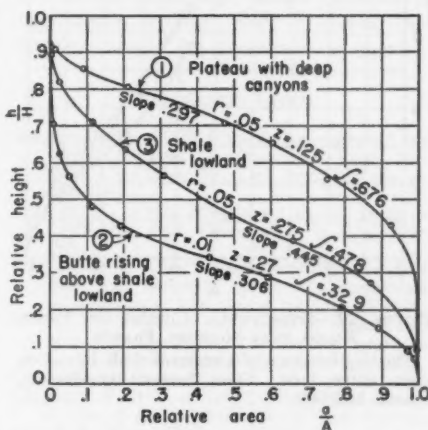


FIGURE 21.—HYPSONETRIC CURVES OF THREE BASINS IN MESA VERDE REGION, NORTHWESTERN NEW MEXICO

From Chimney Rock Quadrangle, New Mexico, U. S. Geological Survey, 1:62,500.

weak material. Here, as is normal in the equilibrium stage, the integral is close to 50% and the curve has a smooth, s-shaped form which is well described by the model hypsometric function with the values $r = 0.05$, $z = .275$.

To summarize the effect of massive, resistant horizontal strata of an erosional escarpment upon the hypsometric function: a high integral characterizes the early phases of development in the zone of canyon dissection close to the cliffs; the integral drops to low values as the proportion of basin of low relief on weak rock increases and the remnants of resistant rock diminish; and finally, when the basin is entirely in weak rock, the curve reverts to the normal form of the equilibrium stage.

A good example of the modified hypsometric curve resulting from the presence of a massive, resistant formation above a weaker rock is found in the dissected plateau near Soissons, France, north and south of the Aisne River. There the Tertiary chalk forms an extensive interstream upland surface at 170-200 meters elevation. The Aisne and its immediate tributaries have cut into weak sands and clays be-

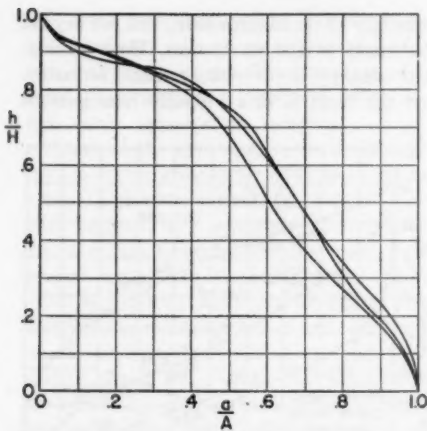


FIGURE 22.—HYPSOMETRIC CURVES OF THREE BASINS NEAR SOISSONS, FRANCE

Showing influence of a resistant chalk formation upon curve form. From Soissons Quadrangle, France, 1:50,000.

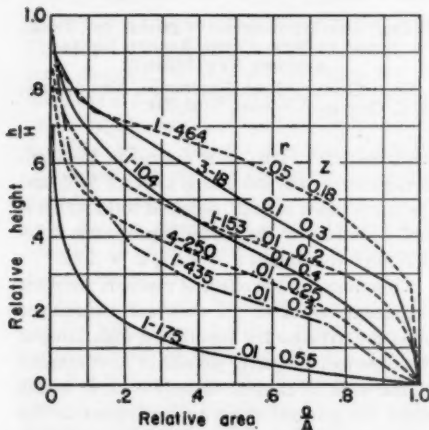


FIGURE 23.—HYPSOMETRIC CURVES OF LARGE DRAINAGE BASINS

From Langbein (1947). Values of r and z , added by writer, were fitted by inspection.

neath the chalk, giving the drainage basins steep inner slopes but very gentle slopes on the extensive divides. Curves of three third-order basins ranging from 14–26 square kilometers in area differ slightly in integral, but are remarkably alike in form (Fig. 22). Note that the resistant chalk produces a high integral and a

pronounced convexity in the upper third of the curve. This curve has a double inflection and does not fit the model hypsometric function.

PRACTICAL APPLICATIONS OF HYPSOMETRIC ANALYSIS

The hypsometric analysis of drainage basins has several applications, both hydrologic and topographic. Langbein (1947) applied the percentage hypsometric curve to a number of New England drainage basins (Fig. 23) of a much larger order of size than those analyzed here, but the curves have basically similar forms and can be described by the model hypsometric function. On Figure 23 the values of r and z are given for the best fit. Fit ranges from fair to excellent, and the results are satisfactory considering that most of these basins lie in a glaciated area combined with complex structure.

Referring to practical value of hypsometric data in hydrology, Langbein states (1947, p. 141):

“For example, snow surveys generally show an increase in depth of cover and water equivalent with increase in altitude; the area-altitude relation provides a means for estimating the mean depth of snow or its water equivalent over a drainage basin. Barrows (1933) describes a significant variation in annual precipitation and runoff in the Connecticut River Basin with respect to altitude. The obvious variation in temperature with change in altitude is further indication of the utility of the area-altitude distribution curve.”

Another application might be found in the calculation of sediment load derived from a small drainage basin in relation to slope. Because the hypsometric function combines the value of slope and surface area at any elevation of the basin, it might help obtain more precise calculations of expected source of maximum sediment derived from surface runoff in a typical basin of a given order of magnitude.

Dr. Luna B. Leopold (personal communication) has applied the hypsometric method to analysis of the relationship of vegetative cover to the areal distribution of surface exposed to erosion in the Rio Puerco watershed, New Mexico. Because of distinctive vertical zoning of grassland, woodland, and forest, the relative

surface
type
function
for cal
increas
function
subject
A m
method
integra
of the
integra
cate ex
suitabl
forces,
row po
ly obs
would
entirely
given
easy tr
or alon
mean
necte
ment,
would
ity. O
can be
topogra
would
tions u

surface areas underlain by each vegetative type can be described by the hypsometric function, which can thus be used as a basis for calculation. Furthermore, because rainfall increases with elevation, the hypsometric function can be used to calculate the total area subject to a given amount of rainfall.

A military application of the hypsometric method is foreseen in the use of the hypsometric integral as a term descriptive of the character of the terrain in quantitative terms. A high integral, such as that in Figure 14 would indicate extensive interstream areas of low relief, suitable to the rapid movement of mechanized forces, but with the valleys forming small narrow pockets suitable for defense and not readily observed from outside. A medium integral would indicate that the land surface was almost entirely in slope, which might be steep in a given region, and lacking in extensive belts of easy trafficability, either in the valley floors or along the divides. A very low integral would mean the development of extensive interconnected valley floors adapted to rapid movement, but with isolated hill summits which would offer defense positions with wide visibility. Obviously these terrain characteristics can be seen at a glance from any contour topographic map, and hypsometric analysis would be of value only in quantitative calculations using empirical formulas in which each

aspect of the terrain is given a numerical statement.

Planning of soil erosion control measures and land utilization may profit from topographic analysis in which such terrain elements as hypsometric qualities, slope steepness, and drainage density are quantitatively stated.

REFERENCES CITED

- Barrows, H. K. (1933) *Precipitation and runoff and altitude relations for Connecticut River*, Am. Geophys. Union, Tr., 14th Ann. Meeting, p. 396-406.
- Fisk, H. N. (1939) *Depositional terrace slopes in Louisiana*, Jour. Geomorph., vol. 2, p. 181-200.
- Horton, R. E. (1941) *Sheet erosion—present and past*, Am. Geophys. Union, Tr., *Symposium on dynamics of land erosion*, 1941, p. 299-305.
- (1945) *Erosional development of streams and their drainage basins; hydrophysical approach to quantitative morphology*, Geol. Soc. Am., Bull., vol. 56, p. 275-370.
- Langbein, W. B. et al. (1947) *Topographic characteristics of drainage basins*, U. S. Geol. Survey, W.-S. Paper 968-C, p. 125-157.
- Rouse, Hunter (1937) *Modern conceptions of the mechanics of fluid turbulence*, Am. Soc. Civ. Eng. Tr., vol. 109, p. 523-543.
- Strahler, A. N. (1950) *Equilibrium theory of erosional slopes approached by frequency distribution analysis*, Am. Jour. Sci., vol. 248, p. 673-696, 800-814.

DEPARTMENT OF GEOLOGY, COLUMBIA UNIVERSITY,
NEW YORK 27, N. Y.

MANUSCRIPT RECEIVED BY THE SECRETARY OF
THE SOCIETY, DECEMBER 12, 1951.

PROJECT GRANT 525-48.

PROBABLE ILLINOIAN AGE OF PART OF THE MISSOURI RIVER, SOUTH DAKOTA

BY CHARLES R. WARREN

ABSTRACT

The east-flowing White River enters the Missouri River about 12 miles below Chamberlain, South Dakota. In the east wall of the 300- to 600-foot trench through which the Missouri flows is exposed a cross-section of a valley now filled with till, cut by the former continuation of the White River eastward to the James River Valley. The floor of this filled valley hangs about 115 feet above the present Missouri. Near by, also east of the Missouri and capping a bluff 550 feet above it, is gravel containing vertebrate fossils stated to be of late Kansan or younger age. This high, fossiliferous gravel was deposited by the White River prior to the cutting of the Missouri trench, and the vertical relations indicate that it antedates the cutting of the till-filled valley. Thus, if the age of the fossils is correct, the glacier that created the Missouri must have been younger than the Kansan. Several lines of evidence indicate that the ice that caused the White River and other streams to divert and form the Missouri was probably Illinoian rather than Wisconsin.

CONTENTS

TEXT			Page
Introduction	1143	Loveland loess related to the Missouri	1151
Origin of Missouri River	1143	Probable Illinoian age of the Missouri	1152
Diversion of White River	1144	General statement	1152
Date of diversion creating the Missouri River	1144	Westward limit of ice of the Illinoian age	1152
Acknowledgments	1144	Pleistocene erosional chronology	1153
Post-Kansan age of White River diversion	1145	Summary and conclusions	1154
Cross section of old valley of White River	1145	References cited	1154
High-level fossiliferous western gravel	1147		
Post-Kansan age of the Missouri River	1148	ILLUSTRATIONS	
Probable pre-Wisconsin age of the diversion	1150	Figure	Page
General statement	1150	1. Map of parts of Chamberlain and Iona quadrangles, South Dakota	1145
Depth and antiquity of the Missouri trench	1150	2. Cross section of former White River valley as exposed in the east bank of the present Missouri River trench	1146
Chronology of events in the trench	1150	3. Diagrammatic cross section showing deposits lying in the Missouri trench near Chamberlain, South Dakota	1149
Relation of the Missouri to the drift border	1151		
Absence of channels related to the drift border	1151		

INTRODUCTION

Origin of Missouri River

It is generally recognized (Fenneman, 1938, p. 564-566) that the course of the Missouri River across South Dakota is of comparatively recent origin, established during Pleistocene time as a result of disruption by glacier ice of an earlier drainage pattern quite different from the present one (G. K. Warren, 1868; 1869, p. 311; Todd, 1885, p. 392; 1923). The general pattern of the pre-diversion drainage

in South Dakota and the manner in which the present Missouri was formed were inferred by Todd (1914), and the details have been considerably clarified by Flint (1949).

Prior to the diversion that formed the Missouri, a series of subparallel streams (including, from north to south, the Grand, Moreau, Cheyenne, Bad, White, and Keya Paha-Niobrara rivers) flowed eastward into the lowland area now drained by the James (Flint, 1949, fig. 1). At some time glacier ice moved southward in the James Valley lowland to form

the James lobe, and its western margin blocked the lower courses of these east-flowing streams. In each of the east-trending valleys, the water of the stream, ponded by the ice and supplemented by glacial meltwater and by water spilling over from the next drainage basin to the north, overflowed at the lowest point in the rim of the ice-dammed basin. Because of the general southward slope of the ice surface in the axial part of the James lobe, the streams were blocked at points that were successively lower and less far west, in successive valleys to the southward; thus, in each case the lowest unblocked route of escape for the ponded waters occurred on the south side of the stream valley at some point west of the ice margin. Because of the general eastward slope of the Great Plains surface, this lowest point would probably in most cases lie not far west of the glacier margin, but the drainage thus established consisted of many separate segments crossing former interfluves, and only locally was it strictly an ice-marginal stream.

The stream segments thus formed carried a large discharge and cut rapidly down through the easily eroded Pierre shale that constituted the previous interfluves. When the ice finally disappeared, it left considerable amounts of drift blocking the former lower courses of the streams, so that the drainage continued to escape by the route established during the time of ice blockade. The glacially integrated stream that resulted is the present Missouri.

Diversion of White River

One of the east-flowing streams whose lower part was thus cut off by the newly integrated Missouri is the White River. Formerly heading, apparently, far west in Wyoming, it is believed to have entered the James Valley near Mitchell, about 40 miles east of its present mouth in the Missouri south of Chamberlain (Flint, 1949, fig. 1). The eastern extension of the former valley of the White is so nearly filled with glacial drift that in places it is scarcely recognizable as a topographic feature (Todd, 1923, p. 478).

Date of Diversion Creating the Missouri River

Although the general mechanism of the diversion that integrated the Missouri has been clearly understood, the exact age of the diver-

sion has been in doubt. It has been inferred that diversions occurred more than once in Montana and northern North Dakota (Flint, 1947, p. 164), but no sufficient evidence of comparable successive diversions is known in South Dakota, and it appears likely that the whole course of the Missouri through South Dakota may have been formed at one time.

Todd (1914, p. 273; 1923, p. 479-488) considered the date of birth of the Missouri to be Wisconsin¹, but Leonard (1916) and Alden (1924, p. 413) showed it to be pre-Iowan in North Dakota, and Flint (1947, p. 163) noted that it "clearly antedates at least one ice invasion." Flint later (1949, p. 71) concluded that, in South Dakota, the Missouri originated in the Kansan. Evidence presented below indicates that the White River was probably diverted by Illinoian ice (See also C. R. Warren, 1949).

ACKNOWLEDGMENTS

Sincerest thanks are due to Professor R. F. Flint, who suggested writing this paper and proposed many of the ideas set forth, both in personal conversations and in unpublished manuscripts that he has permitted me to read. Mr. E. J. Bergner collected from his gravel pit, and donated for study, the vertebrate fossils that provided the critical dating indicating the post-Kansan age of the Missouri trench. Professor C. Bertrand Schultz and Mr. W. D. Frankforter kindly studied the Bergner fossils and determined their age. Professor C. L. Baker first pointed out to me the importance of the Bergner locality and discussed some of the problems in the field. Professors Flint, Schultz, and A. C. Trowbridge have critically read this manuscript. Nearly all of the altitudes used in drawing the cross section (Fig. 2) are based on hand leveling done by Mr. R. R. McDonald.

¹ The standard Pleistocene sequence, used in this paper, is as follows:

Pleistocene epoch	{	Wisconsin age	{ Mankato subage Cary subage Tazewell subage Iowan subage
		Sangamon age	
		Illinoian age	
		Yarmouth age	
		Kansan age	
		Aftonian age	
		Nebraskan age	

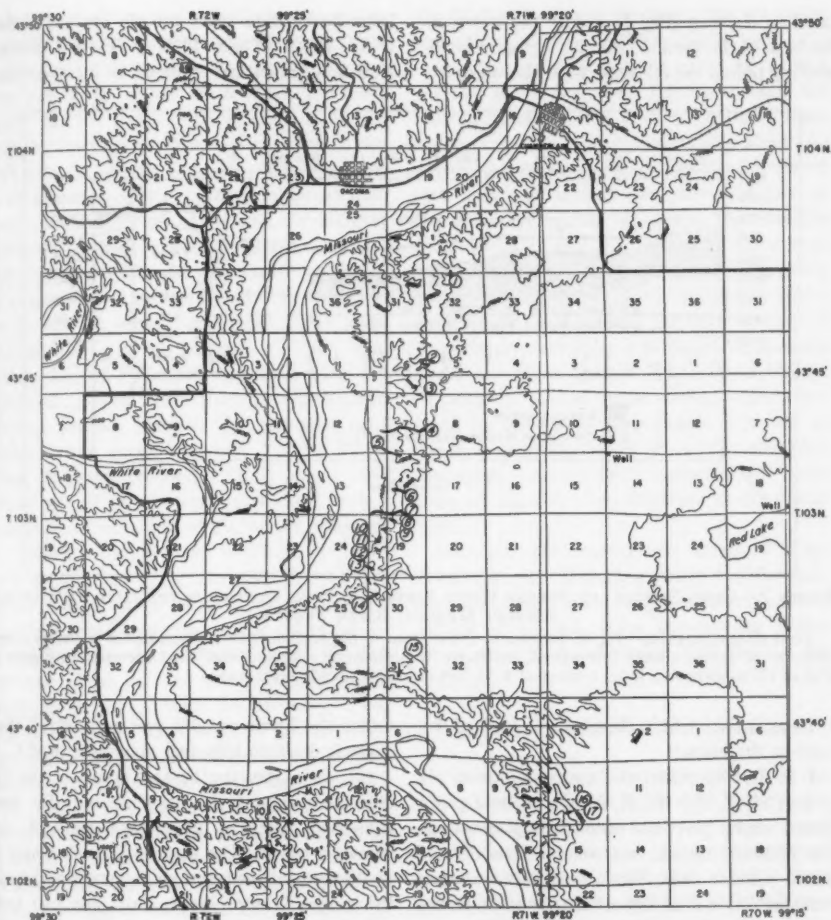


FIGURE 1.—MAP OF PARTS OF CHAMBERLAIN AND IONA QUADRANGLES, SOUTH DAKOTA

Contours, 100-foot interval, generalized from U. S. G. S. quadrangle maps. Traverses numbered 1-17 correspond to the positions of determined altitudes of contacts shown in Figure 2.

POST-KANSAN AGE OF WHITE RIVER DIVERSION

Cross Section of Old Valley of White River

Nearly east of the present mouth of the White River, in the east wall of the Missouri trench (Fig. 1), the former eastward continuation of the valley of the White is exposed in cross section. This cross section was mentioned by Flint (1949, p. 63), but his reconnaissance study failed to locate the deepest point in the old valley, which is now known (Fig. 2) to hang about 115 feet above the normal water level of

the Missouri and approximately 200 feet above the present bedrock floor of the Missouri trench. The 200-foot figure is inferred from the results of recent core drilling by the U. S. Army District Engineer at Chamberlain, about 2 miles north of the north end of the cross section, where the bedrock floor was determined to lie at 1238 feet above mean sea level.

The data on which Figure 2 is based were determined by hand leveling of the contacts as exposed. Traverses were made and altitudes of contacts were determined at the points indi-

cated on the map (Fig. 1) and by the arrows at the base of the section (Fig. 2); at many intermediate points the relations were also observed

Lake, believed to mark the old channel of the White River (Todd, 1899, p. 146), 3 feet of sand and gravel are reported to intervene be-

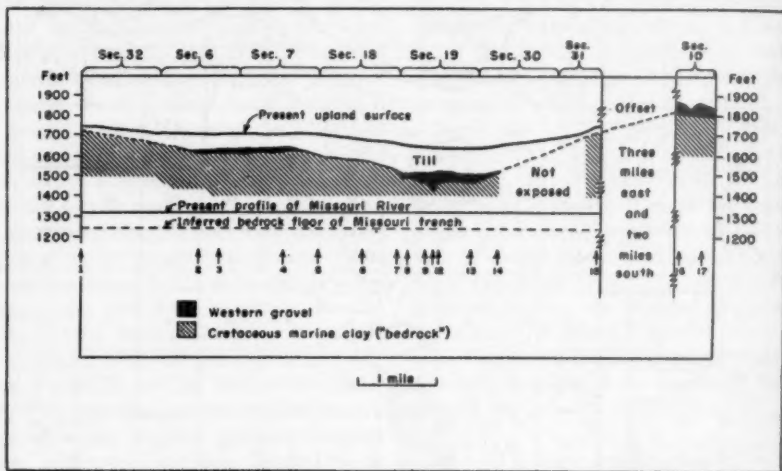


FIGURE 2.—CROSS SECTION OF FORMER WHITE RIVER VALLEY AS EXPOSED IN THE EAST BANK OF THE PRESENT MISSOURI RIVER TRENCH

Vertical exaggeration, 13.2 X. Arrows at the bottom of the section indicate locations of traverses where altitudes of contacts were determined, numbered to correspond with the numbered traverses in Figure 1. Top of till as shown includes a cover of 4-15 feet of loesses of Wisconsin age.

to be as shown, within the limits of error of the scale of the section.

I at first supposed the unusually thick till in sec. 18, T. 103 N., R. 71 W., to be a post-trench veneer plastered onto the sloping wall of the Missouri trench, but several lines of evidence indicate that Figure 2 represents a true cross section of a till deposit that actually thickens in the manner shown, partly filling a depression in the pre-Missouri River surface. This evidence is in part as follows:

(1). The valley occurs in precisely the expected position along the old course of the White that is inferred from topographic and other studies (Todd, 1923, p. 478; Flint, 1949, p. 63). The general form and altitude of the floor of the old valley are corroborated by evidence from two wells, respectively $3\frac{1}{2}$ and $6\frac{1}{2}$ miles east of the line of this section. At the northwest corner of sec. 14, T. 103 N., R. 71 W. (Fig. 1), the glacial drift rests on Pierre shale at approximately 1630 feet. In another well at the southwest corner of sec. 17, T. 103 N., R. 70 W. on the north shore of Red

tween the Pierre at 1488 feet and "clay" that extends down to 1491 feet above sea level.²

(2). In places the basal contact of the till extends at about the same altitude for considerable distances along the wall of the Missouri trench. The contact in such places is at the same altitude out on the spurs and up in the gullies in the trench wall. For two such stretches, the till rests on bodies of gravel rather than directly on the Pierre shale; both the upper and lower contacts of these gravels are in general essentially horizontal, being no higher in the gullies than out on the spurs.

(3). These two bodies of gravel lying in the till-filled valley beneath the till have a distinctive lithology, indicating a western origin (Rothrock, 1944, p. 8). They are similar to gravel occurring on a terrace of the White River 30 miles west of its mouth, far upstream above any possible ice advance. The pebbles in them include many varieties of chert, some of which are identified by Professor Charles L.

² Well data kindly furnished by Professor Charles L. Baker, of the South Dakota Geological Survey.

Baker (personal communication) as coming from the Amsden formation in Wyoming; vein quartz and perthite feldspar, believed to come from pegmatites in the Black Hills; and more locally derived types, such as green quartzite from the Ogallala formation. The stones in the drift brought to this area from the northeast by ice are dominantly granitic and metamorphic rocks, together with Paleozoic limestones; cherts are few, and feldspar pebbles are present only in places where the ice has crossed White River gravels. All terrace gravels known within the trench are either local rocks mixed with such glacial types or mixtures of these with western-derived (White River) rocks. Thus the till-buried gravels with their purely western lithology are not outwash, but represent nonglacial stream deposits formed by the White River. They are perched well up on the east side of the Missouri trench and more than 3 miles east of the mouth of the White, although the Missouri today flows westward between these points, reversing the direction of the former White. These relations argue strongly that the White River gravels were deposited by the White while that stream was still flowing eastward across the site of the trench, before the diversion that created the Missouri. If so, they lie in a valley that formerly drained eastward and that is now filled with till to the depth required by the present topographic surface.

(4). One of the two gravel bodies forms a veneer about 10 feet thick on what appears to be a buried terrace more than a mile wide on the side of the till-filled valley, $1\frac{1}{4}$ miles north of the other gravel body and 100 feet above it. The lower gravel occupies the bottom of the old valley; it is considerably thicker, and its upper half, directly under the till, consists largely of sand. The yellow sand deposit can be traced as a continuous layer along the wall of the present trench (into gullies and out on spurs) for a considerable distance in secs. 19 and 30, T. 103 N., R. 71 W., underlying the till and grading down into a variable thickness of gravel. Such a decrease in grain size would be expected if the White aggraded as a consequence of progressive reduction of its velocity due to blocking by glacier ice advancing westward up its valley. Thus, the two gravel bodies have exactly the character and positions to be expected if they were brought from the west by

the White River and left when the old valley was obliterated by overriding glacier ice.

(5). At several places, the basal contacts of the two gravel bodies on the Pierre shale are marked by continuous lines of perennial seepage springs that extend horizontally along the trench wall for distances up to several hundred feet. Perennial springs are extremely rare in this semiarid region of almost impermeable shale and clay-rich till, and their occurrence here indicates that the gravels from which they emerge can obtain water by infiltration over a considerable area. Thus the two bodies of gravel must extend for a considerable distance under the till in the old White River Valley. Apparently several water bodies occur, isolated by relatively impermeable deposits, as the lines of springs occur at varying altitudes. Presumably, similar barriers prevent the water from all draining away eastward to the James Valley.

For these five reasons and others, it is believed that the till reaches a considerable thickness, and that Figure 2 represents a true cross section of an old valley cut by the White River prior to the diversion that created the Missouri.

High-level Fossiliferous Western Gravel

The recognition of the cross section of the old valley of the White River would be a matter of purely local interest and little importance but for the presence near by of a body of western gravel lithologically like the White River gravel in the old valley, but with quite different topographic relations and containing identifiable and significant vertebrate fossils.

Three miles east and 2 miles south of the southern end of the exposed cross section, in sec. 10, T. 102 N., R. 71 W., is a hill that forms the highest point for nearly 10 miles in any direction. Its summit is protected from erosion by gravel more than 27 feet and possibly as much as 50 feet thick. This high body of gravel consists of chert, feldspar, and other types of rocks identical with those noted above as occurring up the White River. Although overlain by thin till of unknown age, it contains no rocks characteristic of the glacial drift.

The only explanation for the vertical and horizontal relations of this gravel, perched high

on the east side of the Missouri trench, is that it antedates the Missouri River. It must represent a remnant, east of the trench, of one of those Pleistocene gravels that are widespread on the terraces of the White River farther west but have been destroyed by erosion at most places east of the Missouri. If so, the gravel must have been deposited when the White was wandering across the area as it slowly cut down from the altitude of the former Cenozoic (Ogallala) cover toward the profile (recorded by the bottom of the till-filled valley) on which it was flowing just before the diversion that gave birth to the Missouri.

The gravel contains a considerable number of vertebrate fossils. Mr. E. J. Bergner, owner of the land on which the gravel occurs, collected many of these fossils while removing part of the gravel for use, and very kindly donated a selection of them for study.

The Bergner fossils were examined by Professor C. Bertrand Schultz, Director of the University of Nebraska State Museum, and by Mr. Weldon D. Frankforter. They reported as follows (personal communication):

“Faunal list:

EDENTATA

Megalonyx sp. Ground sloth.

CARNIVORA

Felid, large. Large cat, size of *Smilodon* (too incomplete for generic identification).

PROBOSCIDEA

Paralephas cf. *P. jeffersoni* (Osborn). Mammoth. Specimen too incomplete for definite specific identification.

PERISSODACTYLA

Equus excelsus Leidy. Horse.

Equus cf. *E. giganteus* Gidley. Large horse.

ARTIODACTYLA

Camelops kansanus Leidy, referred. Camel.

Camelid, larger than *C. kansanus*. Large camel.

Antilocaprid, similar to *Stockoceros*. Four-horned antelope

Platygonus sp. Peccary.

Mylohyus sp. Peccary.

Remarks

“The presence of ground sloth, southern type mammoth, and peccaries indicates an interglacial, not glacial climate at the time the bones were deposited in the gravels. We would strongly suggest that it is Yarmouth . . . The fossils are not as

numerous or complete as one would desire for a faunal report, but we are sure that the fauna is post-Broadwater or in other words, post-Kansan.”

This evidence indicates that these high gravels cannot antedate glaciation by the Kansan ice. To suppose they antedate that glaciation by any considerable interval seems *a fortiori* impossible.

Post-Kansan Age of the Missouri River

The topographic relations, character, and inferred origins of the gravels in Figure 2 show that after the White River deposited the high fossiliferous gravel at the Bergner locality, sufficient time must have elapsed to allow it to cut downward more than 400 feet before the advancing ice caused it to deposit the lower of the two bodies of western sand and gravel in the buried valley. Downcutting of this vertical amount could conceivably be accomplished rather quickly in the weak Cretaceous sedimentary rocks, but the gravel-veneered terrace shows that the White River also accomplished considerable lateral planation during the cutting. The filled valley beneath the upland surface is about 6 miles wide; if this is average for the pre-diversion valley, the White had an open valley approximately as wide between upland flats as the Missouri trench today, in spite of the greater depth of the Missouri trench and the much greater volume of water it carries. Furthermore, in broad areas west of the Missouri the upland flats themselves, though below the altitude of Mr. Bergner's gravel, carry a thin veneer of western gravel, indicating that the White planed across them after depositing the gravel at the Bergner locality.

Thus it is evident that the White River continued in its eastward course past Chamberlain for a considerable period of time after it deposited the gravel at Bergner's. The glacier ice that advanced up the old valley of the White River, causing the diversion that gave birth to the Missouri, must therefore have arrived considerably later than the deposition of Mr. Bergner's gravel. Unless the determination of the Bergner fossils as late Kansan or younger is greatly in error, the ice sheet that caused the diversion must have been post-Kansan, hence either Illinoian or Wisconsin.

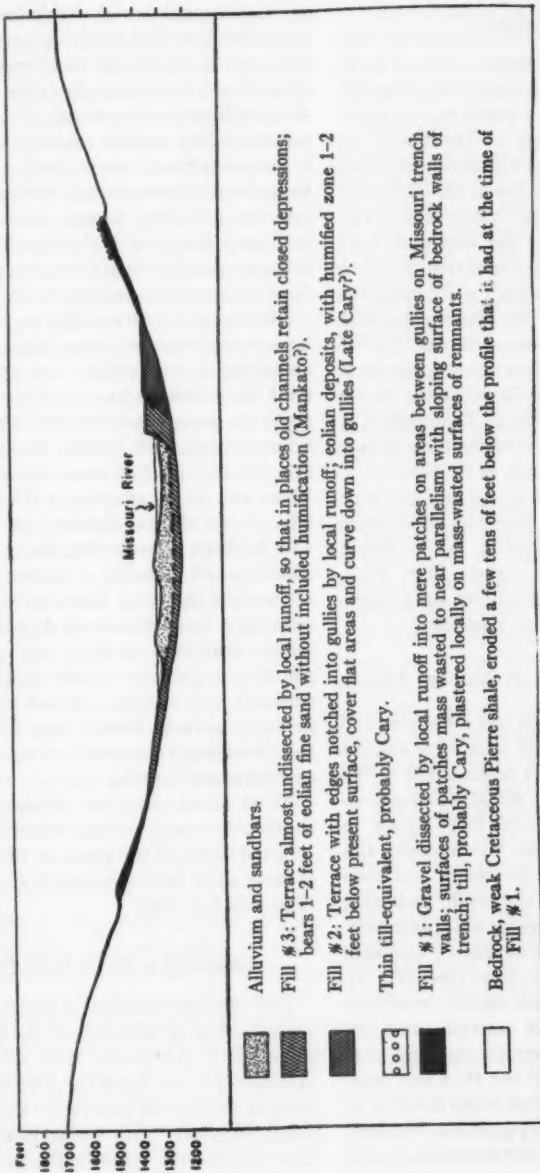


FIGURE 3.—DIAGRAMMATIC CROSS SECTION SHOWING DEPOSITS LYING IN THE MISSOURI TRENCH NEAR CHAMBERLAIN, SOUTH DAKOTA
Width of section approximately 5 miles.

PROBABLE PRE-WISCONSIN AGE OF THE
DIVERSION

General Statement

Till and other drift deposits believed to be Iowan (Flint, 1949) occur west of the Missouri, and it might seem to be a simple matter to determine by the relations of the Iowan till whether or not the trench antedates the Iowan glaciation. However, the Iowan till on the upland west of Chamberlain is less than 2 feet thick, and mass-wasting and slopewash have removed tens of feet of material from the sides of the Missouri trench since the accumulation of a Wisconsin outwash fill. There is therefore little probability that Iowan till can ever be traced from the upland flats down the slopes of the trench, so that any till occurring in the trench might be Tazewell; at Chamberlain it might also be Cary, as ice of the Cary subage invaded the Missouri trench in this area.

No unequivocal proof of age has yet been found, but the following five lines of evidence suggest that at Chamberlain, as in North Dakota (Leonard, 1916; Alden, 1924; Flint, 1947, p. 163), the Missouri River was in existence prior to the Wisconsin glaciation:

Depth and Antiquity of the Missouri Trench

The Missouri trench has had a complex and evidently long history. The walls were first cut to a depth that averaged perhaps 400 to 700 feet. A major stream like the Missouri can obviously have cut downward very rapidly in the weak sedimentary rock that underlies this part of its course, but the trench was then widened by landsliding, slopewash, and other processes almost to its present width and form. After this the trench was extensively aggraded at least twice and probably three times (Fig. 3).

The oldest aggradational deposit recognized in the trench consists of outwash sand and gravel, including some erratic boulders, that was originally at least 160 feet thick and probably thicker (base preserved today down to 40 feet above river level, and probably originally lower in central part of trench; surface aggraded to 200 feet or more above the river). Most of the gravel deposits in this region described by Rothrock (1944) are remnants of this fill. This early outwash deposit was then almost entirely

removed by erosion. The Missouri cut down to a profile that was probably lower than the present one, and flowed on this lowered profile long enough so that the surfaces of the gravel remnants in the trench could waste down to slopes that are in many places but little above the pre-fill walls of the trench. No flat terraces preserving the original constructional surface of the gravel fill are known; local runoff streams have commonly cut channels through the gravel into the underlying marine sedimentary rock, and many remnants of the gravel now consist of mere patches thinly veneering intergully areas on the sloping sides of the trench.

After the gravel fill had been eroded almost to its present topographic expression, silt and sand containing a few pebbles and even boulders filled the trench up to a profile about 50 feet above the present river level but about 150 feet below the earlier fill. Erosion removed much of this fill, and local streams cut small gullies. There was then apparently a third episode of filling, to an altitude slightly below the second one. In sharp contrast with the sloping, mass-wasted gravel remnants of the earliest fill, the remnants of this latest fill stand as flat-topped terraces so fresh that closed depressions in the initial channeled surface are preserved in places, and gullying by rain falling on their surfaces has scarcely notched their steep, generally vertical banks; time has evidently been insufficient to permit them to undergo extensive mass-wasting.

These events since the Missouri began to cut its trench seem too time-consuming to have occurred within 55,000 years, the inferred length of time since the beginning of the Wisconsin (Flint, 1947, p. 400).

Chronology of Events in the Trench

Very thin till mantles in places the mass-wasted slopes of remnants of the earlier thick gravel fill in the trench. This till cannot be Mankato, for the Mankato drift border is 20 miles or more to the east (R. F. Flint, personal communication). Thus ice at least as old as Cary covered the gravel remnants after they had been dissected to essentially their present topographic expression, and the gravel fill, which contains boulders and evidently records an episode of outwash aggradation, cannot be

younger than Tazewell. The Missouri River must therefore be at least as old as Iowan.

If the ice blockade that created this section of the Missouri is assumed to be Wisconsin, hence Iowan, almost the entire cutting of the trench and the widening out of its walls by mass wasting to practically its present width must have occurred in the interval between the Iowan and Tazewell subages, plus the portion of Iowan time after the diversion, whereas the time since the Tazewell has only sufficed to widen the trench by a few tens of feet more. Even allowing for the larger discharge carried by the Missouri during a pluvial time with much meltwater contribution, the interval between the Iowan and Tazewell subages, in this region apparently too short for a recognizable soil profile to develop on the Iowan loess before the beginning of the accumulation of the Tazewell loess (R. F. Flint, personal communication), is believed also too short for the cutting and widening of the trench.

The sequence of events inferred for the Missouri trench fits the Pleistocene chronology inferred in other areas much better if the Missouri began to cut its trench in Illinoian time. The relatively long Sangamon interval would provide ample time for the walls of the trench to reach essentially their present slopes. On this hypothesis, the early gravel could be Iowan or Tazewell or both; if Iowan, its erosion could have begun late in the Iowan subage, allowing more time for the mass wasting that modified its remnants before the arrival of ice of the Cary subage.

Relation of the Missouri to the Drift Border

Flint (1949, p. 70) pointed out that, once an ice-diverted course was established, it would quickly become incised below any pre-diversion divides farther east, so that the Missouri should lie at or west of the drift border of the ice sheet that gave it birth. However, the western limit of glaciation lies west of the Missouri trench, not only near Chamberlain but throughout much of South Dakota (Flint, 1949, fig. 1). As Flint indicated, the explanation of this apparent paradox must be that the Missouri River was created by an ice sheet that antedated the ice whose deposits are found west of the river. The erratics and till on the upland west of the

Missouri are believed to be Iowan (Flint, 1949, p. 70). If the Missouri was created marginal to an ice sheet older than the Iowan drift, it must have originated in pre-Wisconsin time.

Absence of Channels Related to the Drift Border

While the ice of the Iowan subage was at its maximum, it must have blocked the drainage from the west. It would seem that these waters would inevitably have had to find some route of escape, but with one possible exception (Todd, 1923, p. 483-484), no abandoned channels have been recognized west of the Missouri trench. Flint (1949, p. 70-71) explained this by supposing:

"that the expansion of this ice lobe, westward from the site of the Missouri River to the limit of glaciation, took place very rapidly, and that the border of the ice did not pause at its outermost position, but very quickly shrank back to or east of the position of the Missouri."

so that streams like the White River, though dammed and ponded, did not accumulate enough water to overflow their valleys before the route via the Missouri was re-exposed. This mechanism probably cannot be invoked unless the Missouri trench existed prior to Iowan time, for if the Missouri were the result of blocking by ice of the Iowan subage, the White and other valleys would already have been full nearly to overflowing and would surely have spilled over during the time the ice was west of the present Missouri. The only alternatives to Flint's explanation that present themselves are that the water ponded by the ice of the Iowan subage escaped by subglacial or superglacial streams in the Missouri trench, or by percolation through gravels occupying the Missouri trench. These hypotheses seem likewise to require that the trench be in existence before the advent of the ice of the Iowan subage.

Loveland Loess Related to the Missouri³

The Loveland loess is a pre-Wisconsin deposit formerly considered to be Sangamon because it overlies Illinoian drift, but probably

³ Professor A. C. Trowbridge pointed out (personal communication) the value of the Loveland loess in indicating the distribution of ice of the Illinoian age.

actually a late Illinoian accumulation of dust blown up from Illinoian outwash trains in near-by valleys. It has a distinctive reddish color, apparently the result of weathering conditions peculiar to the Sangamon and believed to be diagnostic of loess of Illinoian age. The formation is widespread in Nebraska, Iowa, and neighboring States.

Doubtless partly because ice sheets of the Wisconsin age have extensively modified the pre-Wisconsin surface, very little Loveland loess has been identified in South Dakota. One of the few such deposits, discovered by H. E. Simpson of the U. S. Geological Survey, lies on the edge of the Missouri trench 8 miles west of Yankton. This deposit appears to indicate that the valley now occupied by the Missouri River carried Illinoian outwash at a point far above its junction with the pre-diversion White River and even well above the ancestral lower James (Flint, 1949, fig. 1). Illinoian ice evidently contributed meltwater to a stream west of the present James River. Because no course for such an outwash stream other than the present Missouri is evident, the Missouri must have existed in Illinoian time.

PROBABLE ILLINOIAN AGE OF THE MISSOURI

General Statement

If the Bergner vertebrate fossils are dated correctly, the ice sheet responsible for the diversion of the White River to form the Missouri must have been post-Kansan. The five lines of approach above indicate that the Missouri at and below Chamberlain is very probably pre-Wisconsin in origin. It follows that the glacier ice that blockaded the lower course of the White River, forcing its diversion to form the Missouri, was probably Illinoian.

Flint (1949, p. 71-72) reached his conclusion that the diversion most probably occurred in Kansan time on three lines of evidence:

(1) "The trench, and the diversion, definitely antedate the Wisconsin." This argument is accepted in this paper, and evidence supporting the pre-Wisconsin age has been presented in some detail.

(2) The diversion probably "did not greatly antedate the arrival . . . at the site of the Missouri River" of the ice sheet that deposited a

till then supposed by Flint to be Kansan on the basis of its lithologic resemblance to till in Nebraska and Iowa that had been described as Kansan. This inference agrees with the conclusions of this paper, although the probable pre-Wisconsin till is here considered to be Illinoian rather than Kansan. However, the lithologic characteristics of a till are now considered to be unsafe criteria for establishing its age, and other evidence is relied on in this paper.

(3) "No Illinoian drift, nor other evidence of Illinoian glaciation, has yet been recognized in South Dakota." However, Flint himself in 1947 (p. 283-284) inferred the probability that Illinoian ice invaded areas west of its then-recognized range.

In view of the evidence presented in this paper, Flint (1950) has accepted the probability of an Illinoian age for the diversion.

Westward Limit of Ice of the Illinoian Age

No glacial deposits of Illinoian age have hitherto been identified west of southeastern Minnesota (Flint *et al.*, 1945; Flint, 1947, p. 283). Nevertheless, it has been anticipated (Flint, 1947, p. 284) that whenever climatic conditions were such as to cause extensive glaciation in Illinois and the region to the east, glacier ice should also have invaded areas farther west.

The distribution of Loveland loess in Iowa (Professor A. C. Trowbridge, personal communication), in Nebraska (Professor E. C. Reed, personal communication), and in Kansas (Frye and Leonard, 1949, p. 897) proves that Illinoian ice contributed outwash to the part of the Missouri below Sioux City. To do this it must have reached points much farther west than its deposits have been mapped.

The Loveland Loess deposit 8 miles west of Yankton implies an even greater extension of the Illinoian ice. The geographic relations are such that Illinoian outwash could not have reached this point on the Missouri unless either (1) ice of Illinoian age lay southwest of the pre-diversion White River, in approximately the position of the ice that caused the diversion of the White, or (2) the course of the Missouri past Chamberlain had already been established, and the outwash came from farther up the

Missouri. Because the South Dakota segment of the Missouri is post-Kansan, the evidence strongly indicates that the ice that established the course of the river through this State was Illinoian.

Professor R. F. Flint now considers (personal communication) that the various tills in South Dakota vary so much in themselves and resemble one another so closely that the age of a till cannot be determined by studying its lithologic characteristics, and Professor A. C. Trowbridge, the outstanding authority on the drifts of Iowa, states (personal communication) that "there is no such thing as typical Kansan or Nebraskan or Iowan till." Furthermore, Flint now considers that the loess formerly believed to be recognizable as Iowan is indistinguishable from loess of Tazewell age and even from some Cary loess. Thus the identification of Iowan and pre-Wisconsin tills on the basis of lithology and relation to "Iowan loess" (C. R. Warren, 1947) is now in doubt.

Nevertheless, the body of till lying in the former valley of the White, formerly considered to be Kansan because its lithologic characteristics were considered to be recognizably different from those of Wisconsin tills, buries and protects from erosion the gravel-covered terrace on the side of the pre-diversion valley in a manner suggesting deposition by the ice responsible for the diversion. It is therefore probably Illinoian and probably indicates that ice of the Illinoian age reached Chamberlain. If it is Illinoian, any soil profile or gumbotil developed on it was removed prior to Iowan till deposition. The overlying Iowan till includes much of the material from the probable Illinoian till, and the two are difficult to distinguish lithologically.

Pleistocene Erosional Chronology

It should be emphasized that the conclusions reached in this paper rest primarily on the dating of the Bergner fossils as Kansan or younger. If those fossils can be as old as early or middle Aftonian, the Missouri may have been formed by ice of the Kansan age, as Flint (1949) considered probable. Nevertheless, an Illinoian age for the forming of the Missouri appears to be more consistent with the known erosional history of the region.

West of the Missouri, the White River is now entrenched below a series of gravel-covered terraces believed to be remnants of planation surfaces formed by wandering of the river while it was cutting down in response to regional uplift. Whether these terraces record successive cycles of erosion, corresponding to pulses of uplift or to climatic fluctuations like those inferred by Schultz and Stout (1945) in Nebraska, or whether they are merely nonpaired remnants of surfaces across which the White wandered by lateral planation as it cut slowly downward, the White has accomplished a vast amount of work. Continental Miocene and Pliocene sediments (Ogallala) undoubtedly once covered the entire drainage basin. The White has destroyed all but a small remnant of this Ogallala cover on the divide on the north, stripped it from even wider areas south of its present course, and exported many cubic miles of the underlying Cretaceous sedimentary rock as well. The planation surfaces so developed bear the relation of terraces cut below the Ogallala surface, but they are so widespread that they now occupy the major part of the area and form the general upland surface, below which the present valleys are incised and above which stand buttes capped by remnants of the Ogallala. The development of such a broad erosion surface must have required a relatively long time.

Compared with the large amount of work done in cutting the upland surface, the erosion below the upland level has been relatively slight. The White River cut the valley shown in Figure 2, and thereafter the Missouri cut its trench, but both these valleys are narrow and youthful compared with the broad planation surfaces developed earlier.

The chief difficulty in fitting the development of these features into Pleistocene events as a whole appears to lie in dating the widespread planation by the White River. Obviously the cutting of the upland surface cannot have begun until after the deposition of the Ogallala sediments that now cap the divides. On this evidence the White could have cut the upland surface largely in Pliocene time, but I know of no Pliocene fossils in any of the gravels capping the planation surfaces. On the contrary, remains of Pleistocene forms in one of the highest of them (at the Bergner pit) suggest that a

substantial part of the planation occurred in Pleistocene time; the cutting may even have begun about the beginning of the Pleistocene as a response to regional uplift. Flint (1949) considered the upland surface to be the No. 2 terrace recognized by Alden (1924), and agreed with Alden that it is Pleistocene.

If the late- or post-Kansan dating of the Bergner fossils is rejected, and it is supposed, as Flint supposed in 1949, that the Missouri was created during Kansan time, the now till-filled valley of the White must have been cut in Aftonian time. This would leave only Nebraskan time and part of Aftonian time for that part of the planation that may be ascribed to the Pleistocene. This seems a very short time for such extensive cutting. Moreover, on this hypothesis the Missouri has taken its present course since the beginning of the Yarmouth, which was much longer than the Aftonian and was probably at least $2\frac{1}{2}$ times as long as the Sangamon interglacial age (Flint, 1947, p. 400), and it seems difficult to explain why the river did not cut much more extensively than it has yet done, if it has been working so long in the poorly consolidated sediments of this area.

The entire sequence of events in the White River Valley appears to fit the accepted Pleistocene chronology better on the hypothesis that the diversion to form the Missouri occurred in Illinoian time. Nebraskan, Aftonian, Kansan, and most of Yarmouth time are then available for lateral planation by the White. On this hypothesis, the gravel at the Bergner locality records a profile on which the White River was flowing in late Kansan time or later. The gravel is more than 27 feet thick, much thicker than most of the terrace veneers left by the White, and may record aggradation by the White in response to blocking by ice of the Kansan age at some point to the east. Whatever the cause of its deposition, it stands above most of the upland surface, showing that the White wandered widely, cutting the terraces now preserved and presumably destroying older ones, in post-Kansan (therefore Yarmouth) time. At some time in the Yarmouth, probably late in this interglacial time, the White started to cut downward more rapidly in relation to its lateral cutting, so that by Illinoian time it had become confined in a much narrower

valley, now recognizable in the wall of the Missouri trench (Fig. 2). In response to the accelerated downcutting by the White, tributary streams developed and cut downward; one of these is recognized on the Chamberlain quadrangle. On this interpretation, the Missouri has followed essentially its present course throughout the Sangamon and Wisconsin ages, a time which has proved insufficient to permit extensive widening of its valley.

SUMMARY AND CONCLUSIONS

It has been shown that the White River formerly extended eastward from its present mouth in the Missouri to the James Valley lowland near Mitchell. At a date that was at least as late as Kansan, if the paleontologic determination of the fossils from the Bergner locality is correct, the White was flowing on a profile that at the longitude of the Missouri was more than 400 feet above the one to which it had cut down by the time of the diversion that initiated the Missouri River. The glacier ice that caused the diversion must therefore be of post-Kansan age; it is believed to have been Illinoian rather than Wisconsin. This evidence applies strictly only to the White River at its point of diversion near Chamberlain, but there is strong comparable evidence for an Illinoian age of the diversion of the Bad River near Pierre (D. R. Crandell, unpublished Ph. D. dissertation, Yale University, 1951). Most or all of the stream diversions in South Dakota to which the Missouri River owes its present course and volume may have occurred at about the same time and as a result of the same incursion of glacier ice of the Illinoian age. Thus the Illinoian glaciation, hitherto not certainly recognized in the Dakotas, may have been a major factor in the Pleistocene development and history of that region.

REFERENCES CITED

- Alden, W. C. (1924) *Physiographic development of the northern Great Plains*, Geol. Soc. Am. Bull., vol. 35, p. 385-423.
- Fenneman, N. M. (1938) *Physiography of eastern United States*, McGraw-Hill, New York, 714 pages.
- Flint, R. F. (1947) *Glacial geology and the Pleistocene epoch*, John Wiley, New York, 589 pages.
- (1949) *Pleistocene drainage diversions in South Dakota*, Geog. Annaler, p. 56-74.

- (1950) *Pleistocene stratigraphy of eastern South Dakota*, Geol. Soc. Am., Bull., vol 61, p. 1460-1461.
- et al (1945) *Glacial map of North America*, Geol. Soc. Am., Spec. Paper 60.
- Frye, J. C.; and Leonard, A. B. (1949) *Pleistocene stratigraphic sequence in northeastern Kansas*, Am. Jour. Sci., vol. 247, p. 883-899.
- Leonard, A. G. (1916) *Pleistocene drainage changes in western North Dakota*, Geol. Soc. Am., Bull., vol. 27, p. 295-304.
- Rothrock, E. P. (1944) *Sand and gravel deposits in the Missouri Valley between Little Bend and White River*, S. Dak. Geol. Survey, Rept. Invest. 47, 118 pages.
- Schultz, C. B.; and Stout, T. M. (1945) *Pleistocene loess deposits of Nebraska*, Am. Jour. Sci., vol. 243, p. 231-244.
- Todd, J. E. (1885) *The Missouri Coteau and its moraines*, Am. Assoc. Adv. Sci., Pr. 1884, p. 381-393.
- (1899) *The moraines of southeastern South Dakota*, U. S. Geol. Survey, Bull. 158, 171 pages.
- (1914) *The Pleistocene history of the Missouri River*, Science, n.s., vol. 39, p. 263-274.
- (1923) *Is the channel of the Missouri River through North Dakota of Tertiary origin?* Geol. Soc. Am., Bull., vol. 34, p. 469-493.
- Warren, C. R. (1947) *Iowan till at Chamberlain, South Dakota* (Abstract), Geol. Soc. Am., Bull., vol. 58, p. 1237.
- (1949) *Probable Illinoian age of part of the Missouri River* (Abstract), Geol. Soc. Am., Bull., vol. 60, p. 1926.
- Warren, G. K. (1868) *On certain physical features of the upper Mississippi River*, Am. Natural., vol. 2, p. 479-502.
- (1869) *Some general considerations regarding these rivers, etc.*, 40th Cong., 3d sess., H. Exec. Doc. 1, pt. 2, p. 307-314.

WASHINGTON AND LEE UNIVERSITY, LEXINGTON, VIRGINIA.

MANUSCRIPT RECEIVED BY THE SECRETARY OF THE SOCIETY, JANUARY 28, 1952.

PUBLICATION AUTHORIZED BY THE DIRECTOR, U. S. GEOLOGICAL SURVEY.